論文 / 著書情報
Article / Book Information

題目(和文)	
Title(English)	Role of Intraparticle Reactions and Anisotropic Structure in Pyrolysis and Gasification of Woody Biomass
著者(和文)	PATTANOTAITEERANAI
Author(English)	Teeranai Pattanotai
出典(和文)	学位:博士（工学）, 学位授与機関:東京工業大学, 報告番号:甲第9625号, 授与年月日:2014年9月25日, 学位の種別:課程博士, 審査員:岡崎　健,佐藤　勲,平井　秀一郎,花村　克悟,齊藤　卓志
Citation(English)	Degree:, Conferring organization: Tokyo Institute of Technology, Report number:甲第9625号, Conferred date:2014/9/25, Degree Type:Course doctor, Examiner:,,,,
学位種別(和文)	博士論文
Type(English)	Doctoral Thesis

Role of Intraparticle Reactions and Anisotropic Structure in Pyrolysis and Gasification of Woody Biomass

By
Teeranai Pattanotai

A thesis
Presented in partial fulfillment of the requirements for the degree of Doctor of Engineering

Supervisor
Professor Ken Okazaki

Department of Mechanical and Control Engineering
Tokyo Institute of Technology
June 2014

Abstract

Gasification is one of the most promising technologies for utilizing biomass energy. Woody biomass usually used in commercial gasifiers has relatively large size. Therefore, intraparticle reactions and intraparticle structure play an important role in pyrolysis and gasification of large woody biomass. In this research, intraparticle secondary reactions of tar during pyrolysis were experimentally investigated. It was shown that intraparticle secondary reactions of tar occurred during the pyrolysis of large wood particle, resulting in a decrease in tar yield and an increase of gas products. Gasification characteristics of large wood char were also experimentally studied. An anisotropic structure of wood-derived char was visualized by X-ray computed tomography (CT). The anisotropic structure was found to significantly influence the char reactivity as well as the evolution of particle shape during gasification process.

Table of Contents

* Chapter two is an adaptation of the published paper: Teeranai Pattanotai, Hirotatsu Watanabe, and Ken Okazaki. Experimental investigation of intraparticle secondary reactions of tar during wood pyrolysis. Fuel 2013;104:468–475.

** Chapter three is an adaptation of the published paper: Teeranai Pattanotai, Hirotatsu Watanabe, and Ken Okazaki. Gasification characteristic of large wood chars with anisotropic structure. Fuel 2014;117:331–339.

List of Figures

List of Tables

CHAPTER 1

Introduction

This chapter reports the depletion of fossil fuels and environmental issues due to carbon dioxide emission. The development of existing conversion technologies such as clean coal technology and the promotion of renewable energy resources are necessary to reduce the large amount of carbon dioxide emission. The use of biomass, especially wood, as alternative energy to fossil fuels has attracted attention. The main advantage of biomass energy is its carbon neutrality. Many biomass conversion technologies including thermochemical and biochemical conversions are introduced. However, utilization of biomass energy through gasification process is a promising option. Fundamentals of woody biomass pyrolysis and gasification are explained. Research motivations of this work are initiated from the large size of woody biomass used in gasifiers. Therefore, intraparticle reactions and intraparticle structure become an important role in pyrolysis and gasification of large woody biomass. The objectives of this thesis are the clarification of intraparticle secondary reactions of tar during wood pyrolysis and the investigation of gasification characteristics of wood-derived char with anisotropic structure.

1.1 Energy consumption and environmental issue

For decades, the demand of energy has been growing due to the increase of the world population and the improvement of living standards all over the world including the developed/industrialized nations and the developing countries. The rapid increase in the consumption of fossil fuels began in the twentieth century, mostly by industrialized nations and globally total energy consumption showed an almost exponential increase from 1860 to 1990 as shown in Figure 1.1 [1]. From 1860 to the mid-1930s, total fossil fuel consumption gradually increased but then increased much more rapidly after the beginning of World War II. Since the 1940s, fossil fuels such as natural gas, oil and coal have become the world's largest source of energy [1, 2]. However, fossil fuels are non-renewable energy which will be diminished [2]. It is suggested that the time is not too far before depletion begins to adversely affect petroleum and natural gas reserves. Finally, the world will face the depletion of fossil fuels in the early twenty-second century [2]. Therefore, alternative energy resources such as solar energy, wind and wave energy, hydroelectricity and biomass have become much more attractive.

Most energy environmental specialists agree that the greater consumption of fossil fuel causes the negatively environmental effects. Since the 1960s, climate change and air quality problem have become major issues in many countries [1]. One of the main issues is the greenhouse effect. It is a process by which the thermal radiation from the earth surface is absorbed by greenhouse gases. Primary greenhouse gases in the atmosphere are water vapor, carbon dioxide, methane, nitrous oxide, and ozone. However, it is found that concentrations of carbon dioxide, methane, and nitrous oxide are gradually increasing in the troposphere [1, 3, 4]. The increases in these gases are believed to trap an excessive amount of solar radiation. That may cause the increase in ambient temperature.

The second issues involve ozone formation and destruction. Unnatural ozone formation in the troposphere over populated areas is caused by photochemical interactions of hydrocarbon, carbon monoxide (CO), and nitrogen oxide (NO_x) which primarily produced by human activities such as motor vehicles, incomplete combustion of fossil fuels. The abnormally high concentration of ozone in the troposphere is toxic and may cause negative health effects such as irritation of the respiratory system. On the other hand, the photochemical interactions of organic

chlorofluorocarbon compounds (CFCs) cause the destruction of natural ozone layer destruction in the stratosphere, resulting in increased penetration to the earth's surface of shorter-wavelength ultraviolet light that can cause skin cancers [1, 5]. Other issue is acid rain which caused by sulfur oxide (SO_x) emission from the combustion of sulfur-containing fossil fuels and has harmful effects on building and the growth of biomass [1, 6].

Climate changes refer to the changes in the state of the climate that can be identified by some parameters such as surface temperature and sea level. Over the past 100-year, climate changes were clearly observed. Figure 1.2 shows the observed changes in global average surface temperature, global average sea level and Northern Hemisphere snow cover. Global average surface temperature increased approximately 0.7°C in the past 100-year (1906-2005) [7]. Increases in sea level and decreases in snow and ice are consistent with warming. At the end of the 21st century, the increase in average surface temperature about 1.8–4.0°C and sea level rise in the range of 0.18–0.59 m would be estimated [7].

To deal with global warming from greenhouse gases, many countries are investigating new energy conversion technologies to suppress carbon dioxide emission which released by the great consumption of fossil fuels at the present. The alternative countermeasures for this issue can be classified into three categories as shown below:

(a) Fossil fuel energy with advanced technology

(b) Nuclear energy

(c) Renewable energy

(a) Because, nowadays, the main energy resources still rely on fossil fuel energy. Figure 1.3 shows fossil fuel reserves of coal, oil and natural gas in each continent at the end of 2010 [8]. Figure 1.4 shows fossil fuel reserve-production ratio. It shows that coal, oil and natural gas can supply the world's energy demand for 109, 52.9, and 55.7 years, respectively [9]. Moreover, the technologies which support utilizing fossil fuels have been developing in terms of its efficiency and emission level. Improving efficiency levels in coal combustion increases the amount of energy that can be extracted a single unit of coal, and also decreases carbon dioxide emission. One percentage of improved efficiency in a conventional pulverized coal combustion

plant may result in a 2–3% reduction in CO_2 emission [10]. Improvements in the efficiency of coal-fired power plant can be achieved by technologies including

1) Fluidized bed combustion
2) Supercritical and Ultra-supercritical boilers
3) Integrated gasification combined cycle

Fluidized bed combustion (FBC) is a flexible combustion technology of electricity production. The solid fuels such as coal, biomass and waste can be burned in a reactor comprised of a bed through which gas is fed to keep the fuel. The result is a turbulent mixing of gas and fuel. This provides more effective chemical reactions and heat transfer, resulting in reduction of SO_x and NO_x emissions. Pulverized coal combustion systems with supercritical and ultra-supercritical technology are newly potential coal-fired plants for increasing the efficiencies. These systems operate at increasingly higher temperatures and pressures; therefore they can achieve higher efficiencies than conventional pulverized coal combustion system and significant CO_2 reductions. Supercritical steam cycle technology has been practically used in many countries for decades and it achieves high efficiency more than 40% [10]. Ultra-supercritical steam cycle technology, which operates at much higher temperatures and pressures, is under development however it has been introduced in many countries such as Denmark, Germany and Japan to achieve the target of efficiency up to 50% [10]. An alternative coal conversion technology is integrated gasification combined cycle (IGCC) which coal (or other carbon based materials such as biomass) is converted to syngas using gasifier. The syngas, which is mainly H_2 and CO, is used in gas turbine to produce electricity. Moreover, waste heat from the gas turbine can create steam. Therefore, this system is combined with a steam turbine to generate more electricity. Additional hydrogen can be produced by adding shift reaction, which CO reacts with water vapor to form CO_2 and H_2. Then, CO_2 is captured and stored. Efficiencies of IGCC typically reach 45%, although systems are designed to possibly achieve efficiency around 50%. The challenge of IGCC is reliability and investment for plant construction which is significantly higher than the conventional coal-fired plant. An integrated coal gasification fuel cell combined system (IGFC) is also a new technology for coal utilization which integrates a coal gasifier, solid oxide fuel cells (SOFC), gas turbines and a steam turbine into a cascade-type system. IGFC can provide a high generation efficiency of 55% [11]. Moreover, an alternative way to achieve zero CO_2 emission for coal combustion is a

carbon capture and storage or carbon capture and sequestration (CCS). The method is based on capturing carbon dioxide (CO_2) from large CO_2 sources, such as fossil fuel power plants, and storing it in deep geological formations, in deep ocean masses, where CO_2 does not affect the atmosphere. CCS requires high concentration of CO_2 before storing process. Therefore, coal oxy-fuel or O_2/CO_2 combustion system, which can provide the high CO_2 concentration about 95% in flue gas, should cooperate with CCS effectively.

(b) Nuclear power is considered as a prominent alternative. The first commercial nuclear power plants started operation in the 1950s. There are now over 440 commercial nuclear power reactors operating in 30 countries that supply about 13.5% of the World's electricity in 2012 [12]. Nuclear power plant emits few greenhouse gases during electricity generation, when compared with coal and other traditional power plant. Total lifecycle GHG emissions of nuclear power are averagely 66 gCO_2-eq/kWh [13]. Meanwhile, the lifecycle GHG emissions of coal power plant are approximately 960-1050 gCO_2-eq/kWh [13]. Therefore, nuclear power is an effective GHG mitigation option. Uranium is mainly used as a fuel in nuclear reactor to generate electricity via nuclear fission. Uranium is a relatively common element that is found throughout the world and can be utilized as an energy resource for over 100 years [12]. Typically, uranium is a slightly radioactive metal, thus it must be processed, such as conversion and enrichment process, before it can be used as fuel for a nuclear reactor. One ton of natural uranium can generate approximately 44 million kWh of electricity. Whereas, over 20,000 tons of black coal or 8.5 million cubic meters of gas is required to generate this amount of electrical power. The most concerning points about nuclear power are safety and waste management. Since many accidents of nuclear reactor occurred in the past such as the Three Mile Island accident in 1979, the Chernobyl accident in 1986, and recently the Fukushima accident in 2011, the safety of nuclear reactors has been a very high priority in their design and engineering. It is mentioned that about one third of cost of a typical reactor is due to safety systems and structures. Nuclear power produces wastes of used fuel which are handled and stored safely. The wastes are very hot and radioactive but modest in quantity. The storage place simply need to be shielded from human exposure, and cooled. For example, after the used fuel is removed from a reactor, it is transferred to a large storage pool where it may keep for

up to 20-50 years. After that, the used fuel has only one thousandth of its initial radioactivity remaining that it is much easier to handle and dispose of.

(c) Renewable energy is energy which comes from natural resources such as wind, solar, hydropower and biomass. Renewable energy in 2011 accounted for about 19% of global energy supply, including traditional biomass (9.3%), large hydropower (3.7%), and other new renewable (6%) [14]. Renewable energy can replace conventional fossil fuels in four distinct markets: electricity generation, heat generation, fuels for transportation, and rural (off-grid) energy services [14]. Renewable-energy systems contribute for protection of the environment in terms of GHG emissions. Many renewable-energy technologies have already been commercialized with established markets in at least several countries such as large and small hydropower, woody biomass combustion, geothermal, landfill gas, crystalline silicon PV, solar water heating, onshore wind, and bioethanol. There are many renewable-energy technologies which are under development with demonstrations or small-scale commercial application but approach market introduction such as thin-film PV, tidal range and currents, wave power and biomass gasification and pyrolysis. The large (>10MW) hydroelectricity systems can provide 16% of global electricity or 90% of renewable electricity in 2004 [4]. However, when hydropower is expanding in many countries such as China and India, social disruption and ecological impacts on river ecosystems and fisheries are stimulating public opposition. Wind provides less than 1% of the total electricity production in 2004, but its technical potential greatly exceed this. In Denmark, wind power accounted for 30% of electricity production in 2012 [15]. Countries in Europe, Japan, China, USA and India have largely invested for wind-energy systems [16]. Solar radiation which reached the Earth's surface accounts for several thousand times the annual global energy consumption [17]. There are many technologies for utilizing solar power such as solar thermal electric, solar photovoltaic (PV) and solar heating and cooling. For PV, the potential of this is limited by land, energy-storage and investment constraints [4]. The use of solar energy is rapidly growing all over the world, especially in Germany, Italy, USA, and Japan, due to the declining manufacturing costs and abundant subsidies [12]. The commercial PV modules are mostly based on crystalline silicon cells which have up to 19% of efficiency and about 85% of market share [17]. Biomass is commonly the world's major source of food, stock fodder and fiber as well as a renewable resource of hydrocarbons for heat,

electricity, liquid fuels and chemical. The use of biomass as energy resource is explained in the next section.

There are three main groups of energy resource for suppressing GHG emission and global warming as mentioned above. “What is the best energy resource in the future?” is always questioned but it has no exact answer because every resource has pros and cons. All of technologies should be developed together. The selection for the suitable technology in each country depends on many factors such as geography, own natural resources, investment costs and government’s policy.

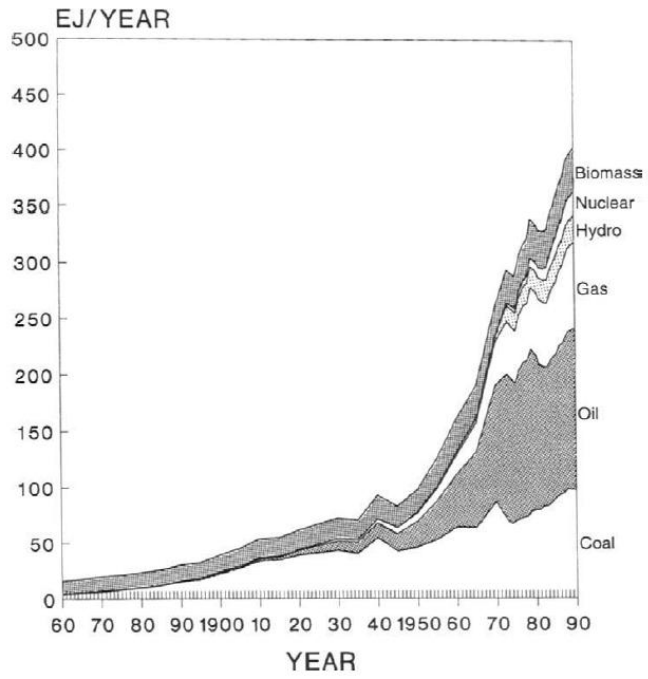

Figure 1.1 World's energy consumption from 1860 to 1990 [1].

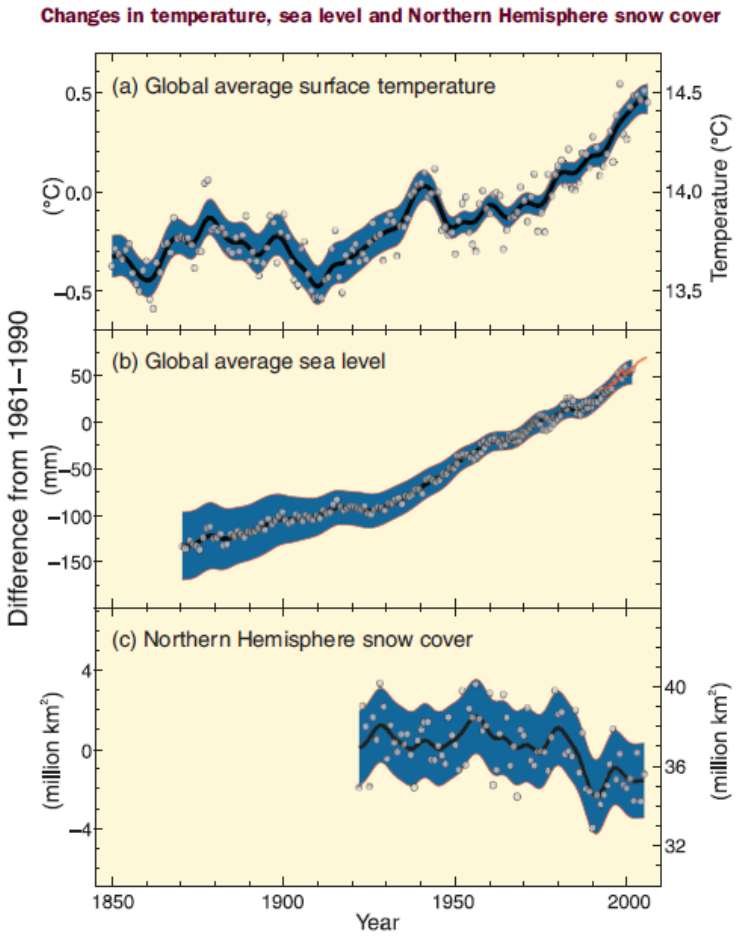

Figure 1.2 Changes in global average surface temperature, global average sea level and Northern Hemisphere snow cover [7].

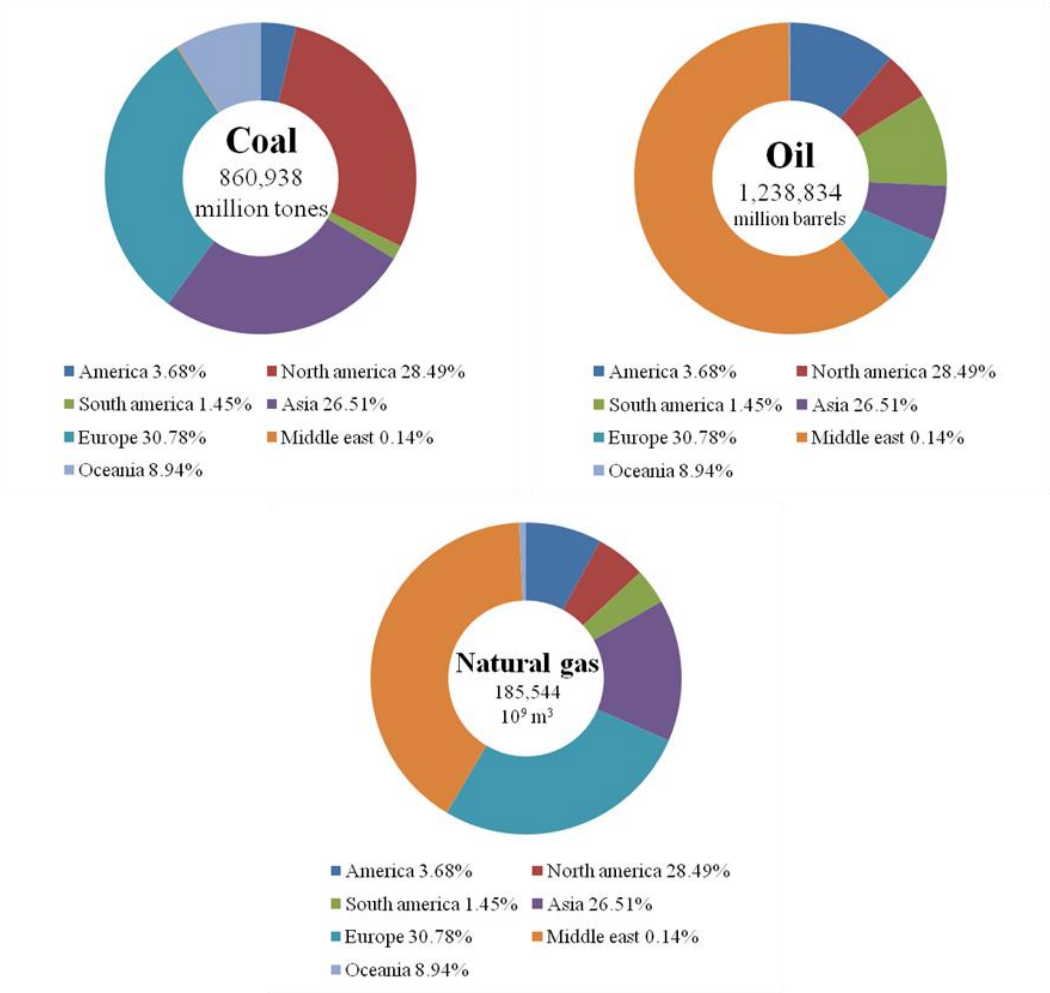

Figure 1.3 Fossil fuel reserves in each continent at the end of 2010 [8].

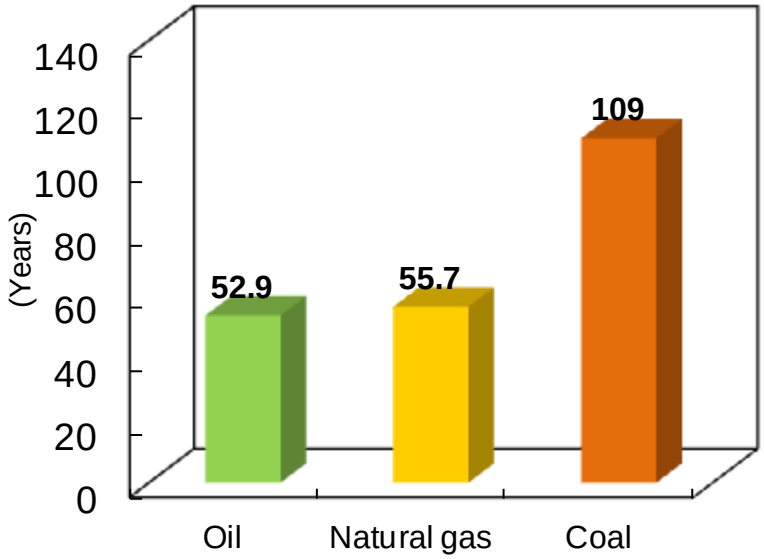

Figure 1.4 Fossil fuel reserves-to-production ratios [9].

1.2 Biomass as renewable energy

Biomass is a great source of energy that can be used for many applications. If the incident solar radiation that strikes the earth's surface is considered, an average daily radiation worldwide is about 198 W/m^2 [17]. The annual insolation on about 0.01% of the earth's surface is approximately equal to total energy consumption by humans each year [1]. The most practical process for capture of solar energy is the growth of biomass or plants with the maximum capture efficiency ranging from 8% to 15% [18]. The large quantities of carbon are fixed in the form of terrestrial and aquatic biomass. In theory, if biomass is harvested and used as an energy resource, it is able to provide about 100 times the world's annual energy consumption [18].

Biomass is biological material derived from living or recently living organisms and is often referred to the plant based material or lignocelluloses. Biomass can be utilized to generate electricity or produce heat. Therefore, biomass is considered as a renewable energy because its energy comes from natural resource which is solar energy. The most conventional way for utilizing the energy from biomass relies on the direct combustion to produce heat. Nevertheless, biomass is able to be converted to other forms of energy such as gaseous fuels (synthesis gas, biogas, hydrogen) and liquid fuels (methanol, ethanol, butanol, biodiesel).

Firstly, biomass had been the major of the world's energy for many centuries before the fossil fuel began. Since the 1940s, fossil fuel energy has become the world's largest energy source. Then, due to the Oil Shocks in the 1970s, biomass was again realized by many countries to be a domestic energy resource that has the potential of reducing oil consumption and imports and improving the balance of payments and deficit problems caused by dependency on the imported oil. Finally, due to environmental concerns about global warming nowadays, biomass became much more attractive energy resource.

1.2.1 Advantages of biomass energy

Biomass is expected to be an alternative energy source to deal with global warming and depletion of fossil fuels owing to many advantages as shown below

(a) Renewable

Renewable energy means energy which comes from natural resources such as solar power, wind, tide and geothermal heat. All of them are renewable or naturally replenished. Biomass is also considered as a renewable energy resource because its energy comes from the sun through the process of photosynthesis. A detail of photosynthesis is explained in the advantage of carbon neutral. The carbon cycle is the biogeochemical process where carbon is recycled and reused through the ecosystem including atmosphere, oceans, biosphere and geosphere. Fossil fuel is one of carbon forms in the carbon cycle. However, it takes time of several million years so that natural processes could replenish the depleted fossil fuels (petroleum, natural gas, and coal). Thus, carbon containing materials that are able to renew themselves over a time span short enough to make them continuously available in large quantities are needed to supply the World's energy demand. Biomass is one of the sources of carbon that can meet these requirements.

(b) Storable and substitutive

Biomass can be considered as a storable energy carrier, unlike gas and liquid fuel. Because biomass is a solid fuel, it may be more convenient for transportation than liquid and gas fuels. Moreover, biomass can be converted to other forms of storable fuels such as bioethanol, biodiesel, hydrogen, syngas, etc. Biomass and its reformed products are expected to substitutive fuels that are able to be used in the existing energy devices. For example, biomass feedstock can be combusted with fossil-fuel technologies by co-firing solid biomass particles with coal; mixing synthesis gas, landfill gas or biogas with the natural gas prior to combustion. Biofuel and gas products are also used as fuels in internal combustion engines as well as gas turbine engines.

(c) Abundant

Biomass is abundant source of energy that can be found in almost countries all over the world. According to the data of global energy resources by IPCC (Intergovernmental Panel on Climate Change), the available energy resource of biomass is estimated to be 250 EJ/yr which can cover nearly an half of annual use rate (490 EJ in 2005) [4]. Globally, biomass provided energy only approximately 46 EJ of bioenergy in 2005 [4]; therefore, biomass has a potential to increase the share

in the global energy resource. About two-third of biomass energy usage (37 EJ/yr) was consumed in developing countries as traditional biomass for household use, whereas approximately 9 EJ/yr of modern biomass was used for heat and power generation [4].

(d) Carbon neutral

Biomass is considered as a carbon-neutral fuel which refers to net zero carbon emission by balancing an amount of carbon released with an equivalent amount sequestered. Figure 1.5 shows life cycle of biomass energy. Biomass captures solar energy as fixed carbon via photosynthesis; during this process; carbon dioxide in the atmosphere is consumed and converted to organic compounds. The key initial step in the growth if biomass is expressed by the equation

$$CO_2 + H_2O + \text{light} + \text{chlorophyll} \rightarrow (CH_2O) + O_2$$

Carbohydrate, represented by CH_2O, is the primary organic product of photosynthesis. Biomass is harvested for many purposes such as for food, feedstock, and materials of construction. A portion of biomass is used as energy source to produce heat or generate electricity via combustion. Alternatively, biomass and any wastes which are residues from its processing or consumption could be converted to synthetic organic fuels. By combustion and utilizing synthetic organic fuels, the fixed carbon in fuels is converted into carbon dioxide which then released to the atmosphere. However, it is noticed that biomass utilization does not contribute to global warming like fossil fuels because the absorbed carbon dioxide by plants during its growth practically balances the released carbon dioxide by it utilization. Whereas, by consuming fossil fuels such as natural gas and coal, the large amount of ancient carbon underground is used and then released to the atmosphere, resulting in the increase of carbon dioxide in the atmosphere.

The basic concept of biomass as the carbon neutral fuel consists of the capture of solar energy and carbon from ambient carbon dioxide in growing biomass. Then biomass is converted to useful forms of energy (synthesis gas, biofuels) or is used directly by combustion. One cycle of biomass utilization is completed when the biomass or derived fuels release the carbon to the atmosphere after its usage.

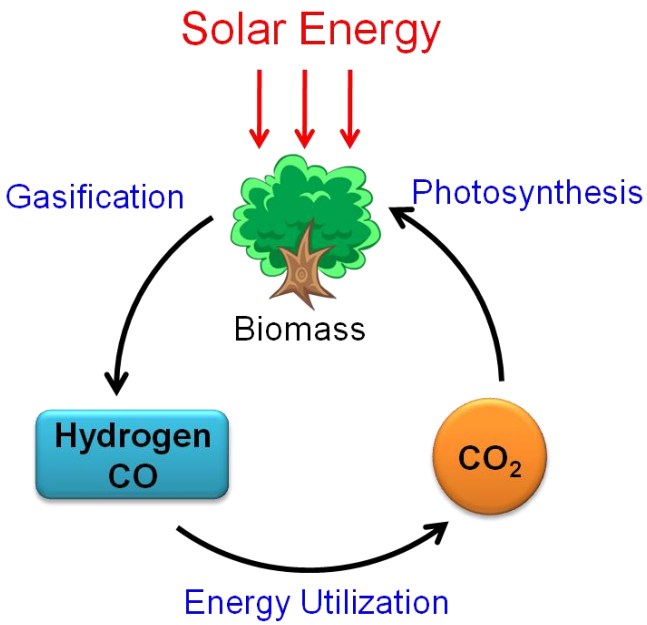

Figure 1.5 Life cycle of biomass energy.

1.2.2 Major components of biomass

The chemical composition of biomass is different from that of coal, oil, etc. The larger amounts of oxygen in plants can be observed. Wood and other biomass is a composite material constructed from oxygen-containing organic polymers [19]. Biomass consists of different types of dead and living cells, the structure and composition of which varies for different parts and species of plant. Typically, the composition of biomass can be divided into cellulose, hemicelluloses, lignin, inorganic minerals and organic extractives.

(a) Cellulose

Cellulose is the largest fraction of biomass about 40-50 wt% of dry wood [20]. Cellulose is a polysaccharide with the formula of $(C_6H_{12}O_6)_n$, consisting of linear chains of several hundred to ten thousand of (1,4)-D-glucopyranose units, in which are linked by β-1,4 glycosidic linkages in linear, unbranched chains. An average molecular weight of cellulose is around 100,000. Figure 1.6 shows a molecular structure of cellulose. Cellulose is the structural component of the primary cell wall of green plants which provides wood's strength.

(b) Hemicellulose

Hemicellulose is the second major chemical component of wood which accounts for 25-30 wt% of dry wood, 28% in softwood and 35% in hardwoods [20]. Hemicellulose is a mixture of polysaccharides, comprising of various polymerized monosaccharide such as glucose, glucuronic acid, xylose, mannose, and arabinose [21]. Hardwood hemicelluloses contain mainly xylans, whereas softwood hemicelluloses contain mainly glucomannans. Figure 1.7 shows main components of hemicellulose. In contrast to cellulose that is crystalline and strong, hemicellulose has a random, amorphous structure with little strength, in which contains short side-chain branches pendent along the main polymeric chain. Hemicelluoses present lower molecular weights (<30,000) than cellulose. The number of saccharide monomers is only 50-200.

(c) Lignin

Lignin is the third major chemical component of wood which accounts for 23-33% of the mass of softwoods and 16-25% of the mass of hardwoods [22]. Lignin is considered as a group of amorphous, high molecular-weight, chemically related compounds, which has no exact structure [21]. The building blocks of lignin are

believed to be a three carbon chain attached to rings of six carbons, called phenyl-propanes [21]. These may have hydroxyl and methoxyl groups attached to the rings. The proportions of each group vary for the different kinds of biomass. Lignin fills the space in the cell walls between cellulose, hemicellulose and pectin component. Figure 1.8 shows a partial structure of hardwood lignin molecule from European beech.

(d) Inorganic materials

Biomass is also comprised of a small amount of inorganic materials such as K, Na, P, Ca, and Mg. These end up in ash after pyrolysis and gasification. It is mentioned that ash in biomass influences pyrolysis and gasification reactions [23-25]. The ash component normally found in woody biomass can suppress the formation of tar [24]. If the effects of ash are desirable, the level of ash in the system can be increased by recycling ash from the outlet. On the other hand, ash may have detrimental effects on combustion equipment through the formation of undesired deposits.

(e) Organic extractives

The last component of biomass is composed of organic extractives. Extractives include fats, waxes, proteins, pectins, starches, resins, and essential oils. These can be extracted from biomass using polar solvents (such as water or alcohol) or nonpolar solvents (such as toluene or hexane).

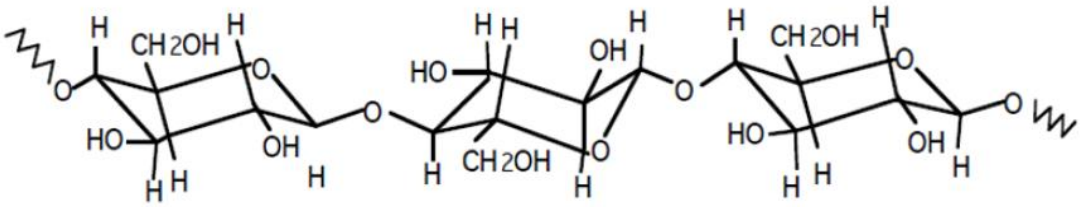

Figure 1.6 Molecular structure of cellulose.

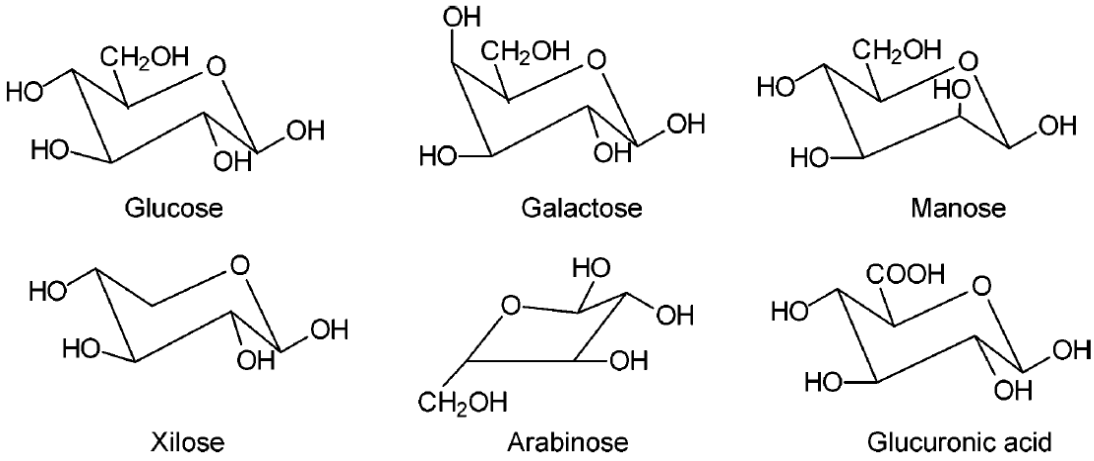

Figure 1.7 Main components of hemicelluloses [19].

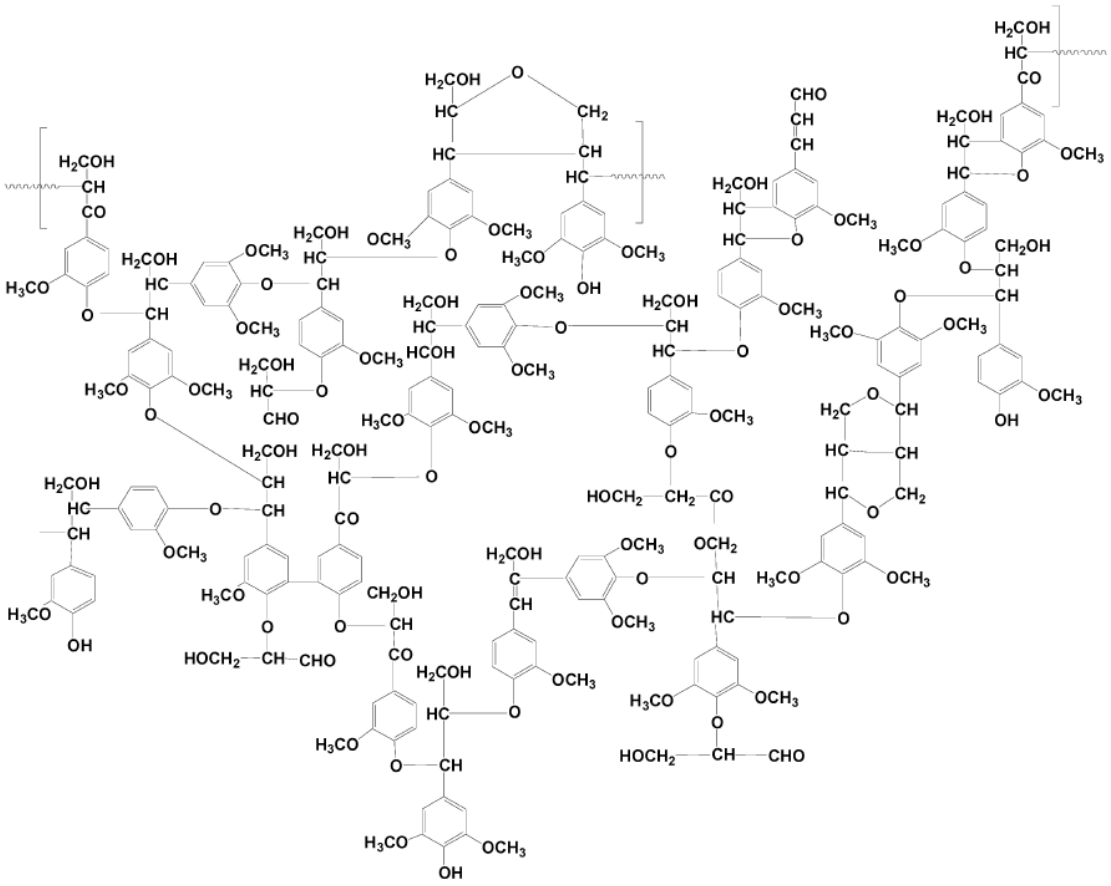

Figure 1.8 shows a partial structure of hardwood lignin molecule from European beech [19].

1.2.3 Types and sources of biomass

Basically, biomass is considered as the world's major source of human food, stock fodder and fiber as well as a renewable energy resource. Woody biomass is always used as construction materials and then it can be reused as an energy resource at the end of their life. Biomass sources can be classified into five main groups including:

(a) Virgin wood

Virgin wood consists of wood and other physical forms such as sawdust, wood chip and bark that have not been passed through chemical treatment or finishes. Virgin wood may be collected from forests and simply logged into appropriate sizes for direct use as fuel. However, wood is too valuable to burn, it is better to use as construction materials by woodworking process [26]. The residues from this process such as bark, sawdust and misshapen or odd-sized pieces and demolition wood from construction are more economic to use as fuel [26]. Virgin wood can be conventionally burned for heat or electricity at a range of scales. Moreover, new technologies which are able to produce liquid or gaseous fuels are being developed.

(b) Energy crops

Cultivation of biomass for use as fuel is known as energy cropping. These may be vegetable oils for conversion to biodiesel, sugar or starch for fermentation to bioethanol, grain for production to liquid transport fuels, and straw for combustion to produce heat or electricity. Maximizing outputs of desired harvest is a key point for energy crops. This may be measured in terms of tons of biomass per area. Moreover, fast-growing wood species such as poplar or willow in moderate climates, and sugar cane in tropical areas might be involved on the activity of energy crops [26]. A consideration that may affect policy on establishing energy crops is the use of agricultural land to grow energy crops in a large scale. It would reduce the area of available to grow food crops. However, food production should have priority over energy crops.

(c) Agricultural residues

Agricultural residues include arable crop residues such as straw or husks, animal manures and slurries, animal bedding such as poultry litter, and most organic material from excess production or insufficient market such as grass silage. Some are wet residues that are not suitable for combustion or gasification and provide low

efficiency for energy conversion. Therefore, any moisture content must be driven off before those processes. Many of agricultural residues may have alternative uses such as fertilizers to improve soil nutrient. This may be displacing significant quantities of synthetic fertilizers. Thus, any decision to use agricultural residues for energy must be made in the context of these alternatives.

(d) Food waste

Food residues and waste are disposed of at all points in the food supply system from production, through processing, transportation and distributions to post-consumer waste. Many food materials are processed to remove inedible or not required components such as peel/skin, shells, husks, fish heads, oil extractives, etc. Many foods and drinks manufacturing industries, which produce liqueur, cheese and dairy products, generate large quantities of organic waste material.

(e) Industrial waste and co-products

Many industrial processes produce waste or co-products which can be divided into woody materials and non-woody materials. These can potentially be used or converted to biomass fuels. Wood wastes include untreated or treated wood wastes and wood composites or laminates. These are technically the same as the virgin wood and can be utilized by many thermal conversion technologies such as combustion, gasification and pyrolysis. Non-woody wastes include paper pulp and wastes, textiles and sewage sludge. This kind of waste is not primarily wood, however is still biomass derived that can be used as a fuel.

1.2.4 Biomass energy conversions

Biomass from various sources as already mentioned is used as feedstocks to produce energy carriers in the form of solid fuels (chips, pellet, briquettes), liquid fuels (biodiesel, methanol, ethanol), gaseous fuels (synthesis gas, hydrogen, biogas), electricity and heat. The conversion technologies of biomass to provide bioenergy can be divided into two main groups: thermochemical conversion and biochemical conversion [21, 27].

(a) Thermochemical conversion

Thermochemical conversion of biomass occurs at elevated temperatures above approximately 300°C (at atmospheric pressure or elevated pressure) that overcome the natural resistance of biomass to conversion. Thermochemical processes can

provide the productive use of wide range of biomass resources. Thermochemical processes of biomass include combustion, pyrolysis, gasification, etc. These processes produce a range of energy forms such as heat, secondary fuels (synthesis gas or biofuel).

(a-1) Combustion

Combustion is an exothermic chemical reaction between fuels and oxidants accompanied by the production of heat and conversion of chemical species. The reaction is spontaneously continued by the heat generated by the reaction. Due to the high moisture of biomass, water is evaporated in the combustion process so that the generated heat from biomass combustion is generally less than that of coal combustion. Thus, biomass can be co-fired with coal at existing thermal power stations [28-30]. The advantage of this technology is that, simply by making some minor modifications on existing equipment to enable biomass combustion.

(a-2) Pyrolysis

Pyrolysis is a thermochemical decomposition of solid fuels at elevated temperature in the absence of gasifying agents such as air or oxygen. Products of pyrolysis process are char, gases and liquids (tars). Pyrolysis can be classified into two main types: conventional pyrolysis and fast pyrolysis. Conventional slow pyrolysis has been used for the production of charcoal for a thousand years. In slow biomass pyrolysis, a feedstock can be held at constant temperature or slowly heated. The vapor residence time varies from 5 min to 30 min for the slow pyrolysis. In fast pyrolysis, biomass is rapidly heated in the absence of oxygen. Heating rates of 1000~10,000 K/s have been claimed [22]. Rapid heating and rapid quenching produced the intermediate liquid products, which condense before secondary cracking of high-molecular-weight species into gaseous products. The intermediate products are estimated that more than 200 species occurred during the pyrolysis of biomass [31]. The desired products of fast pyrolysis are bio-oil and chemicals.

(a-3) Gasification

Gasification is an extension of pyrolysis which converts solid fuels such as biomass, coal into a fuel gas or synthesis gas. This thermal process is mainly to produce the highest yield of carbon and energy in the gas phase, rather than to produce char or a liquid. In contrast to pyrolysis, gasification takes place in the limited amount of air or oxygen at elevated temperature. That results in exothermic reactions which provide heat for pyrolysis and gasification.

(b) Biochemical conversion

Many highly efficient biochemical processes have been developed to harness biomass. The nature of biochemical processes is to break down the molecules of biomass into smaller molecules using enzymes, bacteria and other micro-organisms. Three main routes of biochemical conversion are digestion (anaerobic and aerobic), fermentation and enzymatic or acid hydrolysis [27]. Breaking down biomass (carbohydrates and sugars) to make alcohol is the promising way for biomass utilization to fuels. These methods include methanol fermentation and ethanol fermentation.

(b-1) Methane fermentation

Methane fermentation or biomethanation is a complex microbial process in which organic compounds are degraded into methane and carbon dioxide by variety of anaerobes. This process takes place at room temperature and under atmospheric pressure. First, acetic acid or hydrogen and carbon dioxide are produced by anaerobes. Then, the primary products are converted to methane. This biogas which contains a low heating value of 20-25 MJ/m^3-N can be used for fuel [32]. Moreover, fermented residue is used for liquid fertilizer and raw material of compost.

(b-2) Ethanol fermentation

Ethanol fermentation is a biological process in which saccharine materials such as glucose, fructose and sucrose are metabolized by yeast strains through glycolysis pathway to produce ethanol and carbon dioxide [32]. Ethanol fermentation has been known for several thousand years as brewery of alcohol drinks, manufacture of fermented food and bakery. Ethanol is available in the various fields such as beverage and food industries, medical use, as well as fuel. Large amount of ethanol fuel has been produced from kernels of corn in the USA and from sugar cane in Brazil [32]. Ethanol fermentation is an effective technology to convert biomass to ethanol fuel.

1.3 Principles of pyrolysis and gasification

Pyrolysis (also known as canbonization, destructive distillation, dry distillation, or retorting) is the chemical decomposition induced in organic materials by heat in the absence of oxygen. In practice, oxygen or air cannot be perfectly purged; therefore, pyrolytic systems are operated with less than stoichiometric quantities of oxygen. Pyrolysis process produces char, oils or tar and fuel gases depending on the pyrolysis conditions, especially temperature and heating rate, and the organic material contents of feedstock. Table 1.1 provides a summary of pyrolysis applications and their variants. There are two major differences between combustion and pyrolysis. First, combustion is an exothermic process which generates heat, whereas pyrolysis is an endothermic process which requires the external heat. Second, products of combustion process are carbon dioxide, water and ash, whereas with pyrolysis the products are char, oils or tar and fuel gases.

Pyrolysis can be discriminated into two groups by considering temperature i.e. low temperature and high temperature pyrolysis [33]. At low temperature the major product is tar or heavy oil, whereas at the high temperature the major product is gas [33]. Moreover, pyrolysis processes may be conventional (slow pyrolysis) and fast pyrolysis, depending on the heating rate used in their operations [19]. Slow pyrolysis has been used for thousands of years to produce charcoal. In the slow pyrolysis, biomass is heated to ~500°C with the vapor residence time varying from 5 min to 30 min [19, 33]. Fast pyrolysis is operated at a high temperature (600–1000°C) with high heating rates of 10–200 K/s [34]. Fast pyrolysis produces 60–75 wt % of oils, 15–25 wt % of solid char, and 10–20 wt % of noncondensable gases [19].

1.3.1 Thermal mechanism of biomass pyrolysis

There are various mechanisms of biomass pyrolysis proposed by many researchers [35-42]. A general model for wood pyrolysis as shown in Figure 1.9 is used in this study. In this model, wood is assumed to decompose to three major products: tar, char and gas, by three primary reactions. All of three primary reactions are endothermic. And then, a portion of primary tar decomposes to gas and char by secondary reactions. That is called secondary reactions of tar which are exothermic reactions. Some of other models have been proposed by considering that wood

consists of three major components: hemicellulose, cellulose, and lignin [43, 44]. Cellulose, which is a major component of wood, decomposes at temperature of 240–350°C to produce levoglucosan and dehydrocellulose [19]. Hemicellulose decomposition occurs at 200–260°C producing more volatiles, less tars and less chars than cellulose [19]. Lignin decomposes to produce phenols by the cleavage of ether and carbon-carbon linkages. Lignin decomposition occurs at higher temperature than that of other two components about 280–500°C [19]. Pyrolysis of lignin produces more residue char than that of cellulose [19, 40].

1.3.2 Gasification theory

Gasification is a process which converts carbonaceous materials to a combustible or synthesis gas (with a useable heating value) such as H_2, CO, and CH_4. In general, gasification involves the reaction of carbon with gasifying agents such as air, oxygen, steam, carbon dioxide, or a mixture of these gases at 700°C or higher. By using different gasifying agents, the heating value of gaseous product is also different as shown in Figure 1.10. Gaseous products can be used to generate electric power and heat or as a raw materials for synthesis of chemicals, liquid fuels, or other gaseous fuels [33]. In contrast with combustion, which operates with excess air, gasification process operates at substoichiometric conditions (generally equivalence ratio of 0.3 or less) so that both heat and gaseous fuel are produced as feedstocks are consumed. Meanwhile, combustion produces only heat because its product flue gas has no residual heating value. Some gasifiers use indirect heating to avoid combustion of the feed material in the reactor and the dilution of the product gas with nitrogen and excess CO_2. Figure 1.11 shows a generally agreed sequence of gasification reaction for coal and biomass or the mechanism of gasification. First, biomass is pyrolyzed to produce three main products: char, tar/oils and gas. Then, reactions of these three products with gasifying agents take place and yield synthesis gas. It is noted that the reactions of light hydrocarbon gases and tars with gasifying agents are homogeneous or gas phase reaction, whereas the reactions of char are heterogeneous or solid-gas phase reactions.

Stoichiometric considerations

When the feedstock is fed through the gasifier, the following physical, chemical and thermal processes may occur sequentially or simultaneously, depending on the feedstock material and the reactor design.

Drying

When the feedstock is heated and its temperature increases, water or moisture in the feedstock is first evaporated.

$$\text{Moist feedstock} + \text{Heat} \rightarrow \text{Dry feedstock} + H_2O$$

Pyrolysis/Devolatilization

As the temperature of the dry feedstock increases (300–800°C), the feedstock is pyrolyzed to produce volatiles (gas + tar) and char.

$$\text{Dry feedstock} + \text{Heat} \rightarrow \text{Volatiles (Gas+Tar)} + \text{Char}$$

The volatiles may include gas species (H_2O, H_2, CO_2, CO, CH_4, H_2S, NH_3, etc) and unsaturated hydrocarbons (alkenes, Alkynes, and aromatics or tars), depending on the components of feedstock. Char is the residue solids from devolatilization. Char consists of organic and inorganic materials or ash and has higher concentration of carbon than the dry feedstock.

Gasification

Gasification is the result of chemical reactions between carbon in char and gasifying agents such as steam, oxygen or carbon dioxide as well as chemical reactions between the produced gases and gasifying agents. Gasification reactions can be represented by:

Oxidation reactions

$$C + O_2 \rightarrow CO_2$$

$$C + 0.5O_2 \rightarrow CO$$

$$CO + 0.5O_2 \rightarrow CO_2$$

$$H_2 + 0.5O_2 \rightarrow H_2O$$

Reduction reactions

$$C + CO_2 \rightarrow 2CO$$

$$C + H_2O \rightarrow CO + H_2$$

$$CH_4 + CO_2 \rightarrow 2CO + 2H_2$$

$$CH_4 + H_2O \rightarrow CO + 3H_2$$

Shift reaction

$$CO + 2H_2O \leftrightarrow H_4 + CO_2$$

Other reactions

$$C + 2H_2 \rightarrow CH_4$$

$$CO + 3H_2 \rightarrow CH_4 + H_2O$$

In addition to the gasifying agents (air, steam and oxygen), the gasifier operating temperature and pressure, other factors (such as feedstock composition, feedstock particle size, reactor heating rate, residence time, etc) affect the chemical composition, heating value of the gasifier product gas.

Table 1.1 Pyrolysis applications and their variants [45].

Method	Residence time	Temperature (K)	Heating rate	Product(s)
Carbonation	Days	675	Very low	Charcoal
Conventional	5–30 min	875	Low	Oil, gas, char
Fast	0.5–5 s	925	Very high	Bio-oil
Flash-liquid	<1 s	<925	High	Bio-oil
Flash-gas	<1 s	<925	High	Chemicals, gas
Hydro-pyrolysis	<10 s	<775	High	Bio-oil
Methano-pyrolysis	<10 s	>975	High	Chemicals
Ultra	<0.5 s	1275	Very high	Chemicals, gas

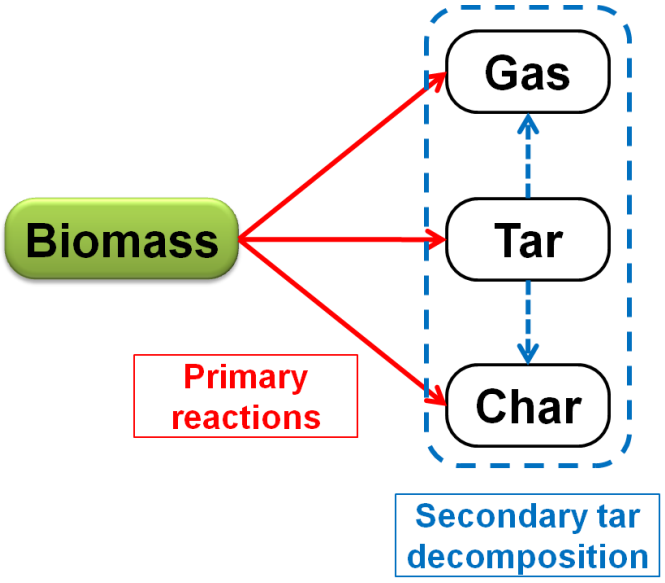

Figure 1.9 Pyrolysis model.

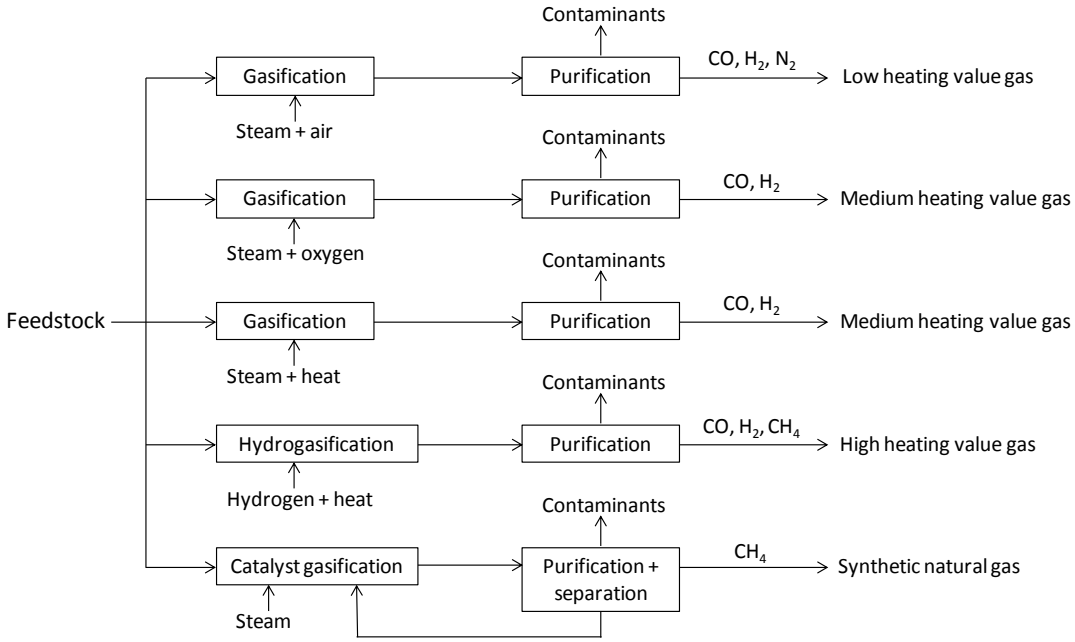

Figure 1.10 Gasification methods [33].

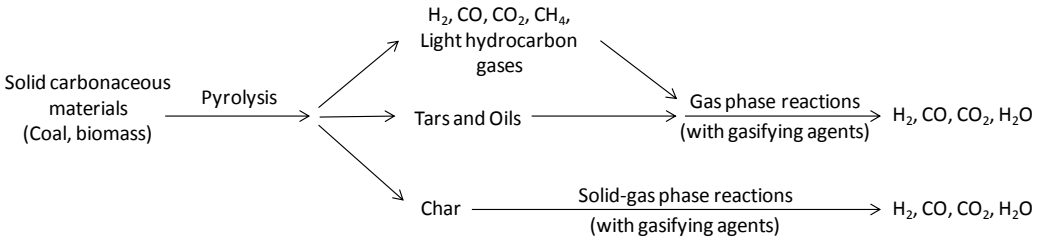

Figure 1.11 Gasification model [33].

1.3.3 Types of gasifier

There are four main types of reactor/furnace [46]:

- quasi-non-moving or self-moving feedstock (fixed bed furnace, cupola furnace, etc)
- mechanical-moved feedstock (screw conveyor, rotary drum, etc)
- fluidically-moved feedstock (fluidized bed, entrained flow reactor, etc)
- special reactors (plasma torch, electric induction, etc)

However, the fixed bed (Figure 1.12) and fluidized bed gasifier (Figure 1.13) are two reactor types mainly used for gasification of biomass [46].

Updraft or countercurrent fixed-bed gasifiers

The fixed-bed countercurrent gasifier is the simplest type of gasifier. The biomass feedstock is fed at the top of the reactor and moves downward. Air is introduced at the bottom, and the gas product leaves at the top. Therefore, the biomass feedstock moves counter to the gas flow and passes sequentially through drying, pyrolysis, reduction, and oxidation zone. The heat for drying and pyrolysis process is mainly supplied by the upward-flowing producer gas and partly by radiation from the oxidation zone. The advantages of this type of gasifier are its simplicity, high char burnout, and low gas-exit temperature [26]. Major drawbacks are the high amounts of tar and pyrolysis products because the pyrolysis gas does not pass the high temperature of oxidation zone. Therefore, the gas cleaning process is needed before utilizing the gas product in engines [26].

Downdraft or cocurrent fixed-bed gasifiers

In the downdraft gasifier, the biomass feedstock is fed at the top. The air is introduced at the top or the side of reactor and the gas leaves at the bottom of the gasifier. Therefore, the feedstock and the gas flow in the same direction. The zones are similar to those in the updraft gasifier. However, the heat for drying and pyrolysis process is mainly delivered by radiation from the oxidation zone. The advantage of this type of gasifier is the low amount of tar because the pyrolysis products including tar pass through the high temperature of oxidation zone and are burned [26, 27]. In practice, a tar-free gas is seldom achieved because not all gases pass through the high temperature zone and the residence time may be too short.

Drawback of the downdraft gasifier is, for example, high amounts of ash and dust particle in the gas because the gas collects small ash particles when it passes the oxidation zone [26].

Fluidized-bed gasifiers

The fluidized-bed gasifier was originally designed to overcome the operational problem of fixed bed gasification of fuel with high ash content [26]. In the fluidized-bed gasifier, the biomass feedstock is fed into a suspended (bubbling fluidized bed) or circulating (circulating fluidized bed) hot solid bed (sand, catalyst, etc). The differences between bubbling- and circulating fluidized bed are the gas velocity and the gas path. Gas velocities for bubbling beds are relatively low, in circulating beds velocities are close to pneumatic flow [46]. Little solids leave from bubbling beds. In circulating beds, entrained solids are recycled using a cyclone. In fluidized-bed gasifier, the feedstock mixes quickly with the bed material, resulting in the rapid pyrolysis with a large amount of pyrolysis gases. The gasification temperature for the fluidized-bed gasifier is relatively low approximately 750–900°C compared with the fixed bed gasifier which operates at maximum temperature approximately 1200–1500°C [26]. The low reaction temperatures results in not very high rate of tar decomposition and relatively low melting points of ash components.

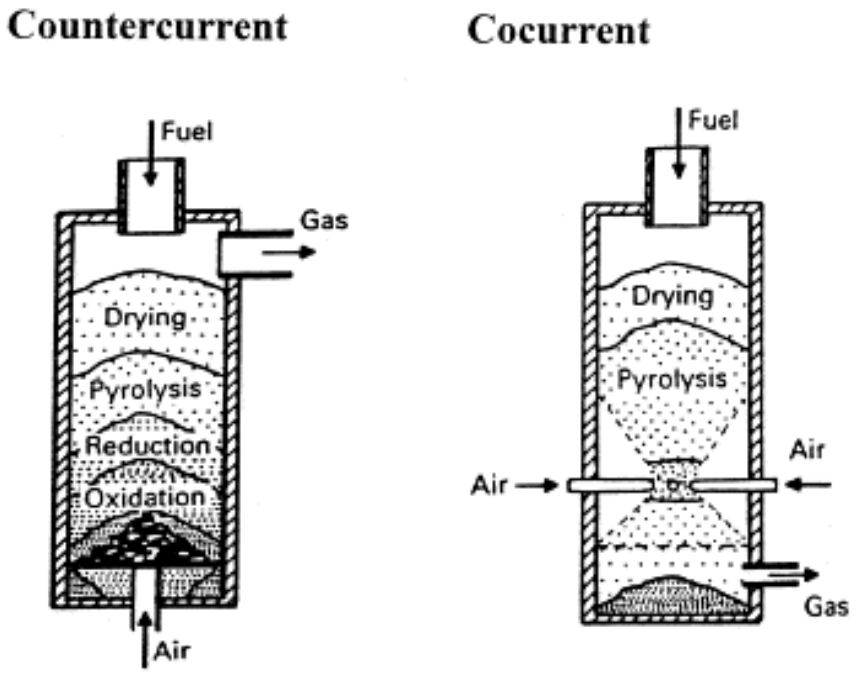

Figure 1.12 Fixed bed reactors [46].

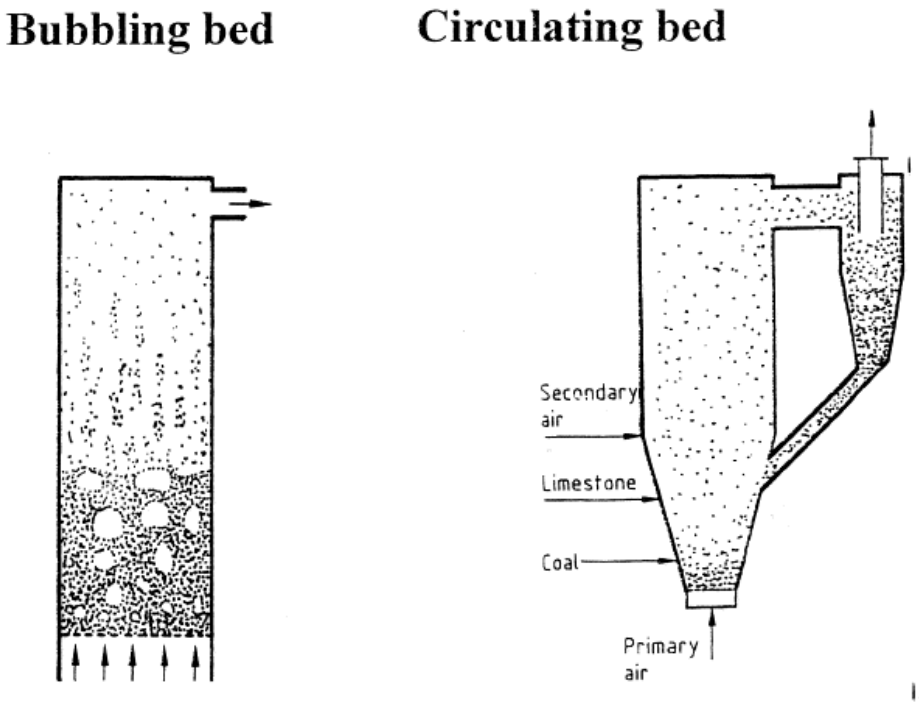

Figure 1.13 Fluidized bed reactors [46].

1.4 Research motivations

Biomass feedstock usually used in commercial applications has relatively large particle size such as that of wood chips and wood pellets [47], because biomass materials unlike pulverized coal cannot be economically processed into fine sizes. Wood pellets measure 6–8 mm in diameter according to Swedish standards [48]. Typical wood chips vary in size from 10×10×5 mm to 15×15×8 mm [49]. Characteristics of pyrolysis and gasification of large biomass particle are different from those of fine particles due to differences in intraparticle mass and heat transfer.

For pyrolysis characteristic, tar reduction in the aspect of intraparticle tar decomposition is focused because tar is an undesirable product from the primary reaction of pyrolysis. Tar formation and condensation in gasification systems leads to blockage of pipeline and adherent tar on turbine blades or heat exchangers. Therefore, tar removal process is needed to be equipped downstream the gasifier to treat the hot gas product. This removal process, which may either done by chemical or physical methods, requires additional costs. However, using large biomass in gasifiers, it may show an advantage in term of tar reduction because large biomass particles may provide a sufficient residence time for tar cracking reactions inside the particles so-called intraparticle tar decomposition. Therefore, the intraparticle tar decomposition has a potential to improve tar reduction in biomass gasification without any additional tar removal process.

For gasification characteristic, the role of anisotropic structure of wood-derived char in gasification process is focused. It is known that woody biomass has an anisotropic structure, leading to its anisotropic properties such as gas permeability. However, little effort has been made to study the effect of anisotropic stricture on gasification. Many researchers [50-54] studied char gasification as well as its reactivity using fine particles of which the anisotropic properties seem to be neglected. Char reactivity is an important parameter because it is the slowest process in gasification [55]. Char reactivity is strongly influenced by its chemical properties, and physical properties such as particle size and pore structure [55, 56]. Therefore, the anisotropic structure of large char particle is expected to play an important role in gasification process, especially in char reactivity as well as gas diffusion into the particle.

1.5 Outline of this thesis

This thesis focuses on the clarification of intraparticle reactions of tar during wood pyrolysis and the investigation of gasification characteristics of wood-derived char with anisotropic structure.

In Chapter 2, intraparticle secondary reactions of tar during pyrolysis process were experimentally investigated. Pyrolysis products (gas, char, and tar) derived from the fine and large wood particle, which represented by sawdust (< 1 mm) and wood cylinder (L 9 mm × Ø 8 mm), were measured. A comparison of sawdust and wood cylinder at specified pyrolysis conditions revealed intraparticle secondary reactions. Products of intraparticle secondary reactions, their reaction temperature, and the act of char as a catalyst for tar decomposition were clarified. A mechanism diagram of intraparticle secondary reactions of tar at both low and high heating rate was also shown.

In Chapter 3, the experimental investigation of gasification characteristic of large wood cylinder with anisotropic structure was performed. The sawdust and wood cylinder (Ø 8 mm) with various lengths were used as samples. For pyrolysis characteristics, the effect of intraparticle secondary reactions of tar on pyrolysis products was confirmed. Scanning electron microscopy (SEM) and X-ray computed tomography (CT) were used to visualize the anisotropic structure of wood-derived char. Quantitative measurement of pore size and shape was made using a digital image analysis. For gasification characteristics, the Arrhenius plot of char reactivity and the evolution of particle shape for the large chars during the gasification were discussed to indicate the importance of pore diffusion and anisotropic structure. Moreover, effects of pyrolysis heating rate on pyrolysis products, char morphology, and char reactivity during the gasification were also studied.

In Chapter 4, the influence of particle aspect ratio on gasification reactivity of anisotropic char was further investigated. Wood cylinders with three particle aspect ratios were pyrolyzed to produce char samples. The 3D X-ray CT image of char structure was shown. The reactivity of char samples was measured at various temperatures. The Arrhenius plot of char reactivity was made to discuss the effect of particle aspect ratio on the char reactivity.

In Charter 5, overall conclusions were drawn from the important results and findings in this research. Moreover, the contribution to this research field was also discussed.

References

[1] D. Klass, Biomass for renewable energy, fuels, and chemicals, Entech International, Inc., 1998.

[2] S. Shafiee, E. Topal, When will fossil fuel reserves be diminished?, Energy Policy, 37 (2009) 181-189.

[3] J.F.B. Mitchell, The "greenhouse" effect and climate change, Reviews of Geophysics 27 (1989) 115-139.

[4] B. Metz, O.R. Davidson, P.R. Bosch, R. Dave, L.A.M. (eds), Contribution of Working Group III to the Fourth Assessment Report of the Intergovernmental Panel on Climate Change, 2007, in.

[5] V. Ramanathan, Greenhouse Effect Due to Chlorofluorocarbons: Climatic Implications, Science, 190 50-51.

[6] Jeffrey J. Lee, Grady E. Neely, Shelton C. Perrigan, L.C. Grothaus., Effect of simulated sulfuric acid rain on yield, growth and foliar injury of several crops, Environmental and Experimental Botany, 21 (1981) 171-185.

[7] R.K. Pachauri, A.E. Reisinger, Climate Change 2007: Synthesis Report, 2007.

[8] BP Statistical Review of World Energy, British Petroleum, 2009.

[9] BP Statistical Review of World Energy, British Petroleum, 2013.

[10] Focus on clean coal, International Energy Agency, 2006.

[11] Clean Coal Technologies in Japan, Next-generation, High-efficiency Integrated Coal Gasification Electric Power Generating Process (A-IGCC/A-IGFC), in, JCOAL.

[12] World energy resources 2013 Survey: Summary, World energy council, 2013.

[13] B.K. Sovacool, Valuing the greenhouse gas emissions from nuclear power: A critical survey, Energy Policy, 36 (2008) 2950-2963.

[14] Renewables 2013 Global Status Report, REN21, 2013.

[15] How 2 guide for wind energy, International Energy Agency, 2014.

[16] Wind force 12, Greenpeace, 2005.

[17] Solar Energy Perspectives, in, International Energy Agency, 2011.

[18] D.L. Klass, Biomass for renewable energy and fuels, in: Encyclopedia of Energy, 2004, pp. 193-212.

[19] D. Mohan, J. Charles U. Pittman, P.H. Steele, Pyrolysis of Wood/Biomass for Bio-oil: A Critical Review, Energy & Fuels, 20 (2006) 848-889.

[20] R.C. Pettersen, The chemical composition of wood, American Chemical Society, Washington DC 1984
[21] P. McKendry, Energy production from biomass (part 1): overview of biomass, Bioresource technology, 83 (2002) 37–46.
[22] A.V. Bridgwater, Biomass fast pyrolysis, Thermal science, 8 (2004) 21 - 49.
[23] Y. Chhiti, S. Salvador, J.-M. Commandré, F. Broust, Thermal decomposition of bio-oil: Focus on the products yields under different pyrolysis conditions, Fuel, 102 (2012) 274-281.
[24] K. Raveendran, A. Ganesh, K.C. Khilart, Influence of mineral matter on biomass pyrolysis characteristics, Fuel 74 (1995) 1812-1822.
[25] P. Nanou, H.E. Gutiérrez Murillo, W.P.M. van Swaaij, G. van Rossum, S.R.A. Kersten, Intrinsic reactivity of biomass-derived char under steam gasification conditions-potential of wood ash as catalyst, Chemical Engineering Journal, 217 (2013) 289-299.
[26] P. Quaak, H. Knoef, H.E. Stassen, Energy from Biomass: A Review of Combustion and Gasification Technologies, World Bank Publications, 1999.
[27] P. Basu, Biomass Gasification, Pyrolysis and Torrefaction: Practical Design and Theory, Academic Press, 2010.
[28] A. Demirbaş, Sustainable cofiring of biomass with coal, Energy Conversion and Management, 44 (2003) 1465-1479.
[29] H. Spliethoff, K.R.G. Hein, Effect of co-combustion of biomass on emissions in pulverized fuel furnaces, Fuel Processing Technology, 54 (1998) 189-205.
[30] B. Damstedt, J.M. Pederson, D. Hansen, T. Knighton, J. Jones, C. Christensen, L. Baxter, D. Tree, Biomass cofiring impacts on flame structure and emissions, Proceedings of the Combustion Institute, 31 (2007) 2813-2820.
[31] H. Emmons, A. Atreya, The science of wood combustion, Proc. Indian Acad. Sci. (Engg. Sci.), 5 (1982) 259-268.
[32] THe Asian Biomass Handbook, The Japan Institute of Energy, 2008.
[33] J. Rezaiyan, N.P. Cheremisinoff, Gasification Technologies: A Primer for Engineers and Scientists, Taylor & Francis, 2005.
[34] B.V. Babu, Biomass pyrolysis: a state-of-the-art review, Biofuels, Bioproducts and Biorefining, 2 (2008) 393-414.
[35] C. Di Blasi, Modeling chemical and physical processes of wood and biomass pyrolysis, Progress in Energy and Combustion Science, 34 (2008) 47-90.

[36] C. Di Blasi, Modeling intra- and extra-particle processes of wood fast pyrolysis, AIChE Journal, 48 (2002) 2386-2397.
[37] K.M. Bryden, K.W. Ragland, C.J. Rutland, Modeling thermally thick pyrolysis of wood, Biomass and Bioenergy, 22 (2002) 41-53.
[38] D.K. Shen, M.X. Fang, Z.Y. Luo, K.F. Cen, Modeling pyrolysis of wet wood under external heat flux, Fire Safety Journal, 42 (2007) 210-217.
[39] N. Bech, M.B. Larsen, P.A. Jensen, K. Dam-Johansen, Modelling solid-convective flash pyrolysis of straw and wood in the Pyrolysis Centrifuge Reactor, Biomass and Bioenergy, 33 (2009) 999-1011.
[40] W.C. Park, A. Atreya, H.R. Baum, Experimental and theoretical investigation of heat and mass transfer processes during wood pyrolysis, Combustion and Flame, 157 (2010) 481-494.
[41] B.V. Babu, A.S. Chaurasia, Modeling for pyrolysis of solid particle: kinetics and heat transfer effects, Energy Conversion and Management, 44 (2003) 2251-2275.
[42] C. Di Blasi, Heat, momentum and mass transport through a shrinking biomass particle exposed to thermal radiation, Chemical Engineering Science, 51 (1996) 1121-1132.
[43] E. Ranzi, A. Cuoci, T. Faravelli, A. Frassoldati, G. Migliavacca, S. Pierucci, S. Sommariva, Chemical Kinetics of Biomass Pyrolysis, Energy & Fuels, 22 (2008) 4292-4300.
[44] C. Dupont, L. Chen, J. Cances, J.-M. Commandre, A. Cuoci, S. Pierucci, E. Ranzi, Biomass pyrolysis: Kinetic modelling and experimental validation under high temperature and flash heating rate conditions, Journal of Analytical and Applied Pyrolysis, 85 (2009) 260-267.
[45] A. Demirbas, Pyrolysis of ground beech wood in irregular heating rate conditions, Journal of Analytical and Applied Pyrolysis, 73 (2005) 39-43.
[46] R. Warnecke, Gasification of biomass: comparison of fixed bed and fluidized bed gasifier, Biomass and Bioenergy, 18 (2000) 489-497.
[47] Y.B. Yang, V.N. Sharifi, J. Swithenbank, L. Ma, L.I. Darvell, J.M. Jones, M. Pourkashanian, A. Williams, Combustion of a Single Particle of Biomass, Energy & Fuels, 22 (2007) 306-316.
[48] M. Ståhl, K. Granström, J. Berghel, R. Renström, Industrial processes for biomass drying and their effects on the quality properties of wood pellets, Biomass and Bioenergy, 27 (2004) 621-628.

[49] R. Abdallah, S. Auchet, P.J. Méausoone, Experimental study about the effects of disc chipper settings on the distribution of wood chip size, Biomass and Bioenergy, 35 (2011) 843-852.
[50] E. Cetin, B. Moghtaderi, R. Gupta, T.F. Wall, Influence of pyrolysis conditions on the structure and gasification reactivity of biomass chars, Fuel, 83 (2004) 2139-2150.
[51] Y. Okumura, T. Hanaoka, K. Sakanishi, Effect of pyrolysis conditions on gasification reactivity of woody biomass-derived char, Proceedings of the Combustion Institute, 32 (2009) 2013-2020.
[52] L. Lu, C. Kong, V. Sahajwalla, D. Harris, Char structural ordering during pyrolysis and combustion and its influence on char reactivity, Fuel, 81 (2002) 1215-1225.
[53] H.-S. Shim, M.R. Hajaligol, V.L. Baliga, Oxidation behavior of biomass chars: pectin and Populus deltoides, Fuel, 83 (2004) 1495-1503.
[54] C. Di Blasi, F. Buonanno, C. Branca, Reactivities of some biomass chars in air, Carbon, 37 (1999) 1227-1238.
[55] S. Link, S. Arvelakis, M. Hupa, P. Yrjas, I. Külaots, A. Paist, Reactivity of the Biomass Chars Originating from Reed, Douglas Fir, and Pine, Energy & Fuels, 24 (2010) 6533-6539.
[56] I.W. Smith, The combustion rates of coal chars: A review, Symposium (International) on Combustion, 19 (1982) 1045-1065.

CHAPTER 2

Intraparticle Secondary Reactions of Tar during Wood Pyrolysis

This chapter is an adaptation of the published article: Teeranai Pattanotai, Hirotatsu Watanabe, and Ken Okazaki. Experimental investigation of intraparticle secondary reactions of tar during wood pyrolysis. Fuel 2013;104:468–475.

Abstract

This chapter presents the experimental investigation of intraparticle secondary reactions of tar during the pyrolysis of woody biomass. For this, pyrolysis products (gas, char, and tar) derived from Japanese cypress sawdust (particle size < 1 mm) and Japanese cypress wood cylinders (8 mm in diameter and 9 mm long) were compared. The samples were pyrolyzed in a thermobalance under argon atmosphere. The final reactor temperature was 600°C, and the heating rate was 0.5 K/s. Under these conditions, the difference between the sawdust and wood cylinder is the intraparticle secondary reactions of tar. The tar yield of the wood cylinder decreases, whereas its total gas and char yields increase when compared with those of the sawdust. These results indicate that intraparticle secondary reactions of tar, which include intraparticle tar decomposition to form gases and polymerization to form char, occur during the pyrolysis of the wood cylinder. It is found that the intraparticle tar decomposition progresses between 400 and 500°C, which is lower than the homogeneous cracking temperature of tar. This observation suggests that the intraparticle tar decomposition can occur heterogeneously on the surface of the microporous char which acts as a catalyst. This study shows that the intraparticle secondary reactions of tar play an important role in the pyrolysis of large wood particles. Moreover, these reactions have the potential to achieve tar reduction in biomass gasification without any additional tar removal process.

2.1 Introduction

Biomass, especially wood, is expected to be developed as a renewable energy resource to deal with global warming and the depletion of fossil fuels. Biomass is a carbon neutral fuel and hence it differs from fossil fuels [1,2]; moreover, it may offer additional advantages of low sulfur and nitrogen content [2,3]. Biomass can be converted to energy forms through various processes, such as thermochemical conversion and biochemical conversion. Gasification and pyrolysis are the most promising thermochemical conversion processes [4]. The energy efficiency of gasification is higher than that of combustion [2,5]. The primary reaction of gasification is pyrolysis, which produces three main products: gas, char, and tar. However, tar is an undesirable product that causes many operational difficulties in biomass gasifiers. Tar formation and condensation in a gasification system lead to blockage and foul of process equipment such as engines and turbines [2,6,7]. Therefore, many researchers have been developing technologies for controlling or suppressing the tar formation during biomass pyrolysis [8–10].

When biomass is pyrolyzed, volatile matter, which includes several tar and gas species, is released by thermal scission of chemical bonds; char is also formed. These reactions are considered as the primary reactions of pyrolysis. Next, a portion of the tar undergoes secondary reactions consisting of its decomposition to secondary gas and secondary tar, and polymerization to secondary char. Secondary tar decomposition may occur homogeneously in the vapor phase and heterogeneously on the surfaces of the pyrolyzing solid or other beds. Moreover, secondary tar decomposition can also occur within (intraparticle) or outside (extraparticle) the biomass particles [11,12]. Extraparticle tar decomposition reactions include homogeneous vapor phase cracking and heterogeneous conversion over the surface of the char or other beds. Boroson et al. [13] studied the homogeneous vapor phase cracking of wood pyrolysis tar using a two-stage reactor and reported 5–88% tar conversions at temperatures of 773–1,073 K with residence times of 0.9–2.2 s.

The biomass feedstock used in commercial gasifiers has a relatively large particle size such as that of woodchips and wood pellets, because biomass materials unlike pulverized coal cannot be economically processed into fine sizes. Wood pellets measure 6–8 mm in diameter according to Swedish standards [14]. During the

pyrolysis of large biomass particles, it was frequently mentioned that intraparticle secondary reactions, including intraparticle tar decomposition, are significant and affect product yields [11,15]. Large biomass particles may provide sufficient residence time for tar cracking reactions inside the particles. Thus, tar may be cracked during transport in the pores of large biomass particles or the char layer. Many researchers have reported positive effects of biomass char on the tar cracking reaction in a two-stage reactor [3,16–20]. However, there is little information and evidence regarding intraparticle secondary reactions of tar. We recently investigated intraparticle tar decomposition experimentally and numerically [21]. A calculation in our previous research indicated the possibility of intraparticle tar decomposition; however, this calculation did not consider heterogeneous reactions because their kinetic parameters were not available. In addition, the gas species produced through intraparticle tar decomposition have not been clarified. Further experimental studies should be conducted to investigate the intraparticle secondary reactions of tar.

In the pyrolysis of fine biomass particles, these reactions are negligible because of the short residence time of the travelling tar inside the particle. A simulation conducted by Di Blasi [11] showed that in small particles (less than 6 mm), intraparticle degradation of tar is negligible. Bryden and Hagge [22] reported that char does not provide additional holding time within the particles for secondary pyrolysis reactions in thermally thin particles (Biot number < 0.2). The characteristics of intraparticle secondary reactions of tar can be clarified according to the differences in such reactions between fine and large biomass particles by comparing the yields of pyrolysis products between fine and large particles.

The purpose of this study is to clarify intraparticle secondary reactions of tar experimentally by comparing the yields of pyrolysis products between the sawdust and wood cylinder, which represent fine and large biomass particles, respectively. Pyrolysis characteristics of both the samples under our experimental conditions were investigated by examining the temperature distribution of biomass particles, ultimate analysis of chars, and the weight fraction histories. Next, we discussed the effects of intraparticle secondary reactions of tar on the product yields and the reaction temperature.

2.2 Experimental

2.2.1 Wood samples

The samples used in this study were Japanese cypress sawdust and Japanese cypress wood cylinders. Photographs of wood samples are shown in Figure 2.1. The properties of Japanese cypress wood (trunk) are shown in Table 2.1. The wood cylinder was milled and then sieved to produce sawdust with particles less than 1 mm in size. The initial weight of the sawdust for each experiment was approximately 50 mg. The wood cylinder had a diameter of 8 mm, length of 9 mm, and initial weight of approximately 180 mg.

2.2.2 Pyrolysis experiments

Figure 2.2 shows a schematic diagram of the experimental apparatus that consists of a gas supply system, thermobalance (ULVAC TGD-9600), tar trap, and gas sampling bag. Photograph of the thermobalance with infrared furnace is shown in Figure 2.3. Pyrolysis experiments on the sawdust and wood cylinder were performed in the thermobalance. A sample was placed in a platinum crucible on a thermocouple (thermometric point). The height of the sawdust sample in the crucible was approximately 4 mm at which secondary tar decomposition on the char surface of other sawdust particles can be neglected [18]. Air inside the experimental setup was purged by a vacuum pump and then replaced by argon. Before pyrolysis, both the sawdust and wood cylinder samples were dried at 110°C for 10 min. This drying period was long enough to dry both samples. Then, pyrolysis was performed at a heating rate of 0.5 K/s in an argon atmosphere flowing at 0.3 l/min. The heating rate was controlled at the thermometric point. Argon was used to sweep volatile matter from the reaction zone in order to prevent extraparticle reactions, which include secondary tar decomposition in the vapor phase. A calculation using the kinetic mechanism and parameters proposed by Boroson et al. [13] showed that extraparticle tar decomposition in the gas phase can be neglected in our experiment. The wood samples were heated at a constant rate to a final temperature of 600°C measured at the thermometric point and were held at this temperature for 5 min. Pyrolysis conditions were summarized in Table 2.2. Tar was collected by an ice-cold trap containing a glass fiber filter (GC-90, ADVANTEC) downstream of the reactor, and the total weight of the trapped tar was measured after pyrolysis was complete. The

weight change of the downstream tube was measured after experiment to determine an amount of tar depositing in the tube. In this study, tar is defined as condensable compounds attached to the filter in the tar trap and inside the downstream tube. Residual matter from the samples in the crucible was considered to be char and it was weighed after pyrolysis was complete. The final product yields shown in this paper were average from three repeated experiments, and the error bars which indicate 95% confidence intervals were also shown.

2.2.3 Measurements within wood cylinder

The temperature within the wood cylinder was measured in the radial direction at three locations: the center (r = 0 mm), an intermediate position (r = 1 mm), and an outer position (r = 2 mm), at a depth of 6 mm from the top of the cylinder using *K*-type thermocouples with a diameter of 0.5 mm. These thermocouples were inserted through holes drilled into the wood cylinder. Figure 2.4 shows the installation of thermocouples inside the wood cylinder. Temperature data were acquired at intervals of 500 ms using a data logger (MEMORY HiLOGGER 8430, Hioki Corp.) during the entire pyrolysis process. To investigate intraparticle secondary reactions of tar by comparing the product yields obtained from the pyrolysis of the sawdust and wood cylinder, the particle temperatures within both the samples should be identical during pyrolysis. This is because the particle temperature is the main parameter controlling the primary reactions of pyrolysis. However, thermal conductivity of wood is generally low [23], and spatial temperature gradients are easily formed in large wood cylinders. To realize the same particle temperature for both the samples and a uniform temperature distribution within the wood cylinder, a low heating rate of 0.5 K/s was used for pyrolysis. When particles within both the samples undergo pyrolysis at the same temperature, the difference between pyrolysis in the sawdust and wood cylinder is the intraparticle secondary reactions of tar. Therefore, the characteristics of these reactions could be studied by comparing the product yields between both the samples.

The ultimate analysis of chars along a radial direction at various temperatures was conducted. The char samples were produced at heating rate of 0.5 K/s with different final temperatures of 400, 500, and 600°C. It was noted that when the final temperature was higher than 400°C, char diameter became about 6 mm due to the

shrinkage. Therefore, each char sample was divided into three parts along the radial direction by about 2 mm: the center, an outer part, and an outermost part as shown in Figure 2.5.

2.2.4 Gas analysis and determination

The product gas passing through the tar trap was collected in a gas sampling bag during the entire pyrolysis process. The total volume of the collected gas was measured by a wet gas flow meter. The product gas in the sampling bag was then analyzed by gas chromatography (GC-8A, Shimadzu Corp.) with a thermal conductivity detector (TCD) with ShinCarbon ST column and a flame ionization detector (FID) with Porapack-Q column. Settings of gas chromatographs were listed in Table 2.3. The concentration of each gas was converted to the yield in terms of the initial weight of the solid samples.

2.2.5 Tar and gas release histories

The tar and gas release histories, which reveal the cumulative yields of tar and gas along the applied temperature history, were investigated to indicate the temperature at which the intraparticle secondary reactions occur. Tar and gas yields were obtained for the pyrolysis of each sample with final temperatures of 200, 300, 400, 500, and 600°C at a heating rate of 0.5 K/s. Each measurement was separately performed. When the final temperature was reached, the process was terminated without a holding time. The experimental procedure and method of collecting tar and gaseous products are those as explained above.

Table 2.1 Proximate and ultimate analyses of Japanese cypress wood (trunk).

Proximate analysis (wt%)	
Volatile matter	78.7
Fixed carbon	13.2
Ash	0.2
Moisture	7.9
Ultimate analysis (wt%, daf)	
C	51.5
H	6.2
O	42.2
N	0.1
S	–

Table 2.2 Pyrolysis conditions.

Heating rate (K/s)	0.5
Final temperature (°C)	600
Holding time (min)	5
Ar flow rate (l/min)	0.3
Pressure (MPa)	0.1

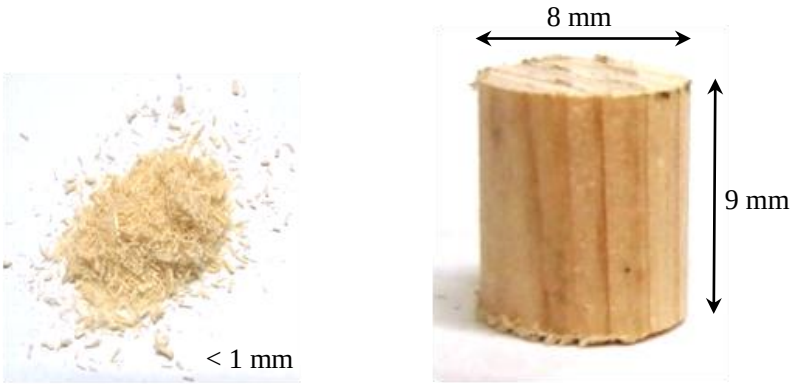

(a) Sawdust (b) Wood cylinder

Figure 2.1 Photographs of wood samples: (a) sawdust and (b) wood cylinder.

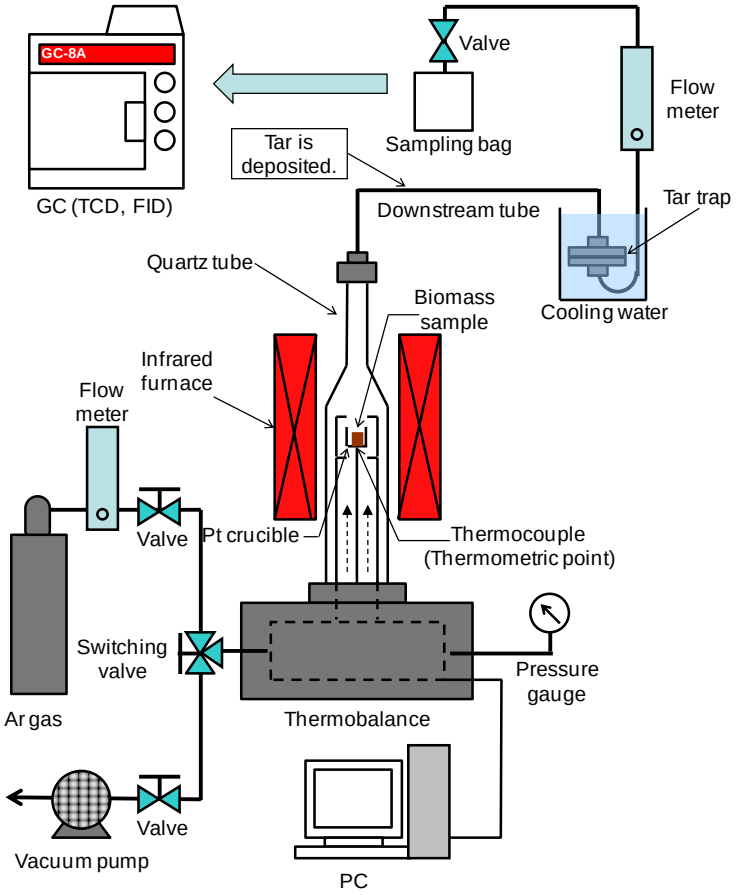

Figure 2.2 Schematic diagram of experimental apparatus with GC analysis.

Figure 2.3 Photograph of the thermobalance with infrared gold image furnace.

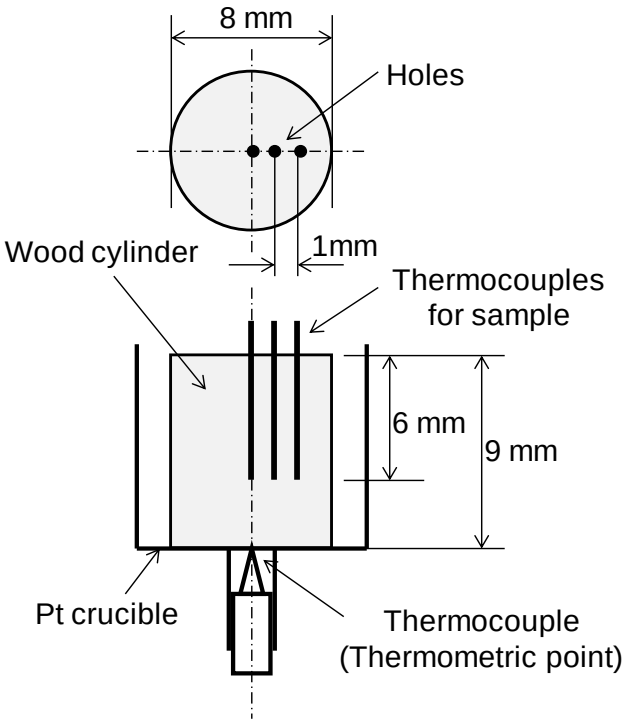

Figure 2.4 Installation of thermocouples inside the wood cylinder.

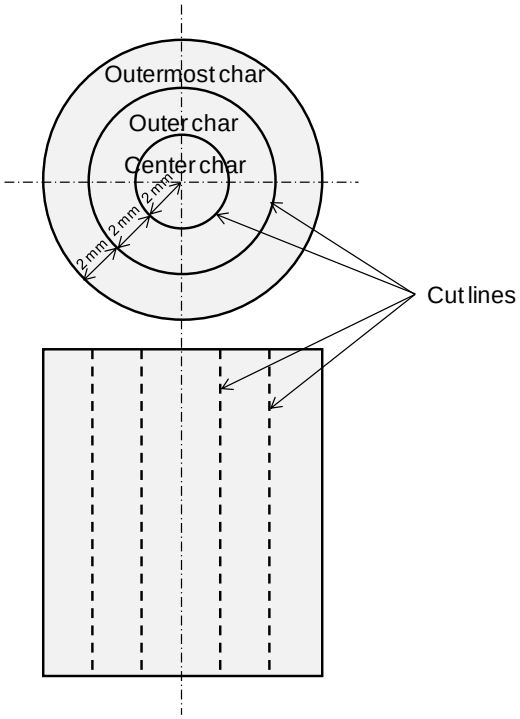

Figure 2.5 Cutting profile of chars for ultimate analysis

Table 2.3 Settings of gas chromatographs.

GC-TCD	
Column	ShinCarbon ST
Carrier gas	Ar
Primary pressure (kPa)	600
Carrier gas pressure (kPa]	140
Injection/detector temperature (°C)	100
Column temperature (°C)	50
Current (mA)	80
Attenuation	2
Analyzed gas	H_2, O_2, N_2, CH_4, CO, CO_2
GC-FID	
Column	Polapack-Q
Carrier gas	N_2
Primary pressure (kPa)	600
Carrier gas pressure (kPa)	120
Hydrogen pressure (kPa)	60
Air pressure (kPa)	50
Injection/detector temperature (°C)	150
Column temperature, initial (°C)	60
Column temperature, final (°C)	120
Range	10^2
Attenuation	2
Analyzed gas	CO, CH_4, CO_2, C_2H_4, C_2H_6, C_3H_8

2.3 Results and discussion

2.3.1 Pyrolysis characteristics

Figure 2.6 shows the temperature histories measured at three locations within the wood cylinder during pyrolysis at a heating rate of 0.5 K/s. The temperatures at these three locations in the radial direction did not differ during pyrolysis. The thermal conductivity of wood across the grain (radial direction) is approximately one-third of that along the grain (axial direction) [24]. Thus, the temperatures along the axial direction should also be uniform, which implies that the temperature of particles within the entire wood cylinder is uniform. Moreover, the temperature of the sawdust sample, which is much shorter than that of the wood cylinder, is also expected to be uniform. Thus, the temperature gradient effect is negligible at this heating rate when we compare the yields of pyrolysis products of both the samples.

Figure 2.7 shows the ultimate analysis of chars along the radial direction at different temperatures. With increasing temperature, carbon element increased, indicating the progress of carbonization. However, the differences in all chemical elements along the radial direction were negligible (less than 1%) at each temperature. This result shows the uniformity of pyrolysis characteristic of wood cylinder during the pyrolysis at heating rate of 0.5 K/s.

Figure 2.8a shows a comparison between the weight fraction histories of the sawdust and wood cylinder, and the thermometric temperature. Both weight fraction histories show that the pyrolysis of Japanese cypress wood starts at approximately 250°C and proceeds rapidly at 300–400°C. The weight loss of both the samples becomes relatively slow at temperatures above approximately 400°C. At temperatures below 380°C, there is no significant difference between the weight fraction histories of the sawdust and wood cylinder. During this period, the total yield of volatile matter released from the wood cylinder is almost the same as that from the sawdust. This indicates that the primary reactions producing primary tar, primary gas, and primary char for both the samples are almost the same at a heating rate of 0.5 K/s. The difference in weight fraction histories between both the samples above 380°C is shown in Figure 2.8b (magnified figure). It indicates that significant polymerization of tar (intraparticle secondary reactions) to form char occurs at temperatures of approximately 380–400°C.

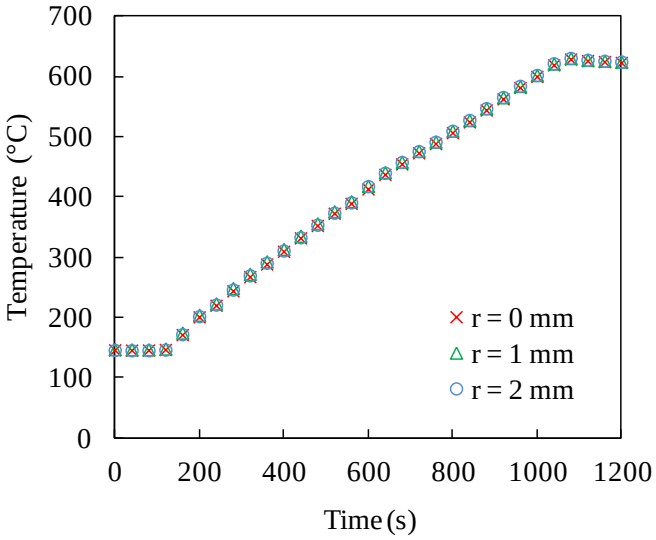

Figure 2.6 Temperature histories at three locations within the wood cylinder during pyrolysis at a heating rate of 0.5 K/s.

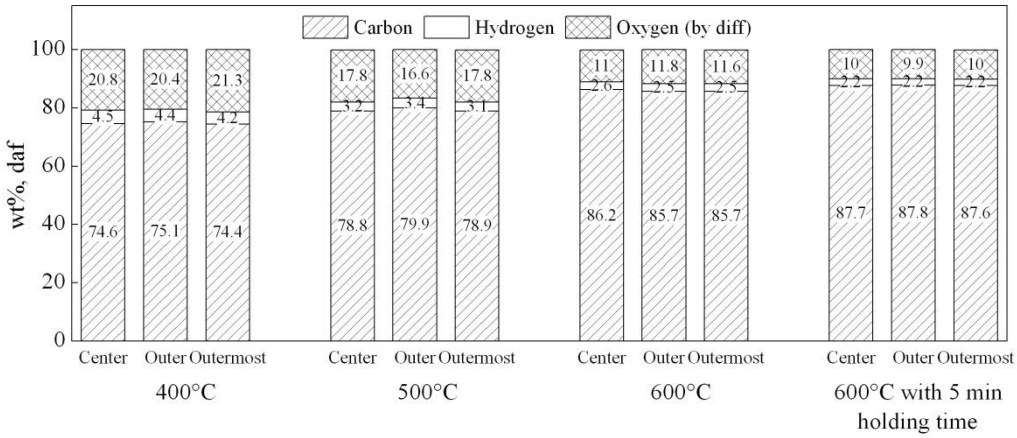

Figure 2.7 Ultimate analysis of chars along a radial direction at various temperatures.

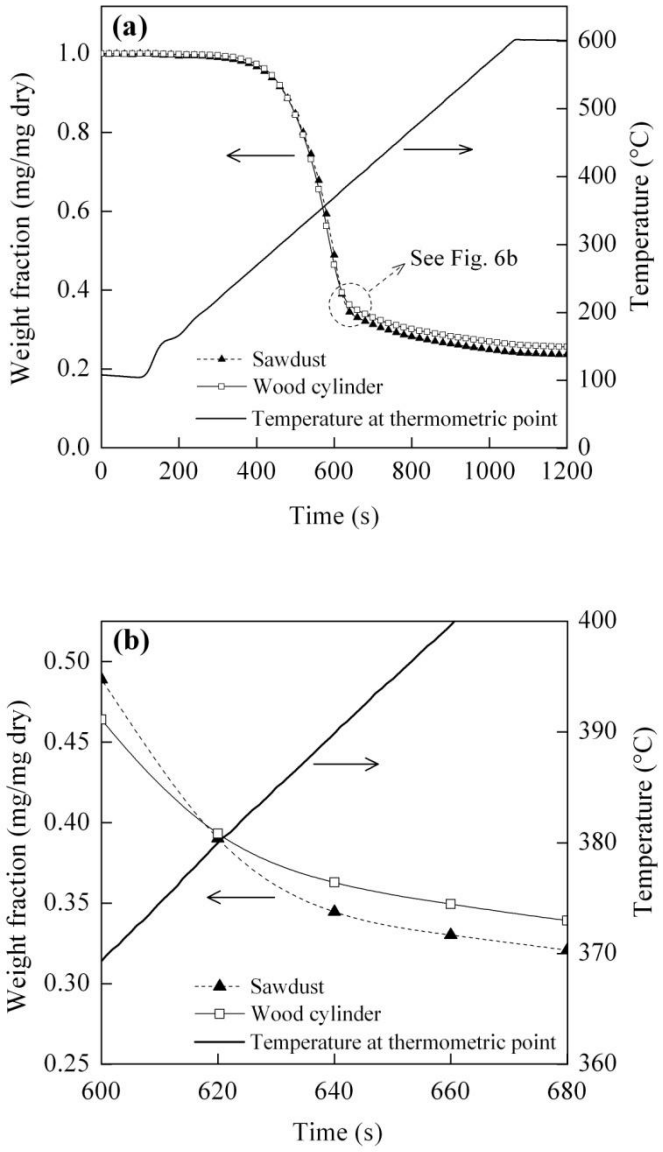

Figure 2.8 Weight fraction histories of the sawdust and wood cylinder, along with the thermometric temperature: (a) for entire pyrolysis and (b) for 600–680 s.

2.3.2 Investigation of intraparticle secondary reactions of tar

Figure 2.9 shows the total tar and char yields obtained from the pyrolysis of the sawdust and wood cylinder. The total tar yield of the wood cylinder was 4.9 wt% lower than that of the sawdust. However, the total char yield of the wood cylinder was 2.7 wt% higher than that of the sawdust. Figure 2.10 shows the yields of individual gaseous products and the total gas yields. The product gas from both the samples consisted of H_2, CH_4, CO, and CO_2. The wood cylinder yielded more CH_4, CO, and CO_2 than that yielded by the sawdust. The total gas yield of the wood cylinder was 1.4 wt% higher than that of the sawdust, mostly owing to a higher CO yield. When compared to the sawdust result, the sum of the increased yields in char and gaseous products of wood cylinder was approximately 84% of the decreased yield in tar. The increased yield in char and gaseous products accounted for approximately 55% and 29% of the decreased tar yield, respectively. Figure 2.11 shows the total product yields of sawdust and wood cylinder. The total yields for both samples were almost the same, which was approximately 81%. This result suggests that some undetectable chemical species in the gas chromatographs are produced in this experiment.

Because the primary reactions in the sawdust and wood cylinder are the same, as discussed above, the yields of the primary products, gas, tar, and char, obtained from both the samples were expected to be the same. However, the product yields measured from each sample after pyrolysis were different. These results indicate that secondary reactions of tar occur in the pyrolysis of the wood cylinder, causing differences in product yields. Nevertheless, extraparticle tar decomposition did not proceed in this experiment because of the very short residence time, as mentioned above. Therefore, the secondary reactions of tar that occurred in the wood cylinder are classified as intraparticle reactions. Our previous research showed further tar reduction by the intraparticle reactions is achievable with increasing heating rate and biomass size [21,25]. The experiments with high heating rate of 30 K/s was discussed in Section 2.3.4. In this study, however, we used low heating rate to make intraparticle temperature uniform for clarifying the intraparticle mechanisms.

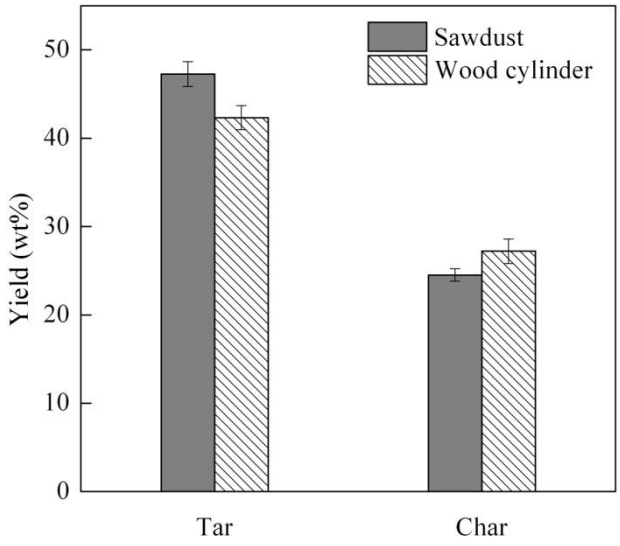

Figure 2.9 Total tar and char yields for the sawdust and wood cylinder. Error bars indicate 95% confidence intervals.

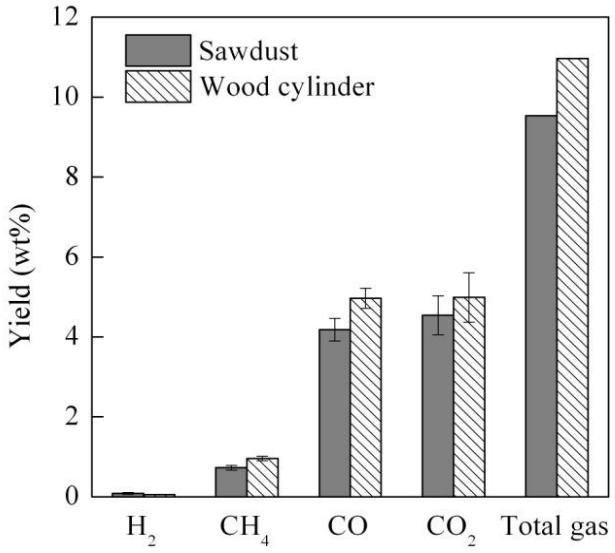

Figure 2.10 Each and total gas yields for the sawdust and wood cylinder. Total gas yield is the sum of the average values of H_2, CH_4, CO, and CO_2. Error bars indicate 95% confidence intervals.

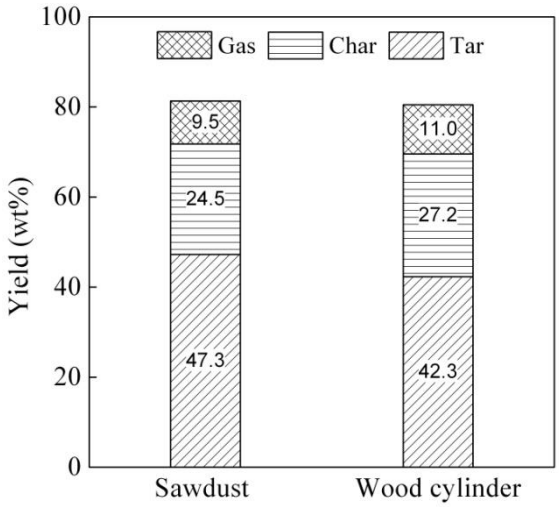

Figure 2.11 Total product yields for the sawdust and wood cylinder.

2.3.3 Tar and gas release histories

Figure 2.12 shows the tar and gas release histories during the pyrolysis of the sawdust and wood cylinder, and the thermometric temperature. Both the samples showed the same cumulative yields of tar and gaseous products in the range of 200–400°C. This trend agrees well with the weight fraction histories (Figure 2.8a), which represent the primary reactions during pyrolysis. The result confirms that intraparticle secondary reactions of tar do not proceed at temperatures below 400°C. Tar formation begins at 200–300°C and then proceeds rapidly at 300–400°C. CO_2 formation also begins at 200–300°C, and CO formation at 300–400°C. CH_4 is produced at relatively high temperatures of approximately 400–500°C. At temperatures above 400°C, differences in the tar and gas yields of the two samples are observed. At 400–500°C, the tar yield of the wood cylinder was less than that of the sawdust; however, the yields of CH_4 and CO were greater. The cumulative yields of CO_2 were almost the same in both the samples during pyrolysis. These results indicate that the primary tar formed at 400–500°C in the wood cylinder is decomposed, and mainly CO is produced through intraparticle tar decomposition (intraparticle secondary reactions). This implies that intraparticle tar decomposition can occur at approximately 400°C.

Thermal cracking of tar in the gas phase (homogeneous reaction) reportedly occurs primarily at temperatures above 600–700°C [5,13]. However, tar decomposition has occurred at approximately 400°C in this study. This result supports the suggestion that intraparticle tar decomposition includes heterogeneous reactions on the surface of microporous char as well as homogeneous reactions. Thus, char acts as a catalyst for tar decomposition. Boroson et al. [3] studied the heterogeneous cracking of wood pyrolysis tar on char surfaces using a two-stage reactor and reported that a significant heterogeneous cracking of tar over the char surfaces was observed at temperatures above 400°C. His evaluation is in good agreement with our experimental result.

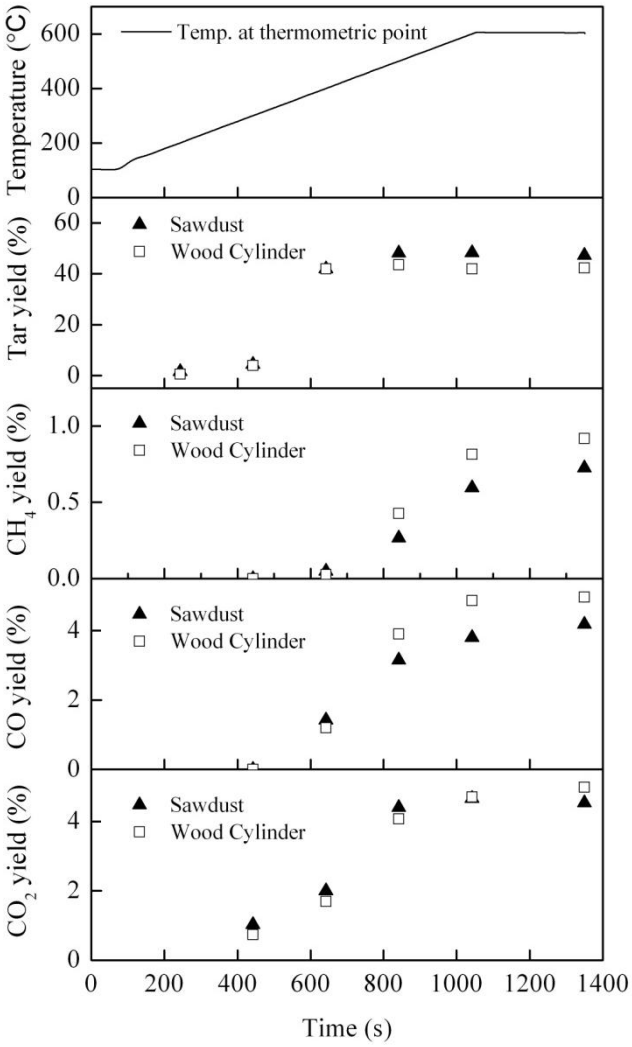

Figure 2.12 Tar and gas release histories of the sawdust and wood cylinder along with the thermometric temperature.

2.3.4 Pyrolysis experiment with high heating rate

In this section, the pyrolysis experiment was also performed at heating rate of 30 K/s. Other conditions, except for heating rate, were the same as described in the section 2.2.2. Figure 2.13 shows temperature histories at three locations within the wood cylinder during pyrolysis at a heating rate of 30 K/s. It is seen that the temperature gradient appears within the wood cylinder during the pyrolysis at the high heating rate. Figure 2.14 shows total tar and char yields obtained from the pyrolysis of the sawdust and wood cylinder at heating rate of 30 K/s. The tar yield of wood cylinder is significantly less than that of sawdust approximately 14% due to intra-particle tar decomposition, whereas a significant difference of the char yield is not observed. Figure 2.15 shows the yields of individual gaseous products and the total gas yields obtained at high rate of 30 K/s. An increase approximately 9% in total gas yield from wood cylinder pyrolysis is observed. Carbon monoxide is seemed to be the major product from intra-particle tar decomposition. These results indicate that tar is decomposed into gases through intra-particle tar decomposition. Moreover, it is noted that the further tar reduction by the intraparticle reactions is achieved by increasing heating rate during the pyrolysis.

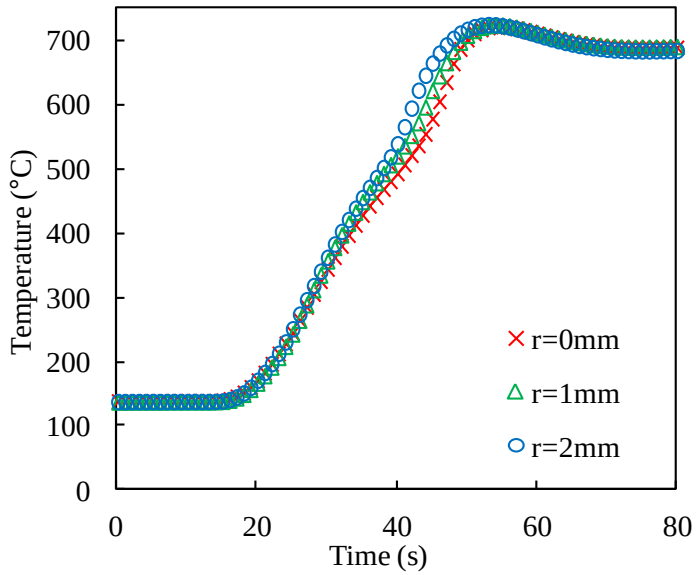

Figure 2.13 Temperature histories at three locations within the wood cylinder during pyrolysis at a heating rate of 30 K/s.

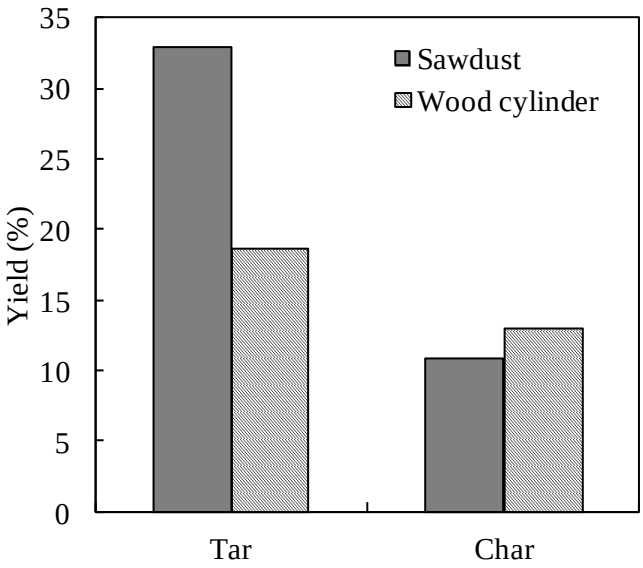

Figure 2.14 Total tar and char yields for the sawdust and wood cylinder pyrolyzed at heating rate of 30 K/s.

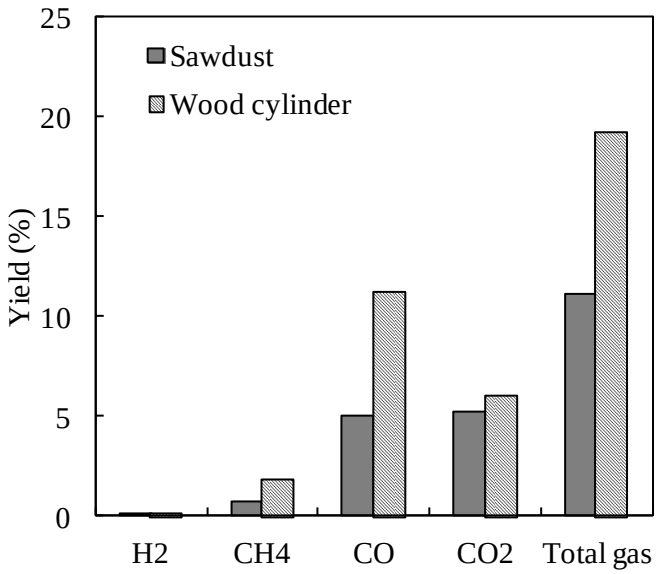

Figure 2.15 Each and total gas yields for the sawdust and wood cylinder pyrolyzed at heating rate of 30 K/s.

2.4 Mechanism of intraparticle secondary reactions of tar

Figure 2.16 shows diagrams of the proposed mechanism of the intraparticle secondary reactions of tar. Figure 2.16a presents the mechanism of the intraparticle secondary reactions of tar at low heating rate. The unreacted wood, pyrolysis zone, and char layer within the particle are overlapped due to the uniform temperature at low heating rate. As temperature increases, char is gradually formed all over the particle and char acts as a catalyst for intraparticle tar decomposition. Figure 2.16b presents the mechanism of the intraparticle secondary reactions of tar at high heating rate. The unreacted wood, pyrolysis zone, and char layer within the particle tend to be distinct from each other because temperature gradient appears at high heating rate. Since the tar produced in the pyrolysis zone is transported toward exterior particles through micropores in the char layer which acts as a catalyst, a portion of the tar is decomposed or polymerized to form secondary gas, secondary tar, and secondary char during this transportation. It is noted that intraparticle secondary reactions of tar can progress in the large biomass particle due to not only the long residence time within its particle but also the effect of catalytic char.

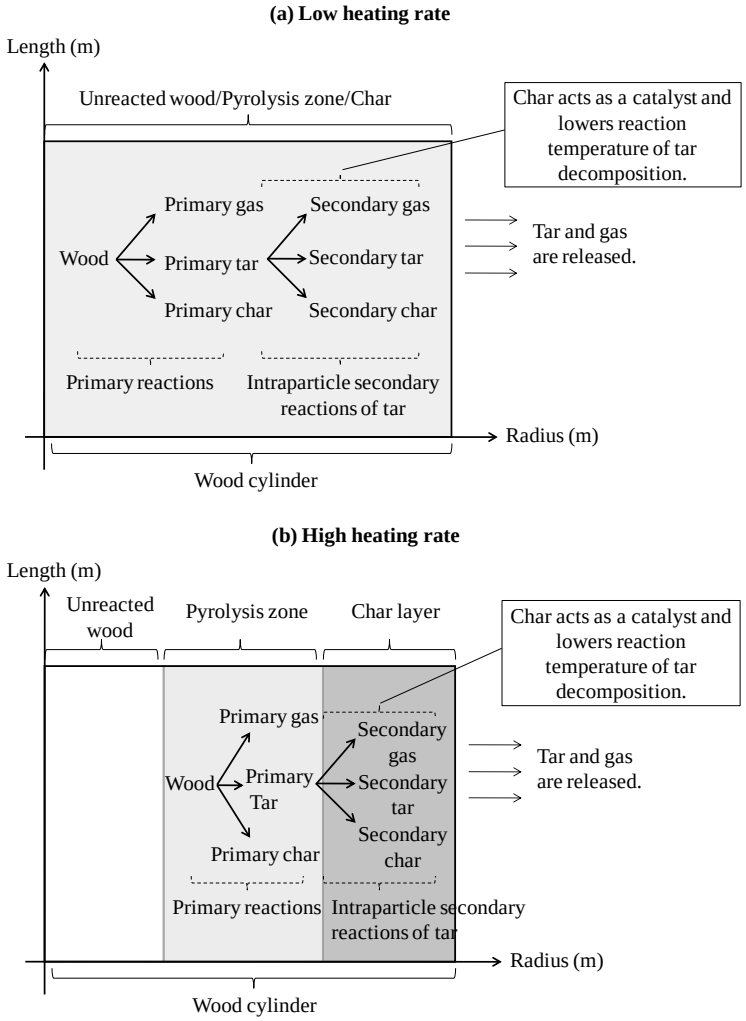

Figure 2.16 Mechanism diagram of the intraparticle secondary reactions of tar: (a) at low heating rate and (b) at high heating rate.

2.5 Conclusion

Intraparticle secondary reactions of tar during the pyrolysis of woody biomass were investigated experimentally. Pyrolysis products of the sawdust and wood cylinder were compared at low heating rate of 0.5 K/s. There was uniform temperature distribution within the wood cylinder. And, the ultimate analysis of chars did not vary along the radial direction. Therefore, a comparison of the sawdust and wood cylinder revealed intraparticle secondary reactions. The weight fraction histories of both the samples were almost the same at temperatures below 380°C, indicating that the same amount of volatile matter was released in each case. However, the weight fraction histories differed above 380°C. This indicates that the polymerization of tar to form secondary char (intraparticle reactions) progressed at approximately 380°C. Intraparticle tar decomposition to form secondary gas (mainly CO) occurred at 400–500°C, which was relatively low for tar cracking, because char worked as a catalyst and lowered the temperature at which secondary tar decomposition progressed. This study showed that the intraparticle secondary reactions of tar played an important role during the pyrolysis of large wood particles. Thus, these reactions have the potential to reduce the amount of tar produced in gasification systems. Controlling the residence time of tar transport inside the particles and the temperature of the char layer are crucial parameters for enhancing intraparticle tar decomposition.

Acknowledgment

This research was partially supported by the JFE 21st Century Foundation.

References

[1] Nunes SM, Paterson N, Dugwell DR, Kandiyoti R. Tar formation and destruction in a simulated downdraft, fixed-bed gasifier: Reactor design and initial results. Energ Fuel 2007; 21:3028–35.

[2] Zhang Y, Kajitani S, Ashizawa M, Oki Y. Tar destruction and coke formation during rapid pyrolysis and gasification of biomass in a drop-tube furnace. Fuel 2010; 89:302–9.

[3] Boroson ML, Howard JB, Longwell JP, Peters WA. Heterogeneous cracking of wood pyrolysis tars over fresh wood char surface. Fuel 1989; 3:735–40.

[4] Li XT, Grace JR, Lim CJ, Watkinson AP, Chen HP, Kim JR. Biomass gasification in a circulating fluidized bed. Biomass Bioenerg 2004; 26:171–93.

[5] Devi L, Ptasinski KJ, Jansen FJJG. A review of the primary measures for tar elimination in biomass gasification processes. Biomass Bioenerg 2003; 24:125–40.

[6] Li C, Suzuki K. Tar property, analysis, reforming mechanism and model for biomass gasification—An overview. Renew Sust Energ Rev 2009; 13:594–604.

[7] Milne T, Evans RJ. Biomass gasifier tars: their nature, formation, and conversion. National Renewable Energy Laboratory Report, NREL/TP-570-25357; 1998.

[8] Han J, Kun H. The reduction and control technology of tar during biomass gasification/pyrolysis: An overview. Renew Sust Energ Rev 2008; 12:394–416.

[9] Abu El-Rub ZY, Bramer EA, Brem G. Review of catalysts for tar elimination in biomass gasification processes. Ind Eng Chem Res 2004; 43:6911–9.

[10] Fagbemi L, Khezami L, Capart R. Pyrolysis products from different biomasses: application to the thermal cracking of tar. Appl Energ 2001; 69:293–306.

[11] Di Blasi C. Modeling intra- and extra-particle processes of wood fast pyrolysis. AIChE J 2002; 48:2386–97.

[12] Fraga AR, Gaines AF, Kandiyoti R. Characterization of biomass pyrolysis tars produced in the relative absence of extraparticle secondary reactions. Fuel 1991; 70:803–809.

[13] Boroson ML, Howard JB, Longwell JP, Peters WA. Product yields and kinetics from the vapor phase cracking of wood pyrolysis tars. AIChE J 1989; 35:121–28.

[14] Stahl M, Granstrom K, Berghel J, Renstrom R. Industrial processes for biomass drying and their effects on the quality properties of wood pellets. Biomass Bioenerg 2004; 27:621–8.

[15] Chan WR, Kelbon M, Krieger-Brockett B. Single-particle biomass pyrolysis: correlations of reaction products with process conditions. Ind Eng Chem Res 1988; 27:2261–75.

[16] Nunes SM, Paterson N, Dugwell DR, Kandiyoti R. Tar formation and destruction in a simulated downdraft, fixed-bed gasifier: Reactor design and initial results. Energ Fuel 2007; 21:3028–35.

[17] Nunes SM, Paterson N, Herod AA, Dugwell DR, Kandiyoti R. Tar formation and destruction in a fixed-bed reactor simulating downdraft gasification: Optimization of conditions. Energ Fuel 2008; 22:3028–35.

[18] Gilbert P, Ryu C, Sharifi V, Swithenbank J. Tar reduction in pyrolysis vapours from biomass over a hot char bed. Bioresource Technol 2009; 100:6045–51.

[19] Phuphuakrat T, Namioka T, Yoshikawa K. Tar removal from biomass pyrolysis gas in two-step function of decomposition and adsorption. Appl Energ 2010; 87:2203–11.

[20] Chembukulam SK, Dandge AS, Kovilur NL, Seshagiri RK, Valdyeswaran R. Smokeless fuel from carbonized sawdust. Ind Eng Chem Process Res Dev 1981; 20:714–9.

[21] Okekunle PO, Pattanotai T, Watanabe H, Okazaki K. Numerical and experimental investigation of intra-particle heat transfer and tar decomposition during pyrolysis of wood Biomass. J Therm Sci Tech 2011; 6:360–375.

[22] Bryden KM, Hagge MJ. Modeling the combined impact of moisture and char shrinkage on the pyrolysis of a biomass particle. Fuel 2003; 82:1633–44.

[23] Suleiman BM, Larfeldt J, Leckner B, Gustavsson M. Thermal conductivity and diffusivity of wood. Wood Sci Technol 1999; 33:465–73.

[24] Di Blasi C. Physico-chemical processes occurring inside a degrading two-dimensional anisotropic porous medium. Int J Heat Mass Tran 1998; 41:4139–50.

[25] Okekunle PO, Watanabe H, Pattanotai T, Okazaki K. Effect of biomass size and aspect ratio on intra-particle tar decomposition during wood cylinder pyrolysis. J Therm Sci Tech 2012; 7: 1–15.

CHAPTER 3

Gasification Characteristic of Large Wood Chars with Anisotropic Structure

This chapter is an adaptation of the published article: Teeranai Pattanotai, Hirotatsu Watanabe, and Ken Okazaki. Gasification characteristic of large wood chars with anisotropic structure. Fuel 2014;117: 331–339.

Abstract

This chapter investigates pyrolysis products, char morphology, and reactivity of char derived from large wood cylinders. Wood samples with various sizes (i.e. sawdust with particle size < 1 mm and wood cylinders with a diameter of 8 mm) were pyrolyzed under an argon atmosphere to produce char samples using a thermobalance. The final pyrolysis temperature was 1173 K and the heating rate was set to 1 or 30 K/s. Then, the reactivity of char samples was measured using an isothermal method at various gasification temperatures from 673 to 1173 K under an oxygen/argon atmosphere. Scanning electron microscopy (SEM) and X-ray computed tomography (CT) were used to observe the char morphology. Quantitative measurements of pore size and shape were made using the digital image analysis. As for the pyrolysis, the effect of intraparticle secondary reactions of tar became significant for the large wood cylinder, resulting in the decrease of tar yield and the increase of char yield. Heating rate during the pyrolysis influenced the pore structure, the radial shrinkage and swelling of the wood cylinder. As for the char gasification, the char reactivity was significantly decreased with increasing cylinder length in the diffusion-controlled zone. In addition, it was found that the char gasification mainly progressed in the direction of pores when the gasification rate was controlled by the diffusion process, indicating the anisotropic evolution of particle shape during the gasification.

3.1 Introduction

Climate change and depletion of fossil fuels have encouraged the development of clean power generation from renewable energy sources. In these issues, biomass fuels, such as woods and agriculture by-products, have attracted attention as renewable energy resources. This is because the woody bioenergy from the sustainably managed sources can provide emission reduction in the long term [1]. Direct use of biomass to produce heat by combustion is not the most efficient way of utilizing biomass energy due to the lower heating value per unit volume compared that of fossil fuels [2,3]. However, biomass can be cofired with coal for power generation in both existing power plants and new high-efficiency technologies such as the integrated gasification combined cycle (IGCC). Moreover, the cofiring biomass with coal has capability to reduce fuel costs [4] and emissions of NO_x and SO_x [4,5,6]. To realize the effective utilization of biomass in these technologies, the intensive study on thermochemical conversion of biomass including pyrolysis and gasification is very essential.

Biomass feedstock usually used in commercial applications has relatively large particle size such as that of wood chips and wood pellets [7], because biomass materials unlike pulverized coal cannot be economically processed into fine sizes. Wood pellets measure 6–8 mm in diameter according to Swedish standards [8]. Characteristics of pyrolysis and gasification of large biomass particle are different from those of fine particles due to differences in intraparticle mass and heat transfer. Our previous paper [9] showed that intraparticle secondary reactions of tar, which include intraparticle tar decomposition to form gases and polymerization to form char, occurred within the large wood cylinder during the pyrolysis.

Char reactivity is an important parameter in the process of char conversion [10]. The char reactivity is influenced by many factors such as the nature of virgin biomass and pyrolysis conditions such as temperature, heating rate, and pressure [11,12,13]. In addition, properties of many biomass materials, such as woods, are anisotropic, owing to the nature of biomass [14,15,16]. For instance, the permeability of gas along fibers is 10^3 higher than transverse wood fibers [17]. The anisotropic characteristic is supposed to influence the gasification characteristics of large wood particle. However, many researchers [11,12,13,18,19] studied char gasification and its reactivity using the fine particles of which the intraparticle transport phenomena

within the anisotropic structure is neglected. In fact, little effort has been made to study the effect of anisotropic structure on gasification.

The purpose of this study was to experimentally investigate the pyrolysis and gasification characteristic of large wood cylinder with anisotropic structure. The effect of intraparticle secondary reactions of tar on pyrolysis products was shown. The char morphology was observed using scanning electron microscopy (SEM) and X-ray computed tomography (CT). Quantitative measurements of pore size and shape were made using the digital image analysis. For the gasification characteristic, the Arrhenius plot of char reactivity and the evolution of particle shape for the large chars during the gasification were discussed. Moreover, the effect of heating rate on pyrolysis products, char morphology, and char reactivity during the gasification was studied.

3.2 Experimental

3.2.1 Wood samples

Wood samples used in this study were Japanese cypress sawdust (SD) and Japanese cypress wood cylinders (WC). Figure 3.1 shows photographs of sawdust and wood cylinders with various lengths. Properties of Japanese cypress wood (trunk) are shown in Table 2.1. The wood cylinder had a diameter of 8 mm and lengths of 2, 5, and 9 mm. Their initial weights were approximately 45, 110, and 200 mg, respectively. Figure 3.2 shows principal axes of wood defined with respect to grain direction for the wood cylinder. It can be seen that the longitudinal axis with respect to fiber grain aligns in the axial direction (z-axis) of the wood cylinder. For sawdust preparation, the wood cylinder was milled and then sieved to produce sawdust with particles less than 1 mm in size. The initial weight of the sawdust for each experiment was approximately 40–45 mg. With this size of sawdust, intraparticle reactions of tar are negligible and intraparticle temperature distribution is uniform [9].

3.2.2 Pyrolysis and gasification experiment

Figure 3.3 shows a schematic diagram of experimental apparatus that consists of a gas supply system, thermobalance (ULVAC TGD-9600), and tar trap. Wood samples were pyrolyzed in the thermobalance to produce char samples. A wood

sample was placed in a center of platinum crucible on a thermocouple (thermometric point). In this experiment, the top and side surface of the wood cylinder were exposed to the surrounding gas. Air inside the experimental setup was purged by a vacuum pump and then replaced by argon. Before the pyrolysis, the wood sample was dried at 383 K for 10 min. This drying period was long enough to dry the largest sample. Then, the pyrolysis was performed at a constant heating rate in an argon atmosphere flowing at 0.8 l/min. The pyrolysis pressure was 0.1 MPa. The heating rate was set to 1 or 30 K/s. The final temperature of pyrolysis was 1173 K with holding time of 5 min. To control the heating rate and the reactor temperature, the temperature at a thermometric point was used as a representative. Pyrolysis conditions were summarized in Table 3.1. After the pyrolysis, the temperature was changed from the final pyrolysis temperature to a desired gasification temperature in the flowing argon. The gasification temperature was varied in the range of 673–1173 K. When the desired temperature was reached, the isothermal gasification was initiated by switching the gas line to a 20% oxygen/argon mixture flowing at 1 l/min. The gasification experiment was terminated when the char was completely gasified. Gasification conditions were summarized in Table 3.2. Tar was collected by an ice-cold trap containing a glass fiber filter (GC-90, ADVANTEC) downstream of the reactor, and the total weight of the trapped tar was measured after the experiment was complete. The weight change of the downstream tube was measured after the experiment to determine an amount of tar depositing in the tube. In this study, tar is defined as condensable compounds attached to the filter in the tar trap and inside the downstream tube. The product yields shown in this paper were average from three repeated experiments, and the error bars of one standard deviation were also shown. It was noted that the pyrolysis temperature was not lower than gasification temperatures in this experiment; therefore, it was implied that pyrolysis process did not progress during gasification process. Pyrolysis and gasification were completely distinguished in this study.

3.2.3 Intraparticle temperature measurement

Temperatures within the 9 mm length wood cylinder during the pyrolysis were measured in the radial direction at three locations: the center (r = 0 mm), an intermediate position (r = 1 mm), and an outer position (r = 2 mm), at a depth of 6

mm from the top of the cylinder using *K*-type thermocouples with a diameter of 0.5 mm. The detailed procedure was explained in Section 2.2.3.

3.2.4 Char reactivity measurement

The char conversion (X) and the gasification rate (R) was calculated by using Eq. (1) and (2), respectively

$$X = 1 - \frac{m}{m_0} \tag{1}$$

$$R = \frac{dX}{dt} = -\frac{1}{m_0}\frac{dm}{dt} \tag{2}$$

where m is the mass of char at time t, m_0 is the initial mass of the char at the time when the gasification begins. It was noted that the sample ash content was neglected because the amount of ash in the Japanese cypress wood was very low (Table 1). In the present study, the char reactivity, R_i, was defined as the gasification rate at $X = 0$. The reactivities of sawdust char and wood cylinder chars were measured at various gasification temperatures as mentioned above.

To study the characteristic of char gasification in more detail, the char reactivity of finely ground char prepared from the different sizes of the original char samples was measured at gasification temperature of 1173 K. In this measurement, the sawdust and wood cylinder chars prepared at heating rate of 30 K/s were milled and then sieved to produce the finely ground char with particles less than 53 μm in size. The initial weight of finely ground char was approximately 8–9 mg.

3.2.5 SEM and X-ray CT analysis

Scanning electron microscopy (SEM) analysis was performed to investigate the surface morphology of char samples using KEYENCE VE-9800 scanning electron microscope. Moreover, X-ray CT (Xradia VersaXRM-500) was used to investigate the internal structure of char samples. The 3D image of 1×1×1 mm char with a resolution of 0.9 μm was obtained from the analysis. The pore diameter (d) and the degree of circularity (f_{circ}) were chosen to explain the differences in the pore structure. WinRoof (Mitani Crop.) software was used to analyze the cross-sectional X-ray CT images. Because the pores are not perfectly circular, the pore diameter, d, was calculated by using Eq. (3)

$$d = 2\left(\frac{A}{\pi}\right)^{1/2} \tag{3}$$

where A is the cross-sectional area of a pore. The degree of circularity, f_{circ}, was calculated by using Eq. (4) to explain the shape of pore

$$f_{circ} = \frac{4\pi A}{P^2} \tag{4}$$

where P is the perimeter.

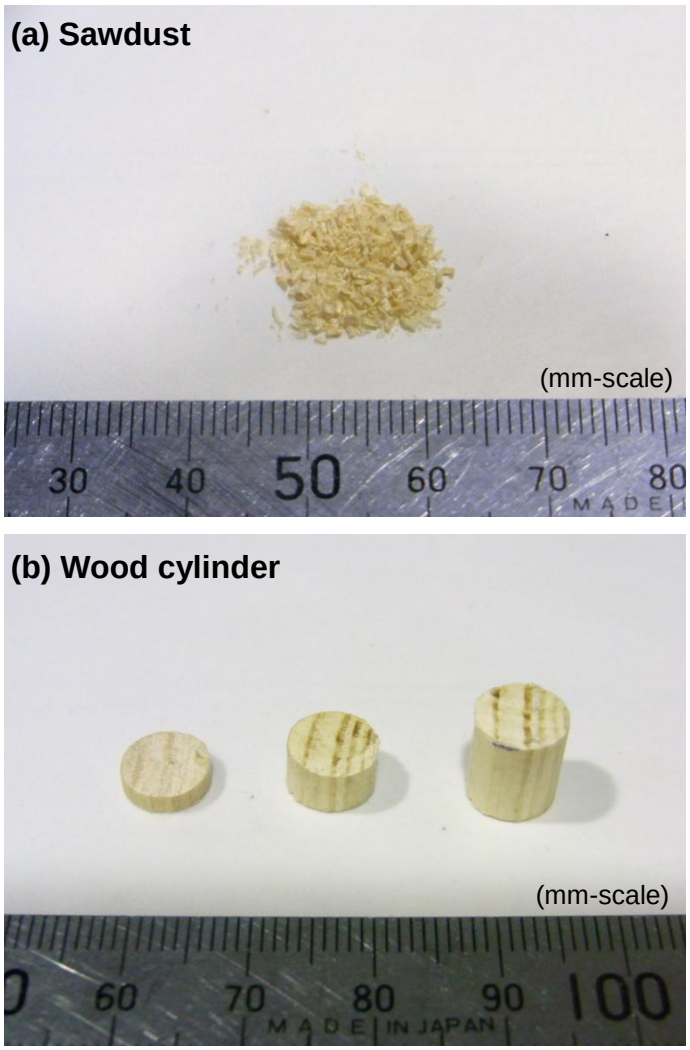

Figure 3.1 Photographs of (a) sawdust and (b) wood cylinders (8 mm in diameter) with lengths of 2, 5, and 9 mm (left to right).

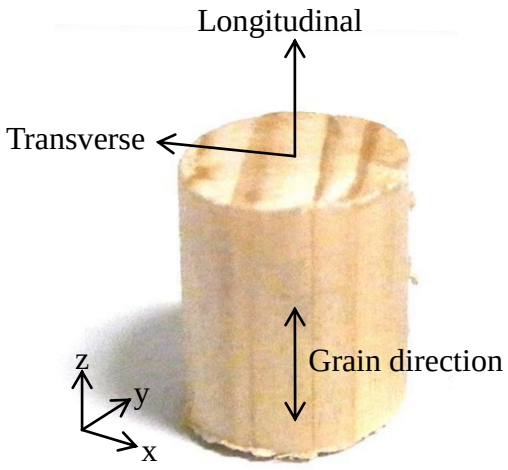

Figure 3.2 Principal axes of wood defined with respect to grain direction for wood cylinder.

Table 3.1 Pyrolysis conditions.

Heating rate (K/s)	1, 30
Final temperature (K)	1173
Holding time (min)	5
Ar flow rate (l/min)	0.8
Pressure (MPa)	0.1

Table 3.2 Gasification conditions.

Temperature (K)	673, 723, 748, 773, 873, 1023, 1173
Ar flow rate (l/min)	0.8
O_2 flow rate (l/min)	0.2
Pressure (MPa)	0.1

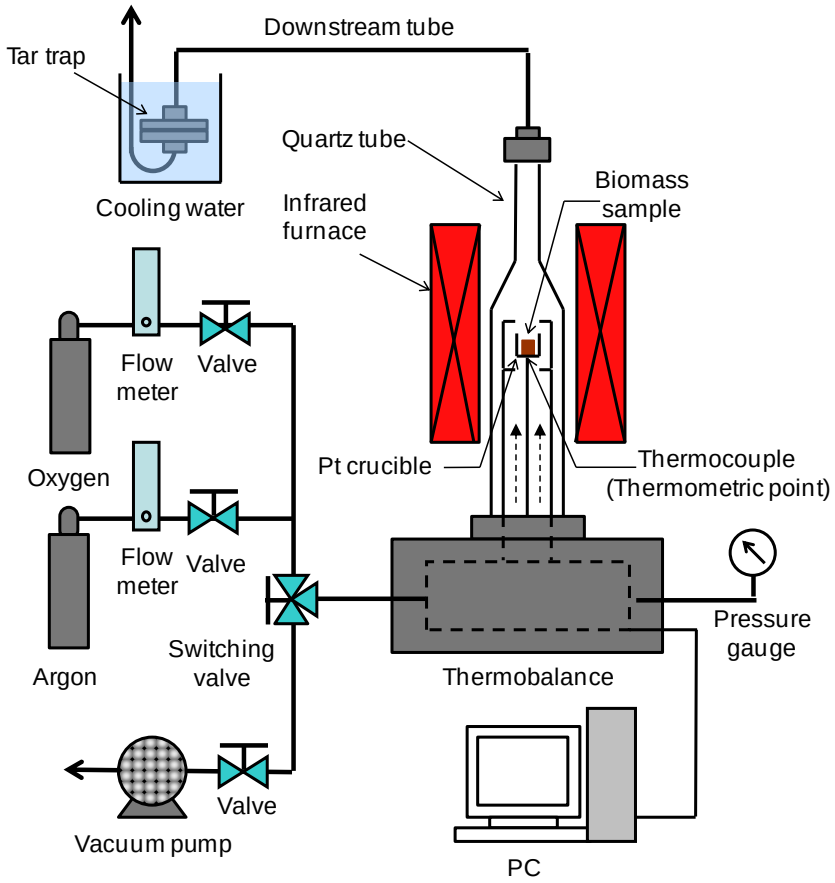

Figure 3.3 Schematic diagram of experimental apparatus.

3.3 Results and Discussion

3.3.1 Pyrolysis characteristics

When the samples are pyrolyzed at low heating rate of 1 K/s, the intraparticle temperature distribution is uniform [20]. Figure 3.4 shows temperature histories measured at three locations within the 9 mm length wood cylinder during the pyrolysis at heating rate of 30 K/s. A decrease and an increase in the slope of the temperatures during 750–765s are due to the effect of endothermic and exothermic reactions, respectively [21]. It can be seen that the temperature gradient appears within the wood cylinder during the pyrolysis at the high heating rate. The temperatures at the outer position (r = 2 mm) are significantly higher than those of the center during 750–765s. The maximum difference in the temperature at between the center and the outer position is higher than 200 K. When the heating rate is set to 30 K/s (referred at the thermometric point), the intraparticle heating rates at the measured locations are reduced to approximately 20 K/s due to the limitation of heat transfer. However, this temperature gradient disappears before the gasification process. Thus, the intraparticle temperature distribution is expected to be uniform during the gasification.

Figure 3.5 shows the tar yields obtained from the pyrolysis of the sawdust and wood cylinders at heating rates of 1 and 30 K/s. The pyrolysis of the sawdust at 30 K/s yields higher tar than that at 1 K/s. This is because when the heating rate becomes higher, the pyrolysis proceeds at higher temperature, resulting in the higher rate of volatiles (tar + gases) formation compared with that of char formation. The tar yields are decreased with increasing wood size at both the heating rates, especially at 30 K/s. We have proposed the mechanism of intraparticle secondary reactions of tar at both low and high heating rate [9]. The decrease in the tar yields of wood cylinder at the low heating rate is caused by the intraparticle tar decomposition with the uniform intraparticle temperature. The larger wood cylinder provides a longer residence time of tar inside the particle, resulting in the further decrease in tar yield. The significant decrease in the tar yields of large wood cylinder at the high heating rate is caused by the decrease of the intraparticle heating rate (as explained above) and the intraparticle tar decomposition enhanced by the temperature gradient (Figure 3.4). This is because it is known that tar yield is decreased with decreasing heating rate and our previous calculation [22] shows that the temperature gradient within the

large wood cylinder can enhance the intraparticle tar decomposition. A primary tar, which is formed inside wood at relatively low temperature, can be decomposed when it is transported toward exterior particle through a surface layer with high temperature. This phenomenon is considered as the enhancement of intraparticle tar decomposition at high heating rate.

Figure 3.6 shows the char yields obtained from the pyrolysis of the sawdust and wood cylinders at heating rates of 1 and 30 K/s. The pyrolysis at heating rate of 30 K/s yields a smaller amount of char than that of 1 K/s due to the lower rate of char formation as explained above. The char yields are slightly increased with increasing wood size at both the heating rates owing to the intraparticle reactions of tar in term of the polymerization. However, the effect of intraparticle reactions on char yield is not so significant.

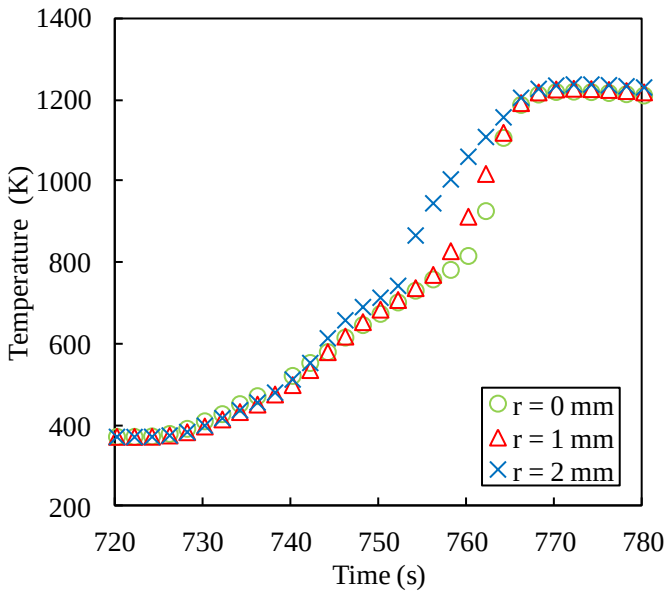

Figure 3.4 Temperature histories at three locations within the wood cylinder during the pyrolysis at heating rate of 30 K/s.

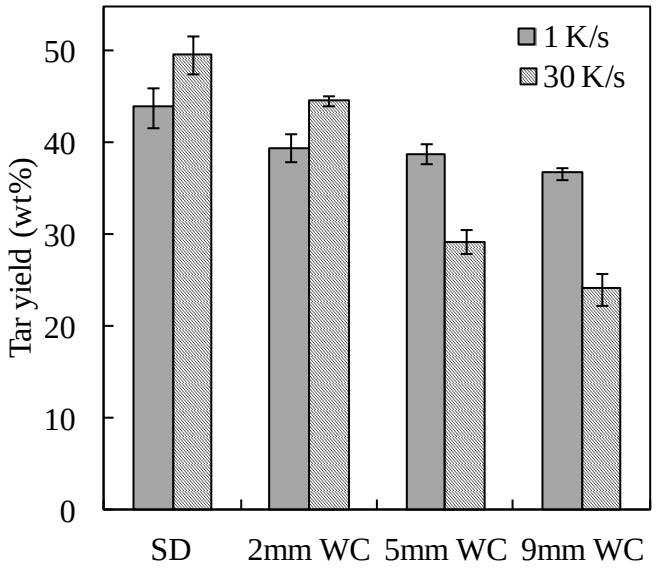

Figure 3.5 Effect of wood size on tar yield. Error bars indicate one standard deviation.

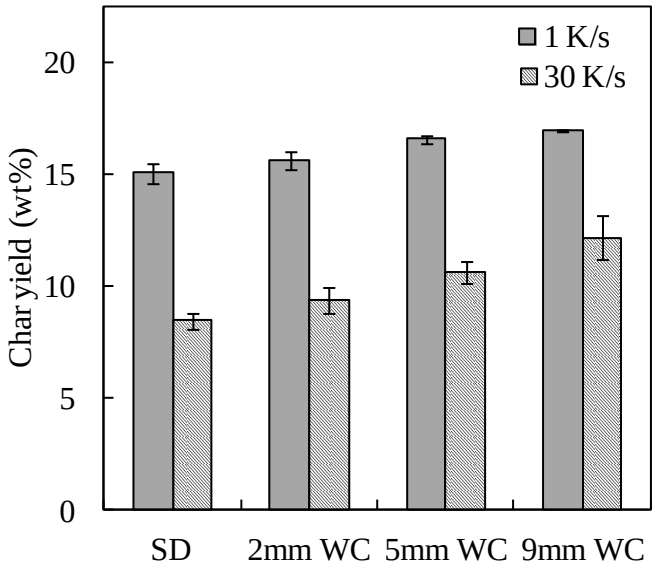

Figure 3.6 Effect of wood size on char yield. Error bars indicate one standard deviation.

3.3.2 Char morphology

Figure 3.7 shows SEM images captured from the top and side surface of wood cylinder char obtained from the pyrolysis at heating rate of 30 K/s. A large number of pores (vessel cells and fiber cells) are observed on the top surface of wood cylinder char whereas its side surface is relatively smooth and consists of a small amount of pores. Figure 3.8 shows the typical X-ray CT images of internal structure of char prepared at 1 K/s (Figure 3.8a) and 30 K/s (Figure 3.8b). By using a series of cross-sectional images, the 3D image of the internal structure is constructed as shown in figure 3.9. Many pores are existed in the wood char. Relatively large pores (2–3μm) are well visualized by using the X-ray CT. The 3D image confirms that the pores of wood cylinder mainly align along the axial direction (grain direction). This anisotropic structure influences the transport of gasifying agents into the inner char during the gasification. The details are discussed later.

When compared the images of pore structure between the chars prepared at 1 and 30 K/s, it is found that the intraparticle structure is significantly influenced by heating rate during the pyrolysis. Approximately 1000 pores were used to determine the distribution of the pore diameter and the degree of circularity as shown in Figure 3.10 and Figure 3.11, respectively. As can be seen from Figure 3.10, the pore diameters for the char at 1 K/s are mainly in the range 10–20 μm. Meanwhile, large pores (>45 μm) are only observed in the char prepared at 30 K/s. These large pores are possibly formed by the expansion of pore walls due to the high internal pressure (as will be discussed in Section 3.1.4) or the collapse of pore walls due to the rapid release of volatile matters at high heating rate. Moreover, the char at 30 K/s consists of larger amount of relatively small pores (<10 μm) when compared with the char at 1 K/s. This is because the expanding pore may push the nearby pores, and these pores become small. For the shape of pore, the peak of pore circularity for the char at 1 K/s is appeared at 0.8–0.9, while it is appeared at 0.6–0.7 for the char at 30 K/s. It means that the pore shape for the char at 1 K/s is more circular than that of the char at 30 K/s. Moreover, the pore circularity distribution for the char at 30 K/s is broader than that at 1 K/s. It indicates that the pore shape for the char at 1 K/s is more uniform than that at 30 K/s.

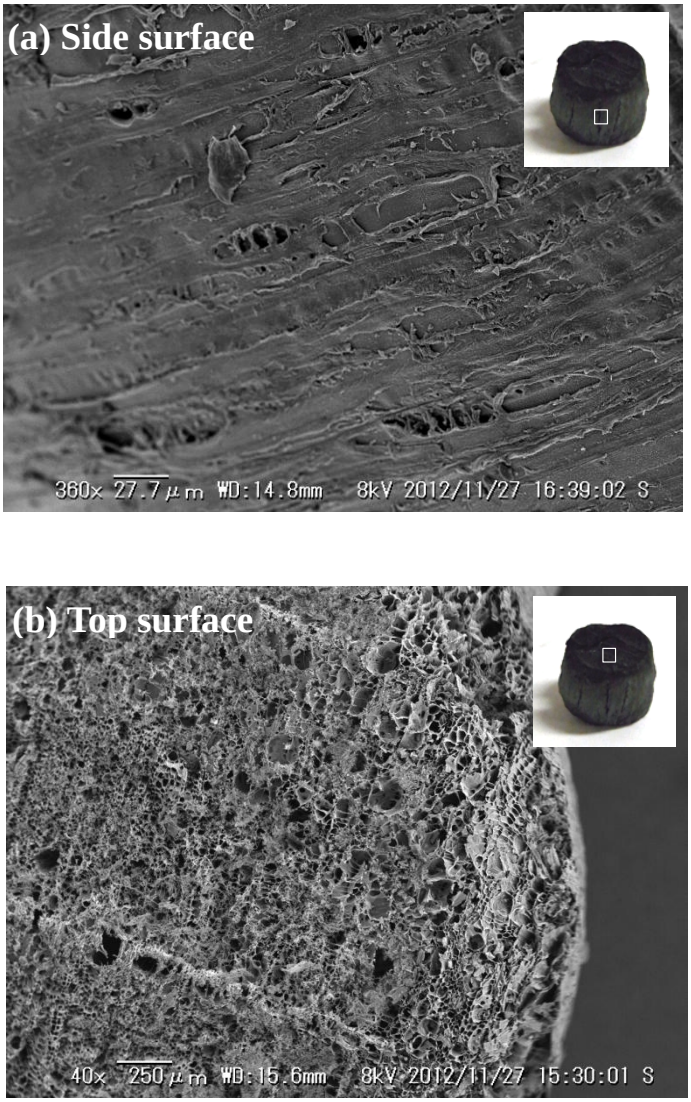

Figure 3.7 SEM images of (a) side surface and (b) top surface of 9 mm wood cylinder char prepared at heating rate of 30 K/s.

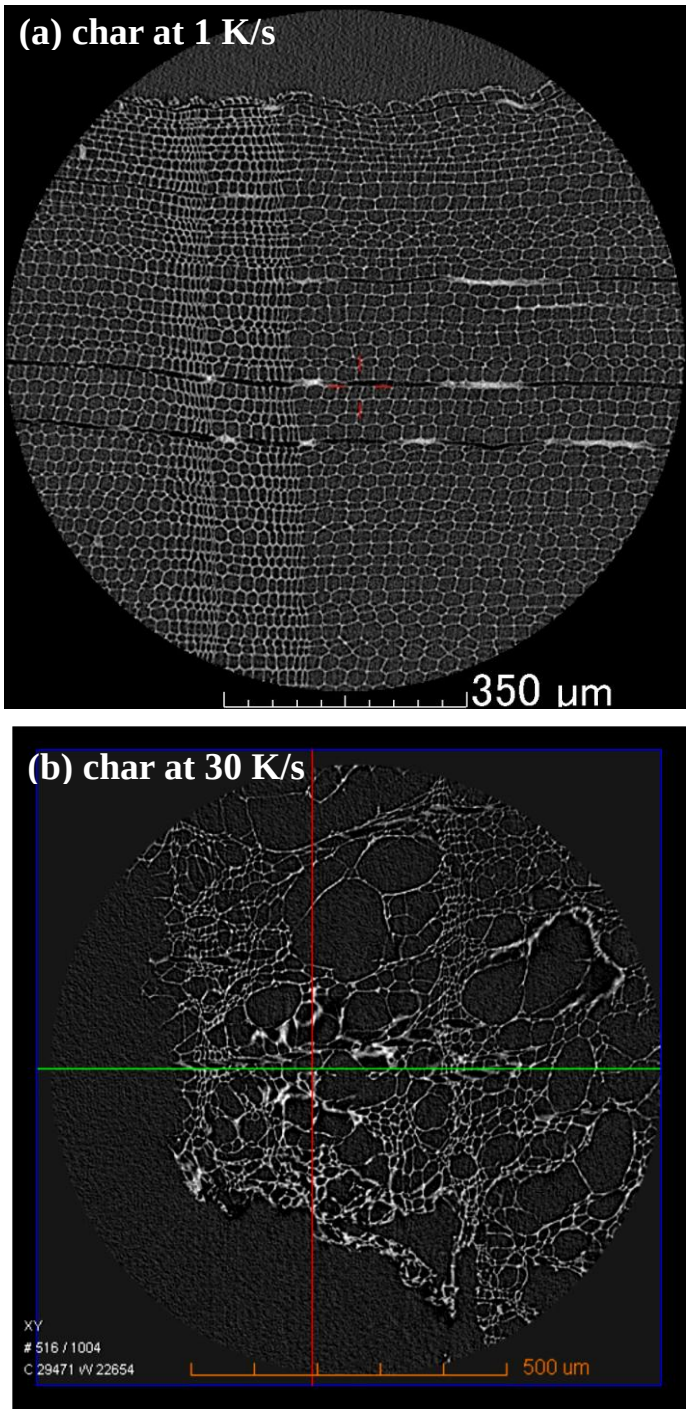

Figure 3.8 X-ray CT cross-sectional images of internal pores in the xy plane for the char at (a) 1 K/s and (b) 30 K/s.

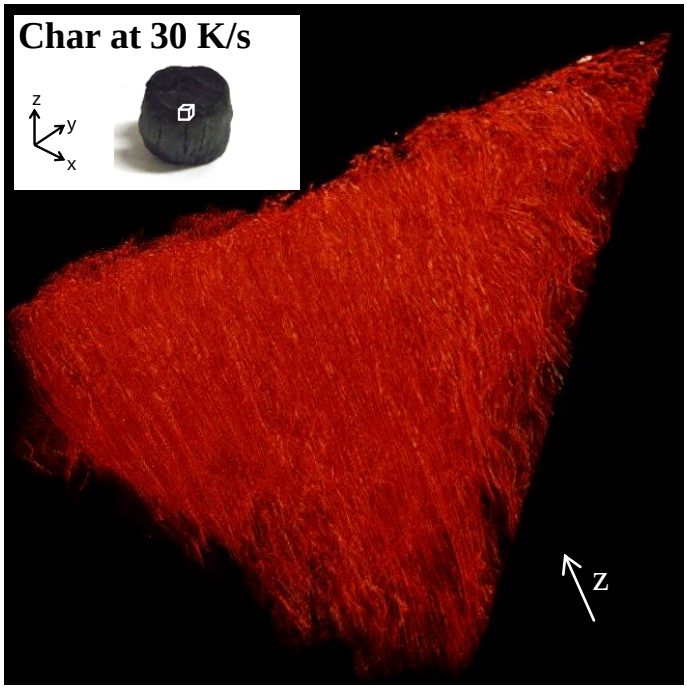

Figure 3.9 X-ray CT 3D image of internal structure for the char at 30 K/s. Pore walls in the 3D image are shown in red color.

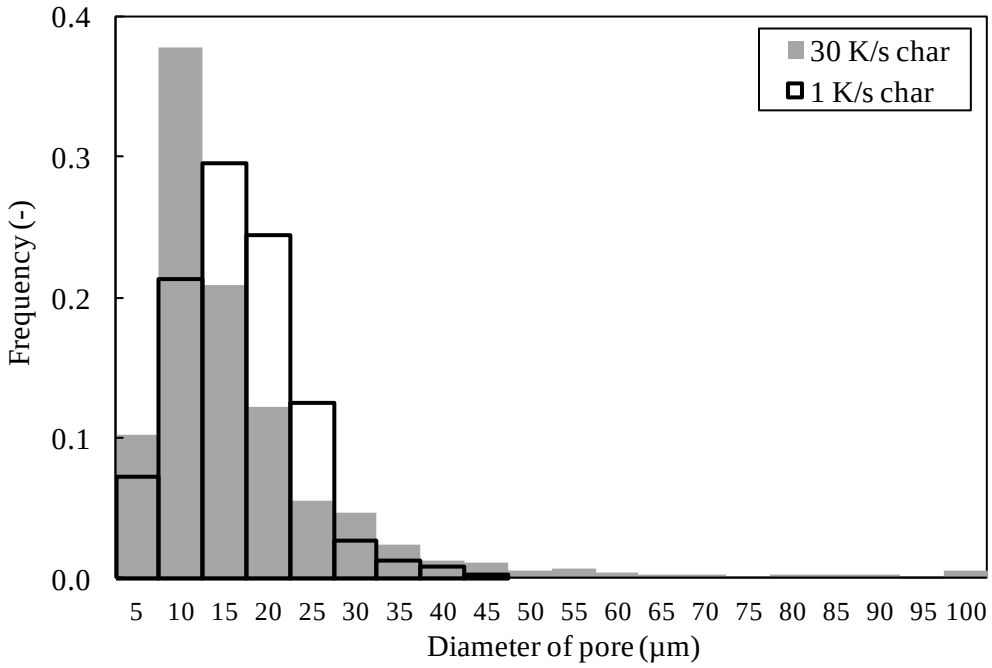

Figure 3.10 Distributions of pore diameter for the chars prepared at 1 and 30 K/s.

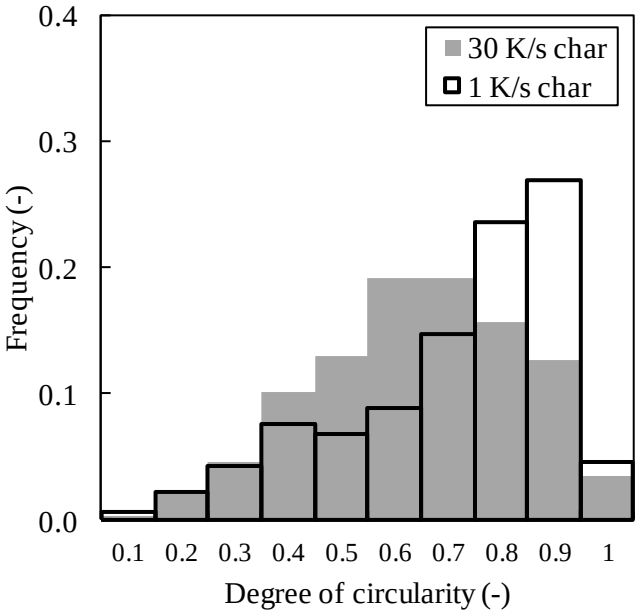

Figure 3.11 Distributions of the degree of circularity of pore for the chars prepared at 1 and 30 K/s.

3.3.3 Shrinking of wood cylinder

This section describes the change in particle size after the pyrolysis at different heating rates. Figure 3.12 shows photographs of the wood cylinder with length of 9 mm and its chars obtained from the pyrolysis at heating rates of 1 or 30 K/s. Parameters chosen in this analysis are the length (L) and the diameter (D) of the wood cylinder. Size and mass of the wood cylinder chars were precisely measured. The measured length ($L_{char,X=0}$) and diameter ($D_{char,X=0}$) for char samples were normalized by the initial length ($L_{wood,initial}$) and diameter ($D_{wood,initial}$) of wood cylinders, respectively. Figure 3.13a shows a plot of the normalized length ($L_{char,X=0}/L_{wood,initial}$) for each wood cylinder size. As can be seen, the normalized lengths are 0.7 for all wood cylinder chars. Figure 3.13b shows a plot of the normalized diameter ($D_{char,X=0}/D_{wood,initial}$) for each wood cylinder size. For all wood cylinder chars prepared at 1 K/s, the shrinking in the radial direction is considerable. Meanwhile, the swelling in the radial direction is observed for the 5 and 9 mm length wood cylinder chars at 30 K/s. The difference in the radial shrinking and swelling between the low and high heating rate char can be explained by an internal pressure during the pyrolysis. The internal pressure of wood particle during the pyrolysis at high hating rate is higher than that at low heating rate [21]. Thus, the higher internal pressure resists the shrinkage in the radial direction for the char at 30 K/s. It is noted that the chars prepared at the low heating rate have heavier weight (Figure 3.6) but smaller size (Figure 3.12) when compared with the chars prepared at the high heating rate. Thus, the significant difference in char apparent density is observed: 270 kg/m^3 for the chars prepared at 1 K/s and 82 kg/m^3 for the chars prepared at 30 K/s (as shown in Figure 3.13c). This observation suggests that the chars prepared at low heating rate have the lower porosity that may lead to the higher diffusion resistance of gasifying agent during the gasification process. Mermound et al. [23] reported the same observation that the porosity of large wood char was increased with increasing heating rate during the pyrolysis.

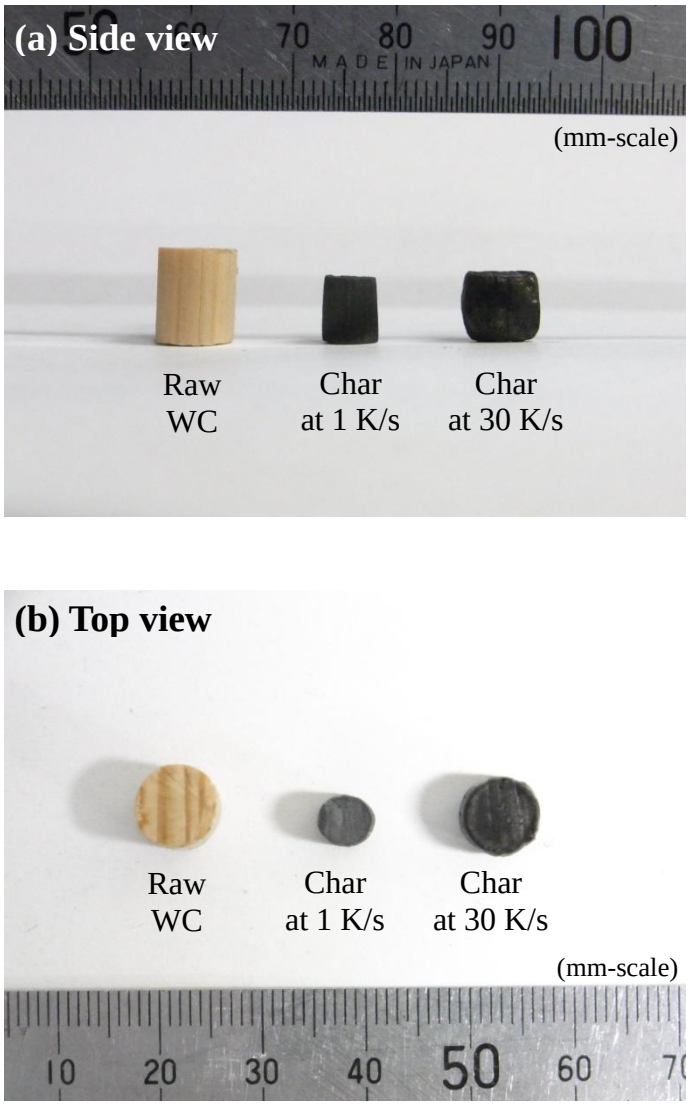

Figure 3.12 Photographs of raw material of wood cylinder and wood cylinder chars prepared at heating rates of 1 and 30 K/s (left to right) captured from (a) side view and (b) top view.

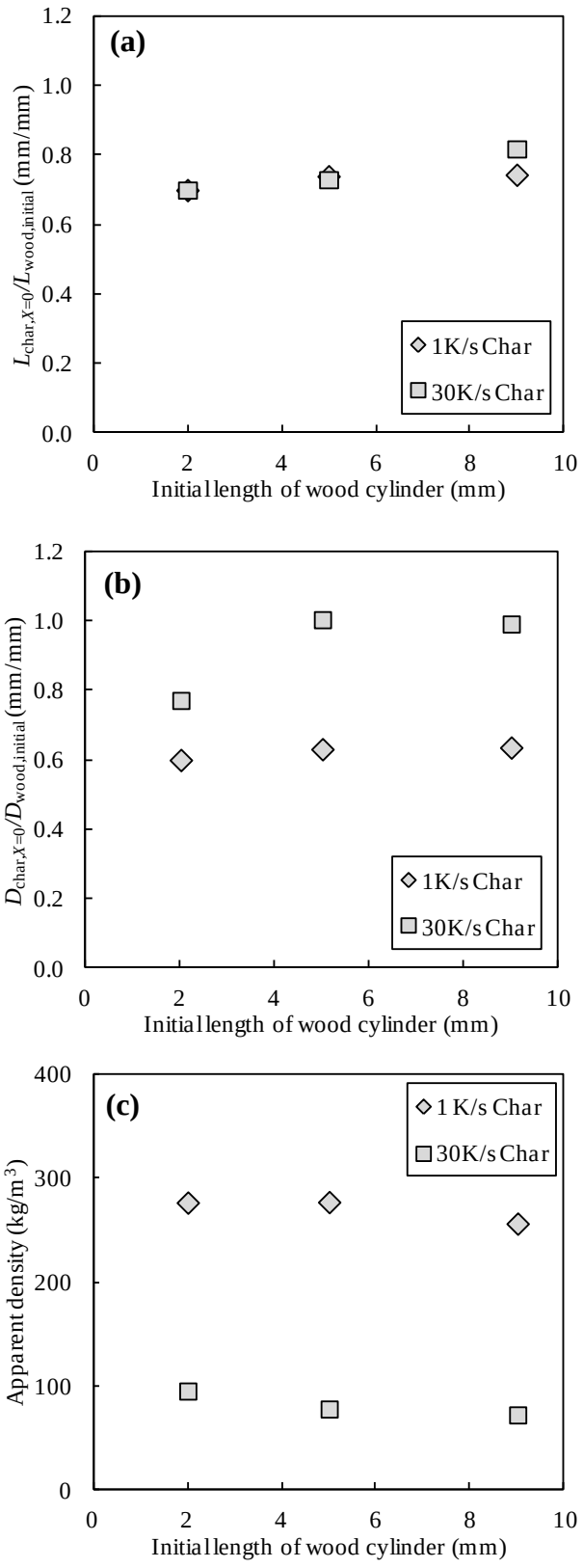

Figure 3.13 Effect of heating rate on (a) axial shrinkage, (b) radial shrinkage, and (c) apparent density of chars.

3.3.4 Char reactivity

The repeatability of the reactivity measurement was checked by performing three repeated experiments at a certain condition. The results show that a deviation of approximately 4% for three reactivity measurements is achieved, indicating the good repeatability. Figure 3.14a shows the Arrhenius plot of reactivity for the sawdust char and wood cylinder chars prepared at heating rate of 1 K/s. At gasification temperature of 673 K, the reactivities are almost the same regardless of char size. Therefore, the gasification reaction at 673 K for all char sizes is controlled by the kinetic of chemical reaction (zone I). In the temperature range of 673–773 K, the reactivities of the sawdust char and the 2 mm length wood cylinder char are linearly increased with increasing temperature, representing the zone I. Meanwhile, the decrease in the reactivities of the 5 and 9 mm length wood cylinder chars is observed in this temperature range (673–773 K) when compared with that of the sawdust. The decrease in slope of reactivity indicates a transition into the internal diffusion-controlled zone (zone II) of char gasification. Therefore, it is implied the rate-limiting process of the gasification for the large char cylinders changes from the chemical control (zone I) to the internal diffusion control (zone II) at lower temperature when compared with the small char cylinders. This is because the pore diffusion becomes dominant in the large wood cylinder char. In the high temperature range of 873–1173 K, the gasification reaction for all char sizes is controlled by the diffusion process and the char reactivities are decreased with increasing cylinder length.

Figure 3.14b shows the Arrhenius plot of reactivity for the sawdust char and wood cylinder chars prepared at heating rate of 30 K/s. The chars prepared at heating rate of 30 K/s show the similar tendency of reactivity as those of 1 K/s. It is found that the reactivities of chars prepared at 30 K/s in the zone II are notably higher than those of chars prepared at 1 K/s.

The measured reactivities of finely ground char are shown in Figure 3.15. At gasification temperature of 1173K, the reactivities of finely ground char are independent from the size of original chars. It is concluded that the chemical kinetic of char gasification is almost the same for all char sizes. This result confirms that the difference in reactivity among the various sizes of chars (Figure 3.13) is caused by the pore diffusion process.

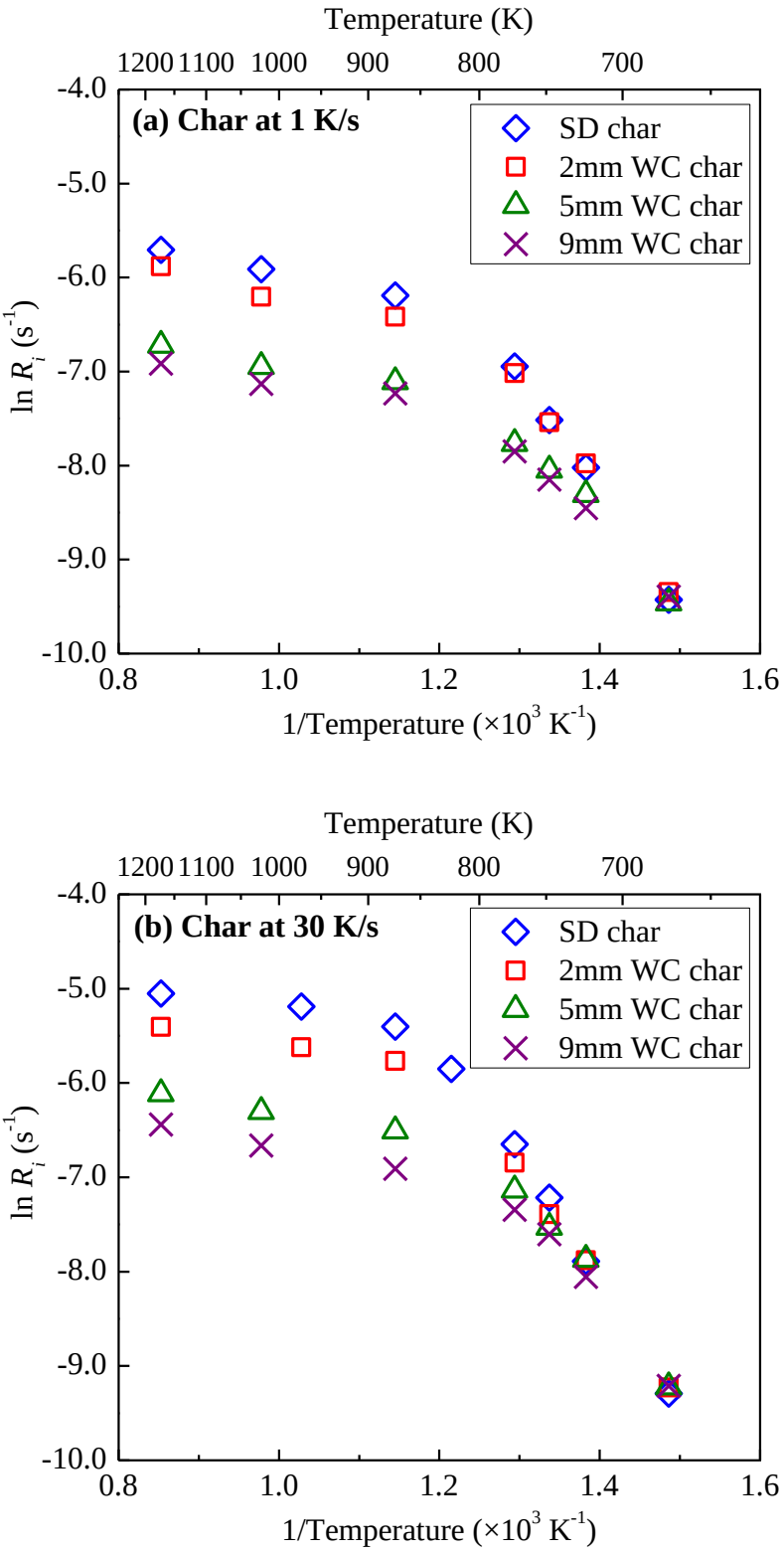

Figure 3.14 Arrhenius plot of reactivity for chars prepared at heating rates of (a) 1 K/s and (b) 30 K/s.

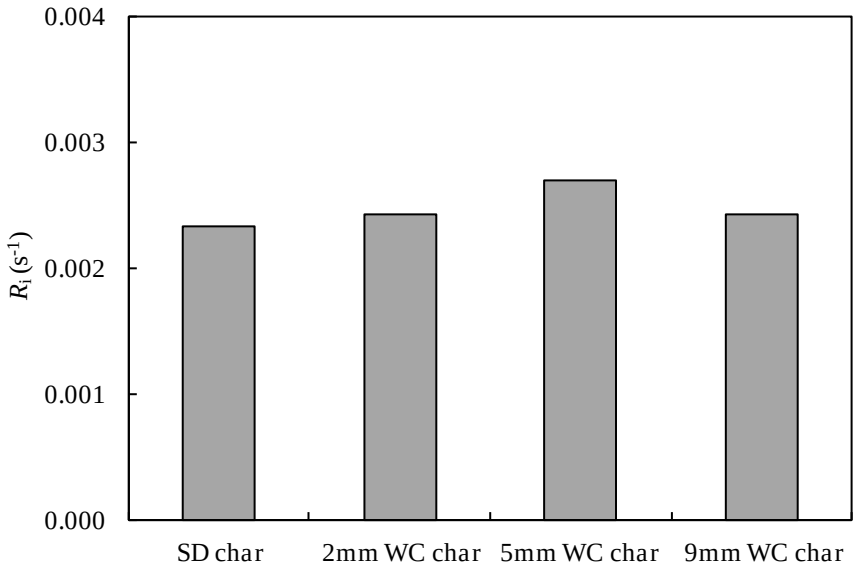

Figure 3.15 Reactivities of finely ground chars prepared from the sawdust and the wood cylinder chars at heating rate of 30 K/s. Gasification temperature is 1173 K.

3.2.5 Evolution of particle shape during gasification

Figure 3.16 shows photographs of the wood cylinder char (X = 0) and its char with X = 0.5 gasified at 673 and 1173 K. When the gasification temperature is 673 K, the char size at X = 0.5 is almost the same as that at X = 0. This result indicates that the char gasification at 673 K proceeds entire the wood cylinder with keeping the constant size. This is because the gasification reaction at 673 K is kinetically controlled at which the diffusion rate is higher than the chemical reaction rate. When the gasification temperature is set to 1173 K, the char shape at X = 0.5 is significantly different from that at X = 0. The length ($L_{\mathrm{char},X}$) and diameter ($D_{\mathrm{char},X}$) of 9 mm length wood cylinder char gasified at 1173 K were measured at X = 0.3, 0.5, and 0.8. The measured length and diameter were normalized by those at X = 0 ($L_{\mathrm{char},X=0}$ or $D_{\mathrm{char},X=0}$) and the results are shown in Figure 3.17. It can be seen that the decrease of the normalized length ($L_{\mathrm{char},X}/L_{\mathrm{char},X=0}$) are higher (approximately 2.5–3 times) than that of the normalized diameter ($D_{\mathrm{char},X}/D_{\mathrm{char},X=0}$) during gasification process. These results indicate that the char gasification at 1173 K mainly progresses from the top of the wood cylinder in the axial direction in which the pores align as shown in the X-ray CT images. This is because the gasification rate at 1173 K is controlled by the internal diffusion process. These phenomena indicate that the gas diffusion along the axial direction (the grain direction) is more dominant than that in the radial direction. The important finding here is that the gasification of large wood char shows the anisotropic shape evolution when the gasification rate is controlled by the internal diffusion process. This information is useful for the numerical simulation of char gasification and the selection of wood shape for the gasifier. This finding suggests that the woody biomass with large surface area in the transverse plane and short length in the longitudinal axis might provide the high gasification rate.

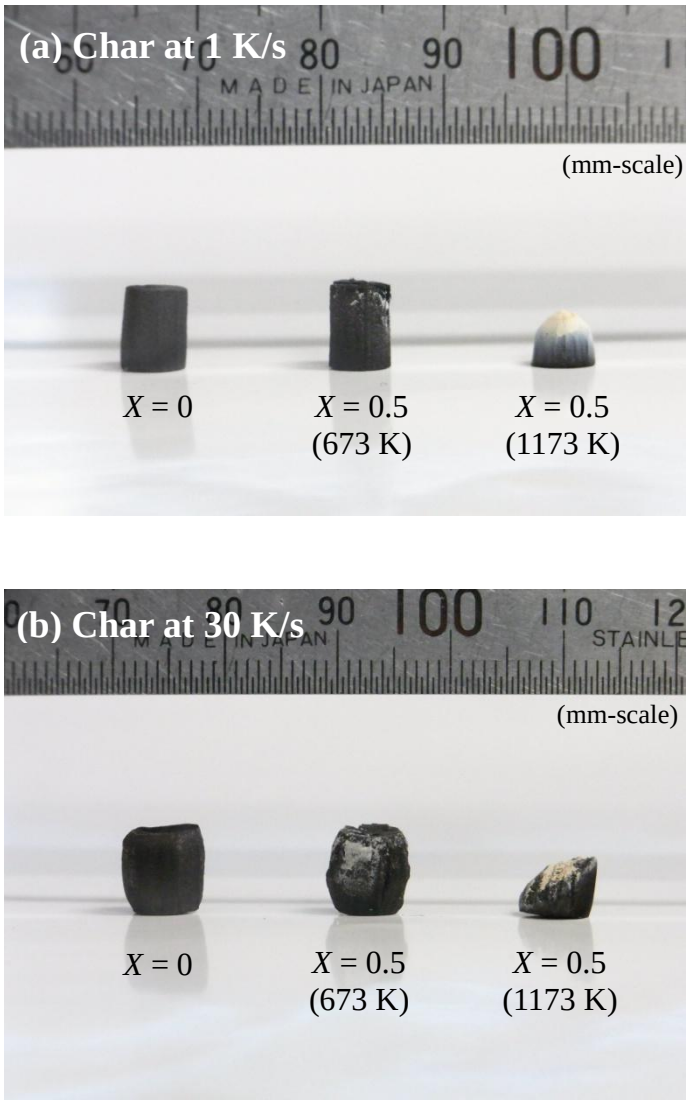

Figure 3.16 Photographs of initial char (X = 0), char at X = 0.5 gasified at 673 K, and char at X = 0.5 gasified at 1173 K (left to right). Char samples are prepared at heating rates of (a) 1 K/s and (b) 30 K/s.

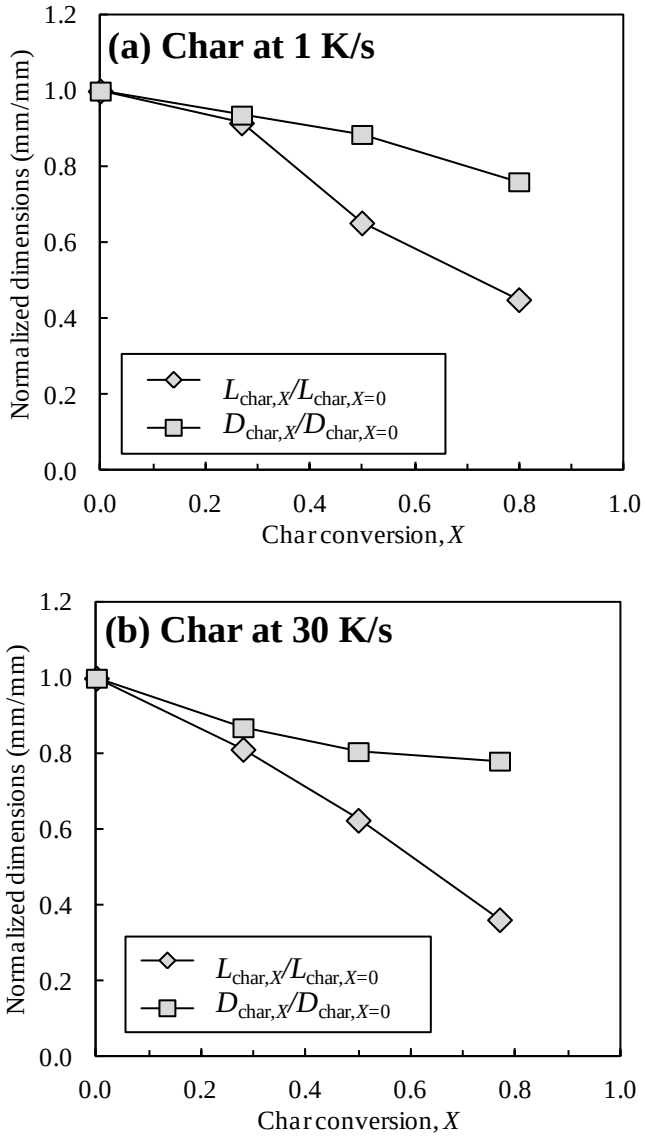

Figure 3.17 Evolution of particle sizes with char conversion for the 9 mm length wood cylinder chars prepared at heating rates of (a) 1 K/s and (b) 30 K/s. Gasification temperature is 1173 K.

3.4 Conclusion

In this chapter, the pyrolysis and gasification characteristics of the large wood cylinder were investigated. For the pyrolysis characteristics, the tar yields were decreased but the char yields were slightly increased with increasing cylinder length due to the intraparticle secondary reactions of tar. The significant decrease in tar yields was observed when the large wood cylinder was pyrolyzed at the high heating rate. The X-ray CT images revealed the internal anisotropic structure of the wood cylinder char. The pores of the wood cylinder char mainly aligned along its axial direction (the grain direction). Moreover, it was found that heating rate during pyrolysis significantly influenced the pore structure, radial shrinkage and swelling of the wood cylinder. For the gasification characteristics, the char reactivity was found to be independent of char size in the kinetically controlled zone. Meanwhile, the char reactivity was significantly deceased with increasing cylinder length in the diffusion-controlled zone. In addition, it was found that the char gasification mainly progressed in the direction of pores when the gasification rate was controlled by the internal diffusion, indicating the anisotropic evolution of particle shape during the gasification.

Acknowledgement

This work was partially supported by HITACHI Corporation (Open-type research fund). The authors would like to thank the Center for Advanced Material Analysis at Tokyo Institute of Technology for SEM analyses. The authors also would like to thank Dr. Masayuki Taniguchi and Ms. Yuki Kamikawa of HITACHI Corporation.

References

[1] Zanchi G, Pena N, Bird N. Is woody bioenergy carbon neutral? A comparative assessment of emissions from consumption of woody bioenergy and fossil fuel. GCB Bioenergy 2012;4:761–72.

[2] Ndiema CKW, Manga PN, Ruttoh CR. Influence of die pressure on relaxation characteristics of briquetted biomass. Energy Convers Manage 2002;43: 2157–61.

[3] Saxena RC, Seal D, Kumar S, Goyal HB. Thermo-chemical routes for hydrogen rich gas from biomass: A review. Renew Sust Energ Rev 2008;12: 1909–27.

[4] Demirbas A, Sustainable cofiring of biomass with coal. Energy Convers Manage 2003;44: 1465–79.

[5] Spliethoff H, Hein KRG. Effect of co-combustion of biomass on emissions in pulverized fuel furnaces. Fuel Process Technol 1998;54:189–205.

[6] Damstedt B, Pederson JM, Hansen D, Knighton T, Jones J, Christensen C, Baxter L, Tree D. Biomass cofiring impacts on flame structure and emissions. P Combust Inst 2007;31:2813–20.

[7] Yang YB, Sharifi VN, Swithenbank J, Ma J, Darvell LI, Jones JM, Pourkashanian M, Williams A. Combustion of a single particle of biomass. Energy Fuels 2008;22:306–16.

[8] Stahl M, Granstrom K, Berghel J, Renstrom R. Industrial processes for biomass drying and their effects on the quality properties of wood pellets. Biomass Bioenergy 2004;27:621–8.

[9] Pattanotai T, Watanabe H, Okazaki K. Experimental investigation of intraparticle secondary reactions of tar during wood pyrolysis. Fuel 2013;104;468–75.

[10] Link S, Arvelakis S, Hupa M, Yrjas, Kulaots I, Paist A. Reactivity of the biomass chars originating from Reed, Douglas Fir, and Pine. Energy Fuels 2010;24:6533–39.

[11] Cetin E, Moghtaderi B, Gupta R, Wall TF. Influence of pyrolysis conditions on the structure and gasification reactivity of biomass chars. Fuel 2004;83:2139–50.

[12] Okumura Y, Hanaoka T, Sakanishi K. Effect of pyrolysis conditions on gasification reactivity of woody biomass-derived char. P Combust Inst 2009;32: 2013–20.

[13] Lu L, Kong C, Sahajwalla V, Harris D. Char structural ordering during pyrolysis and combustion and its influence on char reactivity. Fuel 2002;81:1215–25.

[14] Suleiman BM, Larfeldt J, Leckner B, Gustavsson M. Thermal conductivity and diffusivity of wood. Wood Sci Technol 1999;33:465–73.

[15] Okekunle PO, Watanabe H, Pattanotai T, Okazaki K. Effect of biomass size and aspect ratio on intra-particle tar decomposition during wood cylinder pyrolysis. J Therm Sci Technol 2012;7:1–15.

[16] Di Blasi C. Physico-chemical processes occurring inside a degrading two dimensional anisotropic porous medium. Int J Heat Mass Transfer 1998;41:4139–50.

[17] Larfeldt J, Leckner B, Melaaen MC. Modelling and measurements of the pyrolysis of large wood particles. Fuel 2000;79:1637–43.

[18] Di Blasi C, Buonanno F, Branca C. Reactivities of some biomass chars in air. Carbon 1999;37:1227–1238.

[19] Shim H, Hajaligol MR, Baliga VL. Oxidation behavior of biomass chars; pectin and *Populus deltoides*. Fuel 2004;83:1495–1503.

[20] Watanabe H, Morinaga Y, Okada T, Okazaki K. Experimental and numerical investigation of biomass pyrolysis process focusing on intra-particle heat transfer. Proceeding of the 14th international heat transfer conference 2010;3:161-8.

[21] Park WC, Atreya A, Baum H. Experimental and theoretical investigation of heat and mass transfer processes during wood pyrolysis. Combust Flame 2010;157:481–94.

[22] Okekunle PO, Pattanotai T, Watanabe H, Okazaki K. Numerical and experimental investigation of intra-particle heat transfer and tar decomposition during pyrolysis of wood biomass. J Therm Sci Technol 2011;6:360–75.

[23] Mermoud F, Salvador S, Van De Steene L, Golfier F. Influence of the pyrolysis heating rate on the steam gasification rate of large wood char particles. Fuel 2006;85:1473–82.

CHAPTER 4

Influence of Particle Aspect Ratio on Gasification Reactivity of Anisotropic Char

Abstract

Char derived from pyrolysis of woody biomass has anisotropic structure. During gasification, a gas transport into the char with different geometry and dimension is different due to its anisotropic structure. In this study, the effect of particle aspect ratio (length/diameter) in the gasification of cylindrical char with anisotropic structure was experimentally investigated. Japanese cypress wood cylinders with three aspect ratios were pyrolyzed to produce chars. All wood samples had the same mass and volume; therefore, only the effect of particle aspect ratio was emphasized. The intraparticle structure of char sample was visualized using X-ray CT. Gasification experiment was performed under an oxygen/argon atmosphere. Char reactivity was measured using an isothermal method at various gasification temperatures ranging from 723 to 1423K. It was found that the effect of aspect ratio on char reactivity was not appeared in the kinetically controlled zone. However, the effect of anisotropic structure was significantly appeared in the internal diffusion-controlled zone. Char reactivity was significantly increased with decreasing particle aspect ratio. Because pores inside char samples mainly aligned in the axial direction, a decrease in aspect ratio (an increase in top/bottom surface area) improved gas transport into the particle, leading to the enhancement of char gasification.

4.1 Introduction

The use of woody biomass as fuel has attracted attention because it is considered as a renewable energy resource and has a potential to suppress the emission in the long term [1]. Gasification is an efficient technology for extracting energy from solid fuels such as coal and biomass [2, 3]. To achieve the high efficiency of gasification process, char reactivity is a key factor because the char conversion is considered as a slowest process in gasification when compared with pyrolysis or devolatilization [4, 5]. Generally, the char reactivity is strongly influenced by the nature of biomass and pyrolysis conditions such as temperature, heating rate, and pressure [6]. This is because the pore structure and the chemical properties are affected by changes during pyrolysis process [4, 7].

For woody biomass materials, their pore structure and properties are anisotropic (orthotropic) due to the nature of woody biomass. For example, gas permeability along fibers is 10^3 higher than transverse wood fibers [8]. Many researchers [9-13] studied char gasification and its reactivity using fine particles of which the anisotropic properties seem to be neglected. However, the actual biomass feedstock usually used in the commercial application such as combustors and gasifiers gas has relatively large particle size such as wood chips and wood pellets. Typical wood chips vary in size from 10×10×5 mm to 15×15×8 mm [14]. Therefore, the intraparticle transport phenomena in anisotropic structure should play an important role in gas diffusion during gasification process. Our previous study [15] investigated gasification characteristics of large wood char and showed the importance of pore alignment inside the wood-derived char on the evolution of particle shape during gasification in the internal-diffusion controlled zone; that is; the char gasification mainly progressed in the direction of pores. Therefore, it has a potential to increase the char conversion rate as well as the char reactivity by using the appropriate shape of woody biomass in gasification process.

The purpose of this study is first to visualize the anisotropic structure of wood-derived char using X-ray computed tomography (CT). The advantage of X-ray CT analysis is that the images of intraparticle char structure can be obtained without destruction of char structure. Then, the effects of particle shape in terms of particle aspect ratio on the char reactivity are investigated at various gasification

temperatures. Moreover, the influence of heating rate during pyrolysis process on the anisotropic property of char is also discussed.

4.2 Experimental

4.2.1 Wood samples

Wood samples used in this study are Japanese cypress wood cylinders (WC) with three various aspect rations. Proximate and ultimate analyses of Japanese cypress wood (trunk) are listed in Table 2.1 (Chapter 2). The information and photograph for wood cylinders with three aspect ratios are shown in Table 4.1 and Figure 4.1. It is noted that all samples have the same mass and volume. An initial weight is approximately 48 mg. The principal axes of wood defined with respect to grain direction for the wood cylinder is the same as shown in Figure 3.2 (Chapter 3). It can be seen that the longitudinal axis with respect to fiber grain aligns in the axial direction (z-axis) of the wood cylinder.

4.2.2 Pyrolysis and gasification experiments

Pyrolysis and gasification experiments are conducted in a thermobalance, as shown in Figure 3.3 (Chapter 3). The experimental apparatus consists of a gas supply system, thermobalance (ULVAC TGD-9600), and tar trap. A wood sample is placed at a center of platinum crucible on a thermocouple (thermometric point). Air inside the experimental setup is purged by a vacuum pump and then replaced by argon. The wood sample is dried at 383 K for 10 min before pyrolysis. This drying period was long enough to dry the largest samples. Then, the pyrolysis is performed at a constant heating rate in an argon atmosphere flowing at 0.8 l/min. The pyrolysis pressure is 0.1 MPa. The heating rate is set to 1 or 30 K/s. The final temperature of pyrolysis is 1423 K with holding time of 5 min. To control the heating rate and the reactor temperature, the temperature at a thermometric point is used as a representative. Pyrolysis conditions are summarized in Table 4.2. After the pyrolysis, the temperature is changed from the final pyrolysis temperature to a desired gasification temperature in the flowing argon. The gasification temperature is varied in the range of 723–1423 K. When the desired temperature is reached, the isothermal gasification is initiated by switching the gas line to a 20% oxygen/argon mixture

flowing at 1 l/min. The gasification experiment is terminated when the char is completely gasified. Gasification conditions are summarized in Table 4.3.

4.2.3 Char reactivity calculation

Char conversion (X) and gasification rate (R) are calculated by using Eq. (1) and (2), respectively

$$X = 1 - \frac{m}{m_0} \tag{1}$$

$$R = \frac{dX}{dt} = -\frac{1}{m_0}\frac{dm}{dt} \tag{2}$$

where m is the mass of char at time t, m_0 is the initial mass of the char at the time when the gasification begins. It is noted that the sample ash content was neglected because the amount of ash in the Japanese cypress wood is very low. In the present study, the char reactivity, R_i, is defined as the initial gasification rate at $X = 0$.

4.2.4 X-ray CT analysis

X-ray CT (Xradia VersaXRM-500) is used to investigate intraparticle structure of D8×L2 char samples prepared by the pyrolysis at heating rate of 30 K/s. A series of cross-sectional images with the size of 2×2 mm and 2 μm in resolution is obtained. Moreover, the 3D image of 2×2×2 mm char with the resolution of 2 μm is able to be reconstructed from the analysis.

Table 4.1 Information of wood samples.

Sample	diameter, D (mm)	length, L (mm)	aspect ratio, L/D (–)	mass (mg)
D8×L2	8.0	2.0	0.25	≈48
D6×L3.6	6.0	3.6	0.59	≈48
D4×L8	4.0	8.0	2.00	≈48

Table 4.2 Pyrolysis conditions.

Heating rate (K/s)	1, 30
Final temperature (K)	1423
Holding time (min)	5
Ar flow rate (l/min)	0.8
Pressure (MPa)	0.1

Table 4.3 Gasification conditions.

Temperature (K)	723, 748, 773, 798, 873, 1023, 1173, 1423
Ar flow rate (l/min)	0.8
O_2 flow rate (l/min)	0.2
Pressure (MPa)	0.1

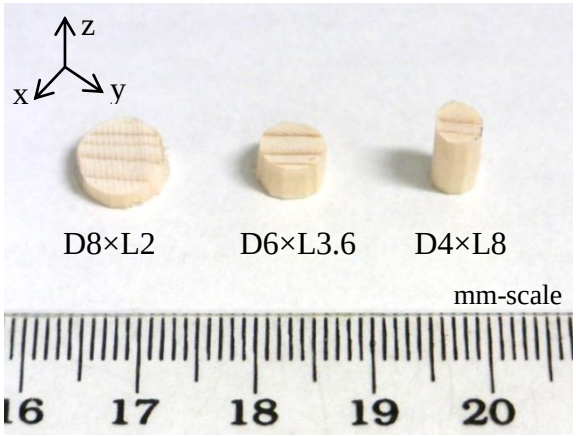

Figure 4.1 Photograph of wood cylinders with three aspect ratios.

4.3 Results and discussion

4.3.1 Intraparticle structure

Figure 4.2 shows X-ray CT cross-sectional images in the xy plane for the D8×L2 char near the top surface, at the middle, and near the bottom surface. It can be seen that the structure of wood-derived char consists of a large amount of pores which are vessel and fiber cells of original wood. Small pores (10–20 μm) with uniform size and shape can be observed in some areas near the top and bottom surface (Figure 4.2a and Figure 4.2c). Meanwhile, most of pores in the middle (Figure 4.2b) are relatively large (50 μm~) and very random in size and shape. Because the char sample is pyrolyzed at high heating rate, the internal pressure of char sample is also high due to the rapid release of volatile matters. That results in the expansion of pore wall and the collapse of pore structure. The details were discussed in our previous paper [15]. However, the internal pressure near the surface seems to be low due to easy release of volatile matters. As a result, the small pores can be observed near the surface.

Figure 4.3 shows X-ray CT cross-sectional images in the xz plane for the D8×L2 char. The pores mainly aligning along the axial direction (z-axis) are visible. By observing a series of cross-sectional images in the xy plane and cross-sectional images in the xz plane (Figure 4.3), it is shown that pores continue from the top/bottom surface to the inside particle. Figure 4.4 shows 3D X-ray CT of D8×L2 char with partially cross-sectioned view near top surface. Partially cross-sectioned view near the top surface (Figure 4.4) shows a honeycomb-like structure of small pores. Pores in the middle seem to be distorted by the high pressure during pyrolysis at high heating rate. However, the alignment of pore in the axial direction is still observable in the middle part, as can be seen in Figure 4.3. This intraparticle visualization by X-ray CT indicates that pores inside the wood-derived char mostly align the axial direction of wood cylinder. And, this kind of structure is considered as the anisotropic structure.

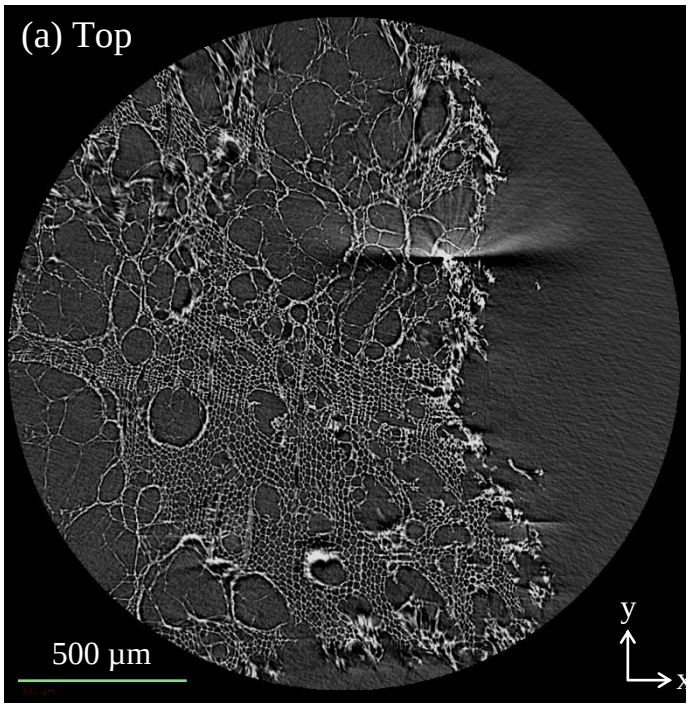
(a) Top
500 µm
y
x

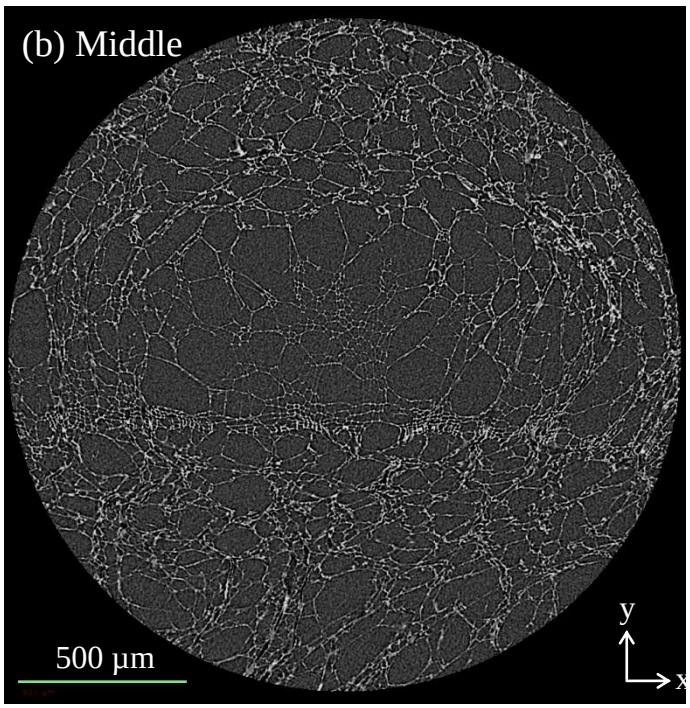
(b) Middle
500 µm
y
x

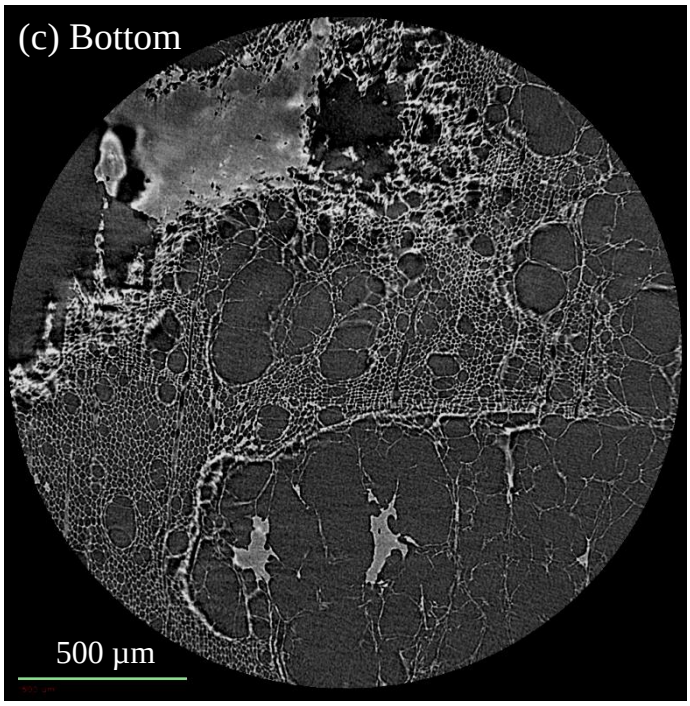

Figure 4.2 X-ray CT cross-sectional image of D8×L2 char in the xy plane: (a) near top surface, (b) at the middle, and (c) near bottom surface.

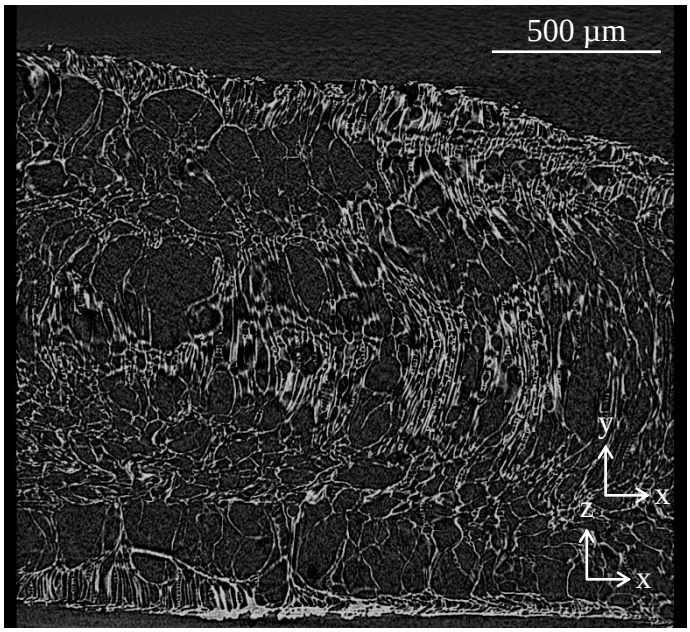

Figure 4.3 X-ray CT cross-sectional image of D8×L2 char in the xz plane.

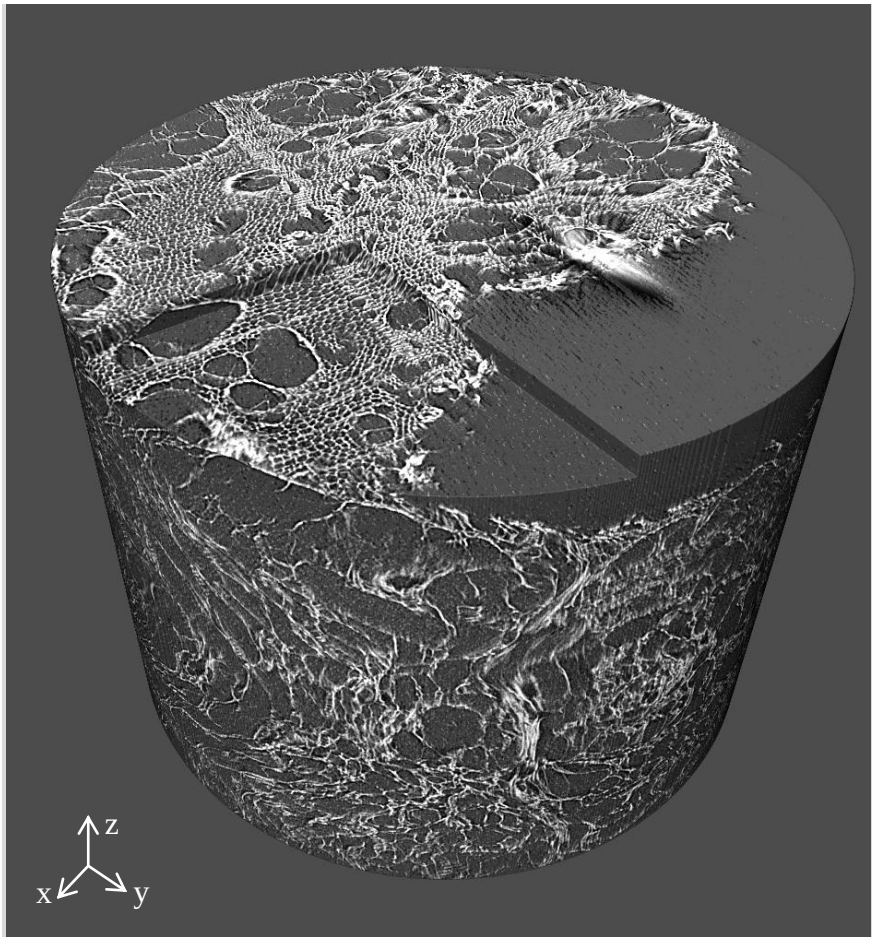

Figure 4.4 3D X-ray CT image of D8×L2 char with partially cross-sectioned view near top surface.

4.3.2 Char reactivity

The results obtained from the char samples prepared at high heating rate of 30 K/s are mainly used to discuss due to its closer heating rate to an industrial process. Arrhenius plot of the reactivity for char prepared at heating rate 30 K/s are shown in Figure 4.5. At low gasification temperatures (673–773K), the reactivity for all char samples is almost the same regardless of particle aspect ratio and linearly increased with increasing temperature. It indicates that the gasification reaction at these low temperatures is controlled by the kinetic of chemical reaction (zone I). In this zone, the diffusion rate is much faster than the chemical reaction rate; therefore, the char gasification occurs throughout the particle. It is concluded that the effect of particle aspect ratio on char reactivity is not appeared in the kinetically controlled zone.

When gasification temperature is above 773K, the decrease in slope of reactivity is observed, indicating a transition from the kinetically controlled zone to the internal diffusion-controlled zone (zone II). Gasification for char particle with high aspect ratio (D4×L8) changes from zone I to zone II at temperature above 773K. Meanwhile, the rate-limiting process for char particle with low aspect ratio (D8×L2) changes at higher temperature of 798K. It is implied that total diffusion resistance of low aspect ratio char is lower than that of high aspect ratio char, resulting in the higher temperature at which the rate-limiting process changes from chemical kinetic to diffusion process. At high temperature range of 873–1423K, the gasification rate for all particle aspect ratios is controlled by the internal diffusion process. In this zone II, the char reactivity is increased with decreasing aspect ratio. The low aspect ratio char (D8×L2) shows the highest reactivity among three char samples. It shows that the effect of anisotropic structure on char reactivity is significantly appeared when the gasification reaction is controlled by the internal diffusion process.

This result can be explained by the anisotropic intraparticle structure. It is known that the alignment of pore structure influences gas transport into the char particle. And, pores inside the cylindrical char used in this experiment align along its axial direction as discussed above. Therefore, the top/bottom surface of cylindrical char becomes more dominant than the side surface for the gas transport. In the zone II the O_2 transport into the char particle is limited by the internal diffusion process. In fact, a decrease in particle aspect ratio of cylindrical shape results in an increase in

top/bottom surface area. That improves O_2 transport into the char sample, leading to the high char reactivity for low aspect ratio char.

The repeatability of reactivity measurement is checked by performing two repeated experiments for three aspect ratio chars at gasification temperature of 1423K. The reactivity for all aspect ratio chars at temperature 1423K with one standard deviation error bars is presented in Figure 4.6. This result shows a good repeatability in this experiment. The char reactivity of D8×L2 char is approximately 22% higher than that of D4×L8 char.

The instantaneous rate of char conversion (dX/dt) for three aspect ratio chars is shown in Figure 4.7. The conversion rate of low aspect ratio char is higher than that of high aspect ratio char for whole gasification period. The important information from this plot is the quantitative comparison of dX/dt for entire gasification process because the difference in dX/dt indicates the difference in Thiele modulus, φ (reaction rate/diffusion rate) of fluid-solid reaction in the zone II [16]. Theoretically, the conversion rate (dX/dt) is decreased with increasing the Thiele modulus. Therefore, it is implied that the Thiele modulus is increased with increasing aspect ratio. Owing to the same reaction rate for all char samples, the diffusion rate for the low aspect ratio char is higher than that for high aspect ratio char. A plot of char conversion (X) as a function of time (t) for three aspect ratio chars at temperature 1423 K is shown in Figure 4.8. The D8×L2 char shows the fastest conversion time among the three samples.

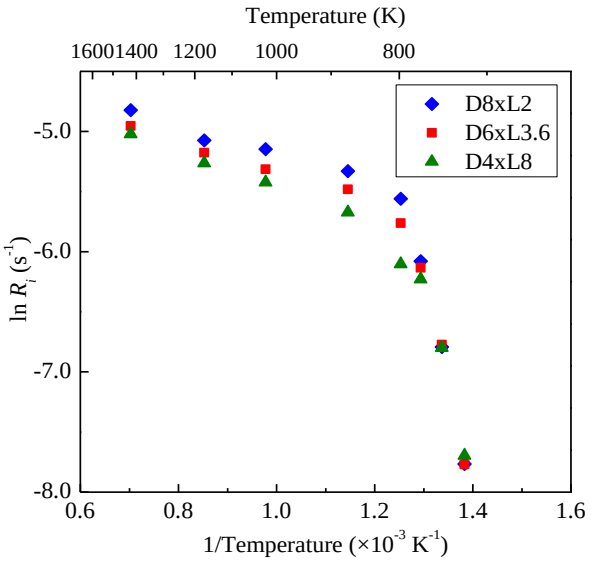

Figure 4.5 Arrhenius plot of reactivity for chars with various aspect ratios prepared at 30 K/s.

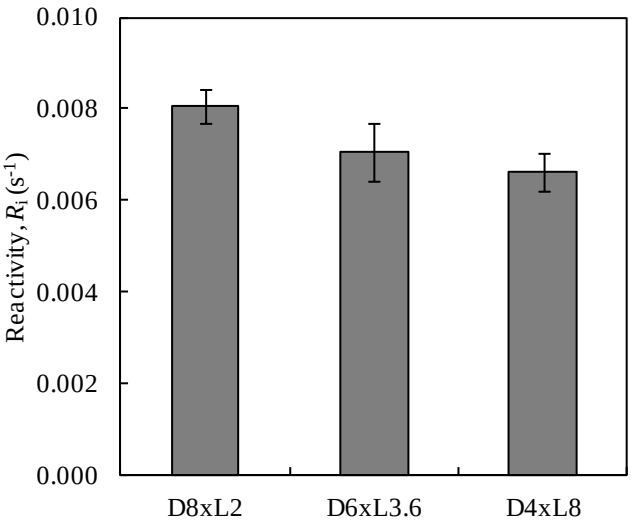

Figure 4.6 Reactivity of three aspect ratio chars prepared at 30 K/s. Gasification temperature is 1423K. Error bars indicate one standard deviation.

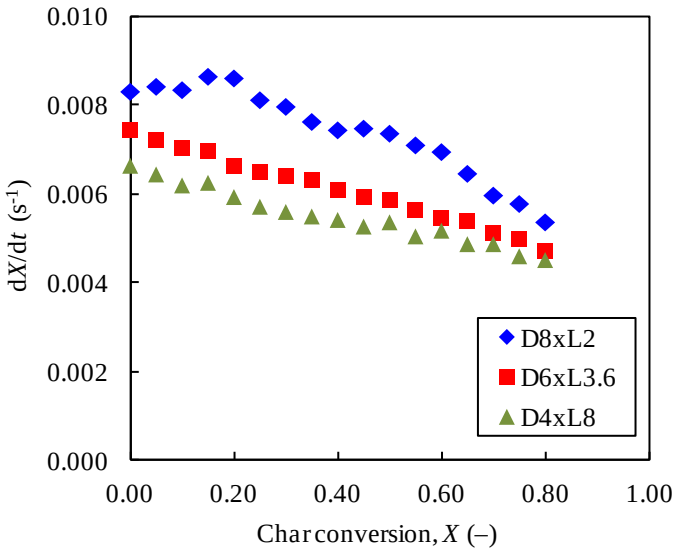

Figure 4.7 Instantaneous rate of char conversion at 1423 K. Chars are prepared at heating rate 30 K/s.

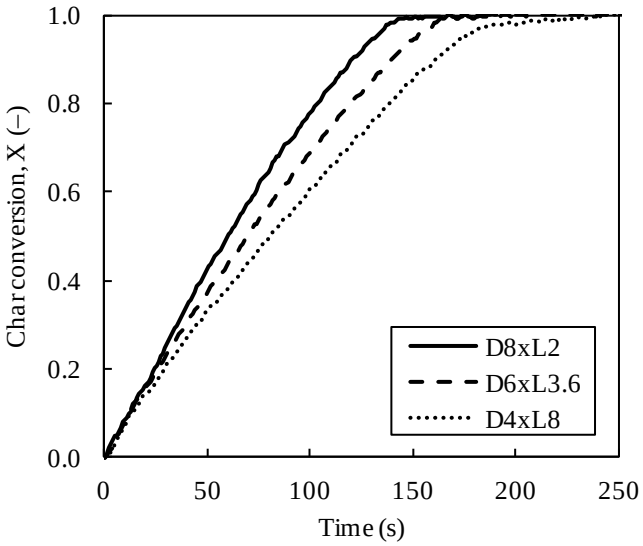

Figure 4.8 Char conversion as a function of time at gasification temperature 1423K. Chars are prepared at heating rate 30 K/s.

4.3.3 Effect of heating rate

Arrhenius plot of reactivity for the chars prepared at heating rate 1 K/s are shown in Figure 4.9. The char prepared at 1 K/s shows the similar tendency of Arrhenius plot as that at 30 K/s. At low temperatures in the zone I, the char reactivity is almost the same regardless of particle aspect ratio. At high temperatures in the zone II, the char reactivity is increased with decreasing aspect ratio. The reactivity for all aspect ratio chars (prepared at 1 K/s) at temperature 1423K with one standard deviation error bars is presented in Figure 4.10. Meanwhile, the reactivity of the D8×L2 (prepared at 1 K/s) is about 41% higher than that of the D4×L8. Compared to the reactivity difference of 22% between the D8×L2 and D4×L8 sample prepared at 30 K/s, this reactivity difference for samples prepared at 1 K/s is significantly larger. The difference in reactivity between the low and high aspect ratio chars may represent the order of anisotropy which is defined as the difference in gas diffusion between the axial direction and the radial direction. If the order of anisotropy is high, the difference in reactivity between low and high aspect ratio char is large. Therefore, it is implied that the order of anisotropy for 1 K/s char is higher than that of 30 K/s char. This can be explained by their char structures. When the char is prepared at low heating rate, the pore structure is perfectly aligned like a honeycomb structure. This kind of structure should show the high order of anisotropy. Meanwhile, the pore structure of char prepared at high heating rate, the alignment of pore is distorted and the portion of pore structure seems to be collapsed as shown in Figure 4.4. That may result in the lower order of anisotropy when compared with the chars prepared at low heating rate. However, it is noted that the significant difference in reactivity between low and high aspect ratio char at heating rate of 30 K/s is observable even for the lower order of anisotropy as shown in Figure 4.6. Figure 4.11 shows the instantaneous rate of char conversion (dX/dt) for three aspect ratio chars prepared at 1 K/s. The plot of char conversion (X) as a function of time (t) for three aspect ratio chars (prepared at 1 K/s) at temperature 1423 K is shown in Figure 4.12. The instantaneous rate of char conversion and the plot of char conversion (X) as a function of time (t) for the chars prepared at heating rate 1 K/s show the same trend as those of the chars prepared at 30 K/s.

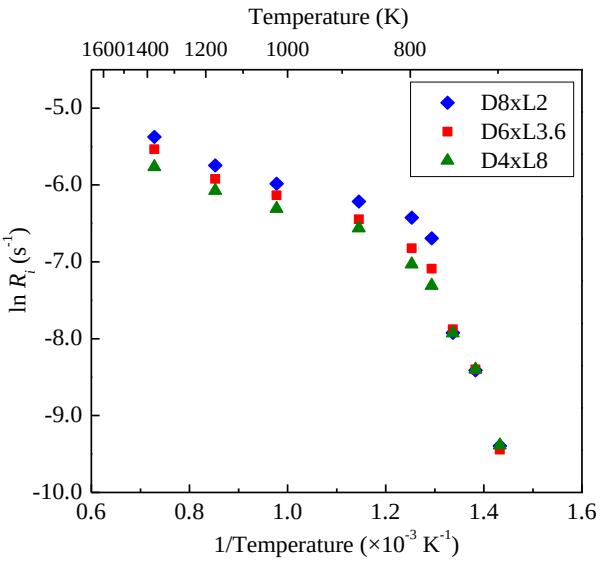

Figure 4.9 Arrhenius plot of reactivity for chars with various aspect ratios prepared at 1 K/s.

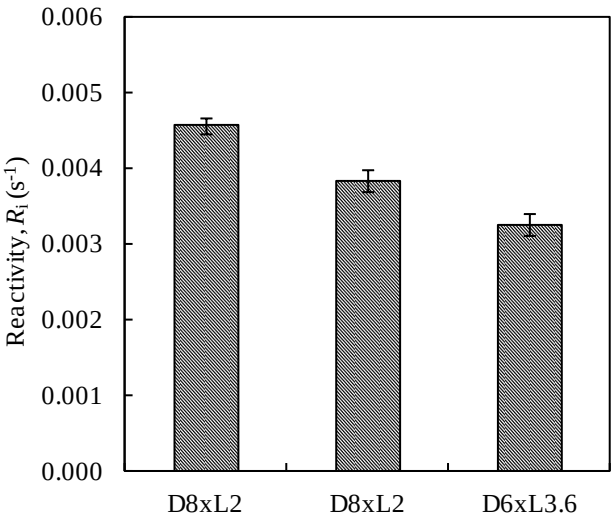

Figure 4.10 Reactivity of three aspect ratio chars prepared at 1 K/s. Gasification temperature is 1423K. Error bars indicate one standard deviation.

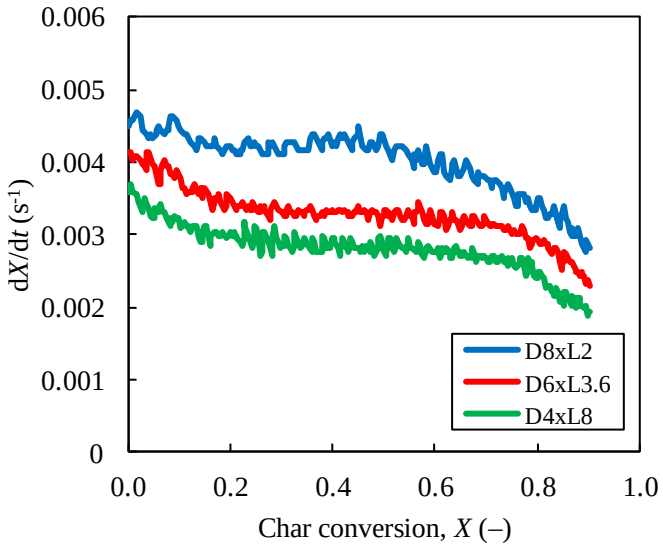

Figure 4.11 Instantaneous rate of char conversion at 1423 K. Chars are prepared at heating rate 1 K/s.

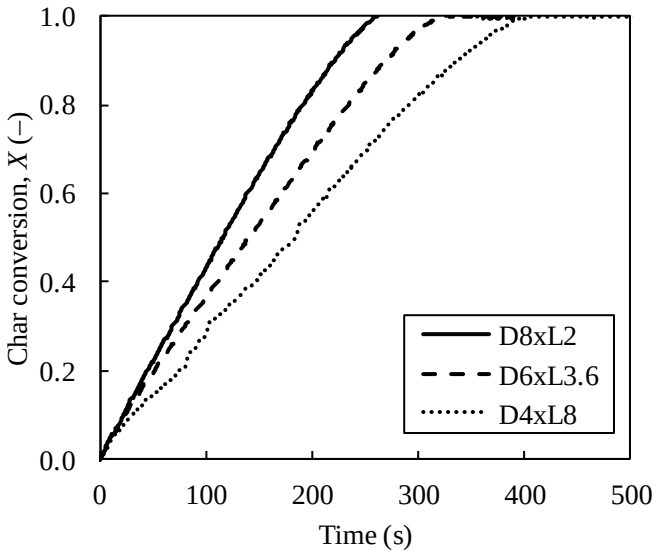

Figure 4.12 Char conversion as a function of time at gasification temperature 1423K. Chars are prepared at heating rate 1 K/s.

4.4 Conclusion

In this study, wood cylinders with three particle aspect ratios were pyrolyzed and gasified to investigate the effect of anisotropic structure on char reactivity. The reactivity was measured at various temperatures in order to make the Arrhenius plot. The X-ray CT images of anisotropic structure of char were also shown. Pores inside the char sample mainly aligned in its axial direction. It was found that the effect of particle aspect ratio on char reactivity was not appeared in the kinetically controlled zone. However, the anisotropic structure significantly influenced char reactivity in the internal diffusion-controlled zone. Char reactivity was significantly increased with decreasing particle aspect ratio. Char with low aspect ratio showed the highest reactivity and fastest conversion time among three samples. This study showed that wood cylinder with low aspect ratio had the high reactivity under gasification in the internal diffusion-controlled zone owing to the influence of anisotropic structure. Therefore, the aspect ratio of wood particle was an important parameter for the reactivity of anisotropic char.

References

[1] G. Zanchi, N. Pena, N. Bird, Is woody bioenergy carbon neutral? A comparative assessment of emissions from consumption of woody bioenergy and fossil fuel, GCB Bioenergy, 4 (2012) 761-772.

[2] S. Sridhar, P. Rozzelle, B. Morreale, D. Alman, Materials Challenges for Advanced Combustion and Gasification Fossil Energy Systems, Metall and Mat Trans A, 42 (2011) 871-877.

[3] J. Fermoso, M.V. Gil, C. Pevida, J.J. Pis, F. Rubiera, Kinetic models comparison for non-isothermal steam gasification of coal–biomass blend chars, Chemical Engineering Journal, 161 (2010) 276-284.

[4] S. Link, S. Arvelakis, M. Hupa, P. Yrjas, I. Kŭlaots, A. Paist, Reactivity of the Biomass Chars Originating from Reed, Douglas Fir, and Pine, Energy & Fuels, 24 (2010) 6533-6539.

[5] E. Cetin, R. Gupta, B. Moghtaderi, Effect of pyrolysis pressure and heating rate on radiata pine char structure and apparent gasification reactivity, Fuel, 84 (2005) 1328-1334.

[6] C. Branca, C. Di Blasi, Global Kinetics of Wood Char Devolatilization and Combustion, Energy & Fuels, 17 (2003) 1609-1615.

[7] I.W. Smith, The combustion rates of coal chars: A review, Symposium (International) on Combustion, 19 (1982) 1045-1065.

[8] J. Larfeldt, B. Leckner, M.C. Melaaen, Modelling and measurements of the pyrolysis of large wood particles, Fuel, 79 (2000) 1637-1643.

[9] E. Cetin, B. Moghtaderi, R. Gupta, T.F. Wall, Influence of pyrolysis conditions on the structure and gasification reactivity of biomass chars, Fuel, 83 (2004) 2139-2150.

[10] Y. Okumura, T. Hanaoka, K. Sakanishi, Effect of pyrolysis conditions on gasification reactivity of woody biomass-derived char, Proceedings of the Combustion Institute, 32 (2009) 2013-2020.

[11] L. Lu, C. Kong, V. Sahajwalla, D. Harris, Char structural ordering during pyrolysis and combustion and its influence on char reactivity, Fuel, 81 (2002) 1215-1225.

[12] C. Di Blasi, F. Buonanno, C. Branca, Reactivities of some biomass chars in air, Carbon, 37 (1999) 1227-1238.

[13] H.-S. Shim, M.R. Hajaligol, V.L. Baliga, Oxidation behavior of biomass chars:

pectin and Populus deltoides, Fuel, 83 (2004) 1495-1503.
[14] R. Abdallah, S. Auchet, P.J. Méausoone, Experimental study about the effects of disc chipper settings on the distribution of wood chip size, Biomass and Bioenergy, 35 (2011) 843-852.
[15] T. Pattanotai, H. Watanabe, K. Okazaki, Gasification characteristic of large wood chars with anisotropic structure, Fuel, 117, Part A (2014) 331-339.
[16] S.K. Bhatia, D.D. Perlmutter, A random pore model for fluid-solid reactions: II. Diffusion and transport effects, AIChE Journal, 27 (1981) 247-254.

CHAPTER 5

Conclusions

Experimental investigation of pyrolysis and gasification of woody biomass was presented in this thesis. Effects of intraparticle reactions and anisotropic structure on pyrolysis/gasification characteristics were emphasized. The important considerations when utilizing large woody biomass in gasifiers were raised in this work. The possibility to decrease tar product and to increase char reactivity was suggested in order to improve the overall efficiency of woody biomass gasification. In this chapter, the summary and important findings in this work were presented. In the last section, contributions and further perspectives of this work were discussed.

5.1 Concluding remarks

In Chapter one, the depletion of fossil fuel and environmental issues due to CO_2 emission encourage the use of renewable energy sources including biomass. Advantages of biomass energy were discussed. Many biomass conversion technologies including thermochemical and biochemical conversions were introduced. However, utilization of biomass energy through gasification process is a promising option. Fundamentals of woody biomass pyrolysis and gasification were explained. Research motivations of this work were raised from the problems and the concerning points while utilizing large woody biomass in gasifiers. Outline and objectives of this thesis were stated and summarized.

In Chapter two, intraparticle secondary reactions of tar during the pyrolysis of woody biomass were investigated experimentally. A comparison of sawdust and wood cylinder pyrolysis at low heating rate of 0.5 K/s revealed intraparticle secondary reactions. The weight fraction histories indicated that the polymerization of tar to form secondary char (intraparticle reactions) progressed at approximately 380°C. Intraparticle tar decomposition to form secondary gas (mainly CO) occurred at 400–500°C, which was relatively low for tar cracking. This was because char worked as a catalyst and lowered the temperature at which secondary tar

decomposition progressed. This chapter clarified that the intraparticle secondary reactions of tar played an important role during the pyrolysis of large wood particles. Thus, these reactions have the potential to reduce the amount of tar produced in gasification systems.

In Chapter three, pyrolysis and gasification characteristics of large wood cylinders were investigated. The sawdust and wood cylinders with various lengths were used as samples. The effect of intraparticle secondary reactions of tar on pyrolysis products was primarily confirmed at both low and high heating rates. The relationship between particle size and tar reduction were shown. The internal anisotropic structure of wood cylinder char was visualized by X-ray CT analysis. X-ray image revealed that pores inside wood cylinder char mainly aligned along its axial direction (the grain direction). Then, Arrhenius plots of reactivity for chars with various sizes were made. Char reactivity was significantly deceased with increasing cylinder length in the internal diffusion-controlled zone. Char gasification mainly progressed in the direction of pores when the gasification rate was controlled by the internal diffusion, indicating the anisotropic evolution of particle shape during the gasification. Moreover, heating rate during pyrolysis was found to significantly influence the pore structure, radial shrinkage and swelling of the wood cylinder. This chapter showed that the alignment of pore and pore diffusion played an important role in the gasification of large wood-derived char.

In Chapter four, the influence of particle aspect ratio on gasification reactivity of anisotropic char was further investigated. Wood cylinders with three particle aspect ratios were used as samples for pyrolysis and gasification experiment in this chapter. The 3D X-ray CT image of char structure was also shown. It was found that the effect of particle aspect ratio on char reactivity was not appeared in the kinetically controlled zone. However, the anisotropic structure significantly influenced char reactivity in the internal diffusion-controlled zone. Char reactivity was significantly increased with decreasing particle aspect ratio. Char with low aspect ratio showed the highest reactivity and fastest conversion time among three samples. This chapter showed that wood cylinder with low aspect ratio had the high reactivity under gasification in the internal diffusion-controlled zone due to the influence of anisotropic structure. Therefore, the aspect ratio of wood cylinder was an important parameter for the reactivity of anisotropic char.

5.2 Contributions and future perspectives

From the results of investigations reported in this thesis, some contributions to the fields of woody biomass pyrolysis as well as gasification can be summarized as follow.

In the first place, this study provided the better understanding of intraparticle reactions of tar during wood pyrolysis. Because the intraparticle reactions are heterogeneous reactions taking place inside the particle, they cannot be directly investigated. Therefore, a comparative study under carefully determined conditions such as heating rate was performed to clarify the intraparticle reactions. The results suggested the advantages of using large woody biomass in terms of tar reduction. Enhancing intraparticle reactions was achievable by increasing heating rate and particle size. Controlling the residence time of tar transport inside the particle and the temperature of char layer are crucial parameters for enhancing intraparticle tar decomposition. Moreover, the catalyst effect of wood-derived char was found to be an important factor for intraparticle tar decomposition.

For characteristics of wood-derived char gasification, the intraparticle anisotropic structure of char particle was well visualized using X-ray CT analysis. The potential of using X-ray analysis in the field of solid fuel conversion (pyrolysis, gasification, and combustion) was shown. Moreover, the digital analysis of X-ray CT image was able to provide the quantitative analysis for the difference char structure prepared at different heating rates. The study showed the important of pore alignment in the char particle. Gasification of large wood char showed the anisotropic shape evolution when the gasification rate was controlled by the internal diffusion process. The investigation of gasification using chars with various aspect ratios showed the increase in char reactivity when the low aspect ratio char was used. This information is useful for the numerical simulation of char gasification and the selection of wood shape for the gasifier. Furthermore, this study suggested that low aspect ratio wood cylinder or woody biomass with large surface area in the transverse plane and short length in the longitudinal axis can provide high char reactivity.

This work was based on the experimental results obtained from the thermobalance (small scale) in which the conditions were precisely controlled. Therefore, an experimental study in the actual or pilot scale gasifier would provide good information as well as a confirmation of results observed in this work.

Acknowledgement

First, I would like to express my sincere gratitude to my adviser Prof. Ken Okazaki for giving me an opportunity at Energy Phenomena Laboratory, and for his guidance, support and encouragement about my research. He always teaches us not only academic knowledge but also the lifestyle experience.

I am grateful to Assist. Prof. Hirotatsu Watanabe, who have helped me improving my research and revising a lot of my manuscripts. Without the intensive discussion with him, finishing my study course would be much more difficult.

I would also like to thank Assoc. Prof. Kazuyoshi Fushinobu for kind helping when I just came to Japan and Prof. Tomohiro Nozaki and Assoc. Prof. Yoichi Murakami for kind interactions in the seminar as well as in my daily life. Moreover, I have to thank Ms. Ayako Nohara for very great administrative supports during my stay in this laboratory.

To EPL members, thanks for all guys for great interactions and giving me a good experience. Firstly, I would like to thank Dr. Takuya Okada and Dr. Pious Okekunle for introducing me about biomass research and the great discussion. To Dr. Willy Wijaya and Dr. Ryan Gresback, both of you were the great doctoral students which make me motivated for completing my course. To Dr. Ding Li, thank you for a great talk during the lab trip. To Kota Kawai, Masashi Tasaki, Kei Kanzawa, Daisuke Kanda, Riku Yamada, Kiyomi Shimomura, Keisuke Maezono, Shota Moriyama, Li Xiaofan, Tomoaki Furuyama, Ryota Nakano, and Kei Yoshikawa: I have to thank all of these friends who have graduated from this laboratory for good interactions in the laboratory including lab trips, conference trips, and many parties. To Yutaka Shoji, and Shunsuke Sugai: I thank for your help over the last few years and good luck for your future. To Jack and Winyu, I am pleased that both of you come to this laboratory so that we can speak Thai language in the laboratory. For new B4 and exchange student; Akihiro Kimura, Shiro Koizumi, Takashi Komeno, and David Tilling; I hope you all will enjoy the research and do the best to get a great output.

I would like to express my gratitude to my family and parents who always love and encourage me during my study in Japan. Not forgotten, I thank all of my Thai friends in Japan especially in Tokyo Tech who make me enjoy my life here.

Finally, I would like to acknowledge Mongbukagakusho (MEXT Japan) for the scholarship support during my study in Tokyo Tech.